Xsuite physics manual

CERN - Geneva, Switzerland

Contents

Chapter 1

Single-particle tracking

XTrack is a 6D single particle symplectic tracking code used to compute the trajectories of individual relativistic charged particles in circular accelerators. It has been developed based on SixTrack.
The physical models are collected from the main references [1, 2, 3, 4, 5, 6, 7], which contain more details of the derivation of the maps.

1.1 Notation and reference frame

The speed, momentum, energy, rest mass, charge of a particle are indicated by v, P, E, m and q, respectively. These quantities are related by the following equations:

$$v = \beta c \qquad E^2 - P^2c^2 = m^2c^4 \qquad E = \gamma mc^2 \qquad Pc = \beta E \tag{1.1}$$

where β and γ are the relativistic factors.
In a curvilinear reference frame defined by a constant curvature h_x in the $\hat{X}, \hat{Z}$ plane and parameterized by s, the position of the particle at a time t can be written as:

$$\mathbf{Q}(t) = \mathbf{r}(s) + x\,\hat{x}(s) + y\,\hat{y}(s), \tag{1.2}$$

and therefore identified by the coordinates s, x, y, t in the reference frame defined by $\hat{x}(s)$ and $\hat{y}(s)$. In particle tracking, s is normally used as independent parameter and t as a coordinate.
The electromagnetic fields $\mathbf{E}$ and $\mathbf{B}$ can be derived in a curvilinear reference frame from the potentials $V(x, y, s, t)$ and $\mathbf{A}(x, y, s, t)$, where

$$\mathbf{A}(x, y, s, t) = A_x(x, y, s, t)\hat{x}(s) + A_y(x, y, s, t)\hat{y}(s) + A_s(x, y, s, t)\hat{z}(s) \tag{1.3}$$

and for which:

$$\mathbf{E} = -\nabla V - \frac{\partial \mathbf{A}}{\partial t} = -\partial_x V\hat{x} - \partial_y V\hat{y} - \frac{1}{1+hx}\partial_s V\hat{z} - \partial_t \mathbf{A} \tag{1.4}$$

$$\mathbf{B} = \nabla \times \mathbf{A} = \left(\partial_y A_s - \frac{\partial_s A_y}{1+hx}\right)\hat{x} + \left(\frac{\partial_s A_x - \partial_x(1+hx)A_s}{1+hx}\right)\hat{y} \tag{1.5}$$

$$+ \quad \left(\partial_x A_y - \partial_y A_x\right)\hat{z}. \tag{1.6}$$

In this reference frame the canonical momenta are:

$$P_x = m\gamma\dot{x} + qA_x, \quad P_y = m\gamma\dot{y} + qA_y, \quad P_s = m\gamma\dot{s}(1+hx)^2 + q(1+hx)A_s. \tag{1.7}$$

and the energy of a particle and the field is

$$E = qV + c\sqrt{(mc)^2 + \frac{(P_s - qA_s(1+hx))^2}{(1+hx)^2} + (P_x - qA_x)^2 + (P_x - qA_x)^2}. \tag{1.8}$$

1.2 Hamiltonian and particle coordinates

If $s(t)$ is monotonically increasing, it is possible to derive the equations of motion using s as the independent parameter, $(-t, E)$ as conjugate coordinates and $-P_s$ as Hamiltonian.

$$P_s = (1+hx)\left(\sqrt{\frac{(E-q\phi)^2}{c^2} - (mc)^2 - (P_x - qA_x)^2 - (P_y - qA_y)^2} + qA_s\right) \tag{1.9}$$

Since in accelerators the orbits of the particles are often a perturbation of the reference trajectory followed by a particle with rest mass m_0, charge q_0, speed $\beta_0 c$ and momentum P_0, one could use the following derived quantities that usually assume small values:

$$p(x,y) = \frac{m_0}{m}\frac{P(x,y)}{P_0} \qquad \chi = \frac{q}{q_0}\frac{m_0}{m} \qquad a(x,y,s) = \frac{q_0}{P_0}A(x,y,s) \tag{1.10}$$

Note that here m is used to indicate the rest mass of particles of species different from the reference particle (which has mass m_0) and not the relativistic mass. Further rescaling the energy and charge density as

$$e(x,y,s) = \frac{m_0}{m}\frac{E(x,y,s)}{P_0} \qquad \varphi(x,y,s) = \frac{q_0}{P_0 c}\phi(x,y,s)\,, \tag{1.11}$$

and as all canonical momenta scale with the same factor, we can define a new Hamiltonian $\tilde{H}$ that still satisfies the same equations of motion:

$$\tilde{H}(x,y,-t,p_x,p_y,e) = \frac{m_0}{m}\frac{1}{P_0}H(x,y,-t,P_x,P_y,E)$$
$$\tilde{H} = -(1+hx)\left(\sqrt{\left(\frac{e}{c} - \chi\varphi\right)^2 - \frac{1}{\beta_0^2\gamma_0^2} - (p_x - \chi a_x)^2 - (p_y - \chi a_y)^2} + \chi a_s\right) \tag{1.12}$$

1.2.1 Longitudinal coordinates

Different sets of longitudinal coordinates can be used:

$$\xi = s\frac{\beta}{\beta_0} - \beta ct \qquad \tau = \frac{s}{\beta_0} - ct \qquad \zeta = s - \beta_0 ct \tag{1.13}$$

$$\delta = \frac{P\frac{m_0}{m} - P_0}{P_0} \qquad p_\tau = \frac{1}{\beta_0}\frac{E\frac{m_0}{m} - E_0}{E_0} \qquad p_\zeta = \frac{1}{\beta_0^2}\frac{E\frac{m_0}{m} - E_0}{E_0} \tag{1.14}$$

where variables in the same columns are canonically conjugate.
The different longitudinal variables can be easily related to each other:

$$\xi = \beta\tau = \frac{\beta}{\beta_0}\zeta \tag{1.15}$$

$$p_\tau = \beta_0 p_\zeta \tag{1.16}$$

$$\delta = \sqrt{p_\tau^2 + 2\frac{p_\tau}{\beta_0} + 1} - 1 = \beta p_\tau + \frac{\beta - \beta_0}{\beta_0} \tag{1.17}$$

$$\delta = \sqrt{\beta_0^2 p_\zeta^2 + 2p_\zeta + 1} - 1 = \beta\beta_0 p_\zeta + \frac{\beta - \beta_0}{\beta_0} \tag{1.18}$$

$$\gamma = \gamma_0(1 + \beta_0 p_\tau) \tag{1.19}$$

$$\beta = \sqrt{1 - \frac{1 - \beta_0}{(1 + \beta_0 p_\tau)^2}} \tag{1.20}$$

For small energy deviations ($\delta \ll 1$, $p_\tau \ll 1$, $p_\zeta \ll 1$), we can neglect the terms of order δ^2, p_τ^2, p_ζ^2 and higher, hence the following approximations hold:

$$\delta \simeq \frac{p_\tau}{\beta_0} \tag{1.21}$$

$$\delta \simeq p_\zeta \tag{1.22}$$

$$\beta \simeq \beta_0 + (1 - \beta_0^2)p_\tau \tag{1.23}$$

1.2.2 Hamiltonian with different coordinate choices

The conjugate pairs can be generated by the following generating functions [1]

$$F_2 = xp_x + yp_y + \left(\frac{s}{\beta_0} - ct\right)\frac{1 + \delta}{\beta} \tag{1.24}$$

$$F_2 = xp_x + yp_y + \left(\frac{s}{\beta_0} - ct\right)\left(p_\tau + \frac{1}{\beta_0}\right) \tag{1.25}$$

$$F_2 = xp_x + yp_y + \left(\frac{s}{\beta_0} - ct\right)\left(\beta_0 p_\zeta + \frac{1}{\beta_0}\right) \tag{1.26}$$

The Hamiltonians are then:

[1] $F_2(-t, p_{\text{new}}, s)$, $e = \frac{\partial F_2}{\partial(-t)}$, $q_{\text{new}} = \frac{\partial F_2}{\partial p_{\text{new}}}$, $H_{\text{new}} = H + \frac{\partial F_2}{\partial s}$

$$H_\delta = \frac{1+\delta}{\beta\beta_0} - (1+hx)\left(\sqrt{\left(\frac{1+\delta}{\beta} - \chi\varphi\right)^2 - \frac{1}{\beta_0^2\gamma_0^2} - (p_x - \chi a_x)^2 - (p_y - \chi a_y)^2} + \chi a_s\right)$$

$$H_\tau = \frac{p_\tau}{\beta_0} - (1+hx)\left(\sqrt{\left(p_\tau + \frac{1}{\beta_0} - \chi\varphi\right)^2 - \frac{1}{\beta_0^2\gamma_0^2} - (p_x - \chi a_x)^2 - (p_y - \chi a_y)^2} + \chi a_s\right)$$

$$H_\zeta = p_\zeta - (1+hx)\left(\sqrt{\left(\beta_0 p_\zeta + \frac{1}{\beta_0} - \chi\varphi\right)^2 - \frac{1}{\beta_0^2\gamma_0^2} - (p_x - \chi a_x)^2 - (p_y - \chi a_y)^2} + \chi a_s\right)$$

Note that things get complicated when using the pair (ξ, δ), as then the Hamiltonian contains terms in β, which in turn depends on the energy. In particular:

$$\frac{\partial\beta}{\partial\delta} = \beta\,\frac{1-\beta^2}{1+\delta} \tag{1.27}$$

For this reason we prefer using H_τ when deriving the equations of motion. Note that when $\varphi = 0$, the Hamiltonian simplifies into:

$$H_\tau = \frac{p_\tau}{\beta_0} - (1+hx)\left(\sqrt{(1+\delta)^2 - (p_x - \chi a_x)^2 - (p_y - \chi a_y)^2} + \chi a_s\right) \tag{1.28}$$

The following identities are useful to derive the equations of motion:

$$\frac{\partial\delta}{\partial p_\tau} = \frac{p_\tau + 1/\beta_0}{1+\delta} = \frac{1}{\beta} \tag{1.29}$$

$$\frac{\partial}{\partial\delta}\left(\frac{1+\delta}{\beta\beta_0}\right) = \frac{\beta}{\beta_0} \tag{1.30}$$

1.3 Symplectic integrators

1.3.1 Hamiltonians of the implemented maps

Xsuite provides maps for the following Hamiltonians

We call $\sqrt{...} = \sqrt{(1+\delta)^2 - p_x^2 - p_y^2}$:

Map	Parameters	Description	
D	l	Drift exact	$H_D = \frac{p_\tau}{\beta_0} - \sqrt{(1+\delta)^2 - p_x^2 - p_y^2}$
De	l	Drift expanded	$H_{De} = \frac{p_\tau}{\beta_0} - \frac{p_x^2+p_y^2}{2(1+\delta)}$
Dc	l	Correction drift exact	$H_{Dc} = H_D - H_{De}$
R	h, l	Curved drift	$H_R = \frac{p_\tau}{\beta_0} - (1+hx)\left(\sqrt{...}\right)$
Br	k0, l	Rectangular bend	$H_{Br} = \frac{p_\tau}{\beta_0} - \sqrt{...} - b_1 x$
B	k0, l, h	Exact Bend	$H_B = \frac{p_\tau}{\beta_0} - (1+hx)\left(\sqrt{...} - k_0\left(x - \frac{hx^2}{2(1+hx)}\right)\right)$
Kh	h, l	Thin curvature kick	$H_{Kh} = -hx$
K0h	k0,l	Weak focusing	$H_{K0h} = k_0 h\frac{x^2}{2}$
K0	k0, l	Dipole kick	$H_{K0} = k_0 x$
K1	k1, l	Quadrupole kick	$H_{K1} = k_1\frac{x^2-y^2}{2}$
K1h	k1, h, l	Quad correction	$H_{K1h} = k_1 h\frac{2x^3-3xy^2}{6}$
Kn	kn, ks, l	Multipole	$H_{Kn} = -\Re\left(\sum_{n=0}^{N}(k_n + i\hat{k}_n)\frac{(x+iy)^{n+1}}{(n+1)!}\right)$
Knh	kn, ks, h	Curved Multipoles	Not yet available
M	k0, k1, l, h	2nd order Hamiltonian	$H_{Kn} = \frac{p_\tau}{\beta_0} + \frac{1}{2}\frac{p_x^2+p_y^2}{(1+\delta)} + (k_0 - h)x + \frac{k_0 h x^2}{2} + k_1\frac{x^2-y^2}{2}$
S	ks,l	Solenoid	$H_S = \frac{p_\tau}{\beta_0} - \sqrt{(1+\delta)^2 - \left(p_x - \frac{k_s}{2}y\right)^2 - \left(p_y + \frac{k_s}{2}\right)^2}$

1.3.2 Magnet models

The maps are combined to obtain the following models of magnetic elements:

Model	$h = 0, ks = 0$	$h \neq 0, ks = 0$
rot-kick-rot	[D], [K0 K1 Kn]	[R], [K0 K0h K1 K1h Kn Knh]
bend-kick-bend	[Br], [K1 Kn]	[B], [K1 K1h Kn Knh]
matrix-kick-matrix	[M], [Kn Dc]	[M], [K1h Kn Knh Dc]
drift-kick-drift-exact	[D], [K0 K1 Kn]	[D], [Kh K0 K0h K1 K1h Kn Knh]
drift-kick-drift-expanded	[De], [K0 K1 Kn]	[De], [Kh K0 K0h K1 K1h Kn Knh]

1.3.2.1 Map for the exact bend

$$x(s) = \frac{1}{hk_0}\left(h\sqrt{(1+\delta)^2 - p_x(s)^2 - p_y^2} - \frac{dp_x(s)}{ds} - k_0\chi\right) \tag{1.31}$$

$$p_x(s) = p_x\cos(hs) + \left(\sqrt{(1+\delta)^2 - p_x^2 - p_y^2} - k_0\chi\left(\frac{1}{h} + x\right)\right)\sin(hs) \tag{1.32}$$

$$y(s) = y + \frac{p_y sh}{k_0\chi} + \frac{p_y}{k_0\chi}\left(\sin^{-1}\left(\frac{p_x}{\sqrt{(1+\delta)^2 - p_y^2}}\right) - \sin^{-1}\left(\frac{p_x(s)}{\sqrt{(1+\delta)^2 - p_y^2}}\right)\right) \tag{1.33}$$

$$p_y(s) = p_y \tag{1.34}$$

$$\delta(s) = \delta \tag{1.35}$$

$$\zeta(s) = \zeta - \frac{\beta_0}{\beta}\left[\frac{(1+\delta)sh}{k_0\chi} + \frac{(1+\delta)}{k_0\chi}\left(\sin^{-1}\left(\frac{p_x}{\sqrt{(1+\delta)^2 - p_y^2}}\right) - \sin^{-1}\left(\frac{p_x(s)}{\sqrt{(1+\delta)^2 - p_y^2}}\right)\right)\right] \tag{1.36}$$

1.4 Cavity time, energy errors and acceleration

A cavity kick depends on:

$$\sin(2\pi fT + \phi) \tag{1.37}$$

where T is laboratory time.
For the most general case:

$$\sin(2\pi fT + \phi) = \sin\left(2\pi f\frac{s-\zeta}{\beta_0 c} + \phi\right) \tag{1.38}$$

Most codes drop the term $2\pi fs/(\beta_0 c)$ that is

$$\sin(2\pi fT + \phi) \to \sin\left(-2\pi f\frac{\zeta}{\beta_0 c} + \phi\right) \tag{1.39}$$

to make sure that a particle that is syncrhonous to the reference trajectory is in phase with the cavity.

1.4.1 Implementing energy errors

One can define

$$\begin{aligned} s &= s_0 + n(L_0 - L) + nL \\ f_{\text{rev}} &= \beta_0 c/L \\ f &= hf_{\text{rev}} \end{aligned} \tag{1.40}$$

where s_0 is the path length at the cavity turn at 0, L_0 is the design circumference, n is the turn number, h is the harmonic number, L is the new path length with an energy

error. Indeed one could write $L = L_0(1 + \eta\delta_s)$ where η is a constant property of the lattice.
Multiple cavities can have their own defined L.
Using these definitions, then

$$\sin(2\pi fT + \phi) = \sin\left(2\pi h f_{\text{rev}} \frac{s_0 + n(L_0 - L) - \zeta}{\beta_0 c} + \phi\right) \tag{1.41}$$

$$= \sin\left(2\pi h f_{\text{rev}} \frac{n(L_0 - L) - \zeta}{\beta_0 c} + \phi'\right) \tag{1.42}$$

where $\phi' = \frac{2\pi h s_0}{L} + \phi$.
In MAD-X twiss and MAD8, indeed the longitudinal coordinates is directly $\zeta' = n(L_0 - L) - \zeta$ and the term $n(L_0 - L)$ is added smoothly in each thick element. This forces all the cavities to share the same L or f_{rev}.
In SixTrack or MAD-X track, one could simply define a turn dependent phase

$$\phi = \phi_0 + 2\pi h f_{\text{rev}} n(L_0 - L) \tag{1.43}$$

which is very general or in alternative add a special element that perform at each turn the following transformation:

$$\zeta_{\text{new}} = (L_0 - L) - \zeta_{\text{old}} \tag{1.44}$$

1.4.2 Acceleration

Accelaration can be achieved by renormalized the relative variables using a new momentum reference. This has the side effect that the fields of the magnets (expressed in normalized strength) follow the energy ramp and that the cavity frequency (if expressed in terms of the harmonic number (NB we should perhaps change this in the Xtrack interface) is updated.
The re-normalization if done once at each turn is:

$$p_{x,\text{new}} = p_{x,\text{old}} \frac{P_{0,\text{old}}}{P_{0,\text{new}}} \qquad p_{y,\text{new}} = p_{y,\text{old}} \frac{P_{0,\text{old}}}{P_{0,\text{new}}} \tag{1.45}$$

$$\delta_{\text{new}} = (\delta_{\text{old}} + 1)\frac{P_{0,\text{old}}}{P_{0,\text{new}}} - 1 \qquad p_{\tau,\text{new}} = \frac{p_{\tau,\text{old}}\, P_{0,\text{old}}\, c + E_{0,\text{old}} - E_{0,\text{new}}}{P_{0,\text{new}} c} \tag{1.46}$$

$$\zeta_{\text{new}} = s\beta_0 \left(\frac{1}{\beta_{0,\text{new}}} - \frac{1}{\beta_{0,\text{old}}}\right) - \zeta_{\text{old}} \qquad \tau_{\text{new}} = s\left(\frac{1}{\beta_{0,\text{new}}} - \frac{1}{\beta_{0,\text{old}}}\right) - \tau_{\text{old}} \tag{1.47}$$

(1.48)

1.5 Beam elements

1.5.1 Drift

A drift is a straight, field-free region ($h(x,y) = 0$, $V = 0$ and $\mathbf{A} = 0$). The exact and expanded Hamiltonian for a drift space are

$$H_\tau = \frac{p_\tau}{\beta_0} - \sqrt{(1+\delta)^2 - p_x^2 - p_y^2} \approx \frac{p_\tau}{\beta_0} - \delta + \frac{1}{2}\frac{p_x^2 + p_y^2}{1+\delta}. \tag{1.49}$$

The map is given by solving the equations of motion:

$$\frac{\mathrm{d}p_i}{\mathrm{d}s} = -\frac{\partial H}{\partial q_i} \qquad \frac{\mathrm{d}q_i}{\mathrm{d}s} = \frac{\partial H}{\partial p_i} \tag{1.50}$$

As there is no explicit dependency on the position coordinates in the Hamiltonian, the momenta remain unchanged in a drift.
For the position coordinates, we get:

$$(x)' = \frac{p_x}{p_z} \approx \frac{p_x}{1+\delta} \tag{1.51}$$

$$(y)' = \frac{p_y}{p_z} \approx \frac{p_y}{1+\delta} \tag{1.52}$$

$$(\tau)' = \frac{1}{\beta_0} - \frac{1}{\beta}\frac{1+\delta}{p_z} \approx \frac{1}{\beta_0} - \frac{1}{\beta} - \frac{1}{\beta}\frac{p_x^2 + p_y^2}{2} \tag{1.53}$$

$$p_z = \sqrt{(1+\delta)^2 - p_x^2 - p_y^2} \tag{1.54}$$

1.5.1.1 Expanded Drift

The map relative to the expanded Hamiltonian is then

$$x_p = \frac{p_x}{1+\delta} \qquad y_p = \frac{p_y}{1+\delta} \tag{1.55}$$

$$x \leftarrow x + x_p l \qquad y \leftarrow y + y_p l \tag{1.56}$$

$$\zeta \leftarrow \zeta + l\left(1 - \frac{\beta_0}{\beta}\left(1 + \frac{x_p^2 + y_p^2}{2}\right)\right) \tag{1.57}$$

1.5.1.2 Exact Drift

The map relative to the exact Hamiltonian is then

$$x \leftarrow x + \frac{p_x}{p_z} l \qquad y \leftarrow y + \frac{p_x}{p_z} l \tag{1.58}$$

$$\zeta \leftarrow \zeta + l\left(1 - \frac{\beta_0}{\beta}\frac{1+\delta}{p_z}\right) \tag{1.59}$$

1.5.1.3 Polar Drift

It is possible to define a "polar" drift that has the effect of rotating the reference frame [8] for instance in the x-z plane

$$p_x \leftarrow p_x \cos\theta + p_z \sin\theta \qquad p_z \leftarrow -p_x \sin\theta + p_z \cos\theta \tag{1.60}$$

$$z = -x \sin\theta \qquad x' = p_x/p_z \qquad y' = p_y/p_z \tag{1.61}$$

$$x \leftarrow x\cos\theta - x'z \qquad y \leftarrow y - x'z \qquad \tau \leftarrow \tau + z\frac{1}{\beta}\frac{1+\delta}{p_z}. \tag{1.62}$$

where θ is the angle bringing the new $\hat{x}$ towards the old $\hat{z}$. The map can be also generated by combining a rotation with a $-x\sin(\theta)$-length drift. In case of an $\hat{x}$ rotation the role of x and y are interchanged.

1.5.2 Dipole

In a curvilinear reference system with a constant curvature h in the horizontal plane a uniform magnetic field can be derived by the vector potential:

$$A_x = 0, \qquad A_y = 0, \qquad A_s = -B_y\left(x - \frac{hx^2}{2(1+hx)}\right). \tag{1.63}$$

With the following normalization $k_0 = \frac{q_0}{p}B_y$ is the inverse of the bending radius of the reference particle.
The exact and expanded Hamiltonian for a horizontal bending magnet is (eq. 2.12 in [2])

$$H = \frac{p_\tau}{\beta_0} - (1+hx)\sqrt{(1+\delta)^2 - p_x^2 - p_y^2} + \chi k_0\left(x + \frac{hx^2}{2}\right) \tag{1.64}$$

$$\simeq \frac{p_\tau}{\beta_0} + \frac{1}{2}\frac{p_x^2+p_y^2}{1+\delta} - (1+hx)(1+\delta) + \chi k_0\left(x + \frac{hx^2}{2}\right) \tag{1.65}$$

1.5.2.1 Thin dipole

The map for a thin dipole kick (horizontal or vertical) from the expanded Hamiltonian is (eq. 4.12 in [4]):

$$p_x \leftarrow p_x + (h_x l - \chi k_0 l) + h_x l\delta - \chi k_0 l h_x x \tag{1.66}$$

$$p_y \leftarrow p_y - (h_y l - \chi\hat{k}_0 l) - h_y l\delta - \chi\hat{k}_0 l h_y y \tag{1.67}$$

$$\tau \leftarrow \tau - \frac{h_x x - h_y y}{\beta} l. \tag{1.68}$$

1.5.2.2 Thick dipole

Defining the following quantities,

$$G_x = \chi\frac{k_0 h_x}{1+\delta}, \qquad G_y = \chi\frac{\hat{k}_0 h_y}{1+\delta} \tag{1.69}$$

$$C_{x,y} = \cos(\sqrt{G_{x,y}}L), \qquad S_{x,y} = \sin(\sqrt{G_{x,y}}L) \tag{1.70}$$

the map relative to the expanded Hamiltonian is (eq. 4.11 in [2])

$$x \leftarrow C_x \cdot x + \frac{S_x}{\sqrt{G_x}}\frac{1}{1+\delta}\cdot p_x + \frac{\delta}{h_x}(1-C_x) \tag{1.71}$$

$$p_x \leftarrow -\sqrt{G_x}(1+\delta)\cdot S_x \cdot x + C_x \cdot p_x + \delta\sqrt{1+\delta}\cdot S_x \tag{1.72}$$

$$y \leftarrow C_y \cdot y + \frac{S_y}{\sqrt{G_y}}\frac{1}{1+\delta}\cdot p_y + \frac{\delta}{h_y}(1-C_y) \tag{1.73}$$

$$p_y \leftarrow -\sqrt{G_y}(1+\delta)\cdot S_y \cdot y + C_y \cdot p_y + \delta\sqrt{1+\delta}\cdot S_y \tag{1.74}$$

$$\zeta \leftarrow \zeta + L\left(1-\frac{\beta_0}{\beta}\right) \tag{1.75}$$

$$-\frac{\beta_0}{\beta}\left[\frac{h_x S_x}{\sqrt{G_x}}\cdot x + \frac{1-C_x}{h_x}\cdot p_x + \frac{h_y S_y}{\sqrt{G_y}}\cdot y + \frac{1-C_y}{h_y}\cdot p_y + \delta\left(2L - \frac{S_x}{\sqrt{G_x}} - \frac{S_y}{\sqrt{G_y}}\right)\right] \tag{1.76}$$

$$-\frac{1}{4}\frac{\beta_0}{\beta}\left[G_x\left(L-\frac{C_x S_x}{\sqrt{G_x}}\right)\left(x-\frac{\delta}{h_x}\right)^2 + \left(L+\frac{C_x S_x}{\sqrt{G_x}}\right)\frac{p_x^2}{(1+\delta)^2} - \left(x-\frac{\delta}{h_x}\right)\frac{2S_x^2}{1+\delta}\cdot p_x\right. \tag{1.77}$$

$$\left. + G_y\left(L-\frac{C_y S_y}{\sqrt{G_y}}\right)\left(y-\frac{\delta}{h_y}\right)^2 + \left(L+\frac{C_y S_y}{\sqrt{G_y}}\right)\frac{p_y^2}{(1+\delta)^2} - \left(y-\frac{\delta}{h_y}\right)\frac{2S_y^2}{1+\delta}\cdot p_y\right]. \tag{1.78}$$

1.5.2.3 Dipole Edge effects

Considering the dipole edge effects from a dipole of length L and bending angle θ, the map is

$$p_x \to p_x + \frac{1+\delta}{\rho}\tan(\alpha)\cdot x$$
$$p_y \to p_y - \frac{1+\delta}{\rho}\tan(\alpha)\cdot y,$$

where the bending radius ρ and α are defined as

$$\rho^{-1} = \frac{h_x}{\sqrt{1+\delta}} \qquad \alpha = \frac{1}{2}\frac{L}{\rho} = \frac{\theta}{2}.$$

1.5.2.4 Fringe field

Based on: `https://cds.cern.ch/record/2857004`
The map of the fringe field of a bending magnet can be written as:

$$y^f = \frac{2y}{1+\sqrt{1-2\frac{\partial\Phi}{\partial p_y}y}} \tag{1.79}$$

$$x^f = x + \frac{1}{2}\frac{\partial\Phi}{\partial p_x}y^{f2} \tag{1.80}$$

$$p_y^f = p_y - \Phi y^f \tag{1.81}$$

$$\zeta^f = \zeta + \frac{\beta_0}{\beta}\frac{1}{2}\frac{\partial\Phi}{\partial\delta}y^{f2} \tag{1.82}$$

where:

$$\Phi\left(p_x, p_y, \delta\right) = \frac{k_0 x'}{1+y'^2} - gk_0^2 f_{\text{int}}\left(\frac{(1+\delta)^2 - p_y^2}{p_z^3} + x'^2\frac{(1+\delta)^2 - p_x^2}{p_z^3}\right) \tag{1.83}$$

We define:

$$\phi_0(x', y') = \frac{x'}{1+y'^2} \tag{1.84}$$

$$\phi_x(p_x, p_y, \delta) = \frac{(1+\delta)^2 - p_x^2}{p_z^3} \tag{1.85}$$

$$\phi_y(p_x, p_y, \delta) = \frac{(1+\delta)^2 - p_y^2}{p_z^3} \tag{1.86}$$

So we can rewrite:

$$\Phi\left(p_x, p_y, \delta\right) = \frac{k_0 x'}{1+y'^2} - gk_0^2 f_{\text{int}}\left(\frac{(1+\delta)^2 - p_y^2}{p_z^3} + x'^2\frac{(1+\delta)^2 - p_x^2}{p_z^3}\right) \tag{1.87}$$

so we can rewrite:

$$\Phi\left(p_x, p_y, \delta\right) = k_0\phi_0(x', y') - gk_0^2 f_{\text{int}}\left(\phi_y(p_x, p_y, \delta) + x'^2\phi_x(p_x, p_y, \delta)\right) \tag{1.88}$$

The derivatives can be written as:

$$\frac{\partial\Phi}{\partial p_x} = k_0\left(\frac{\partial\phi_0}{\partial x'}\frac{\partial x'}{\partial p_x} + \frac{\partial\phi_0}{\partial y'}\frac{\partial y'}{\partial p_x}\right) - gk_0^2 f_{\text{int}}\left(\frac{\partial\phi_y}{\partial p_x} + 2x'\frac{\partial x'}{\partial p_x}\phi_x + x'^2\frac{\partial\phi_x}{\partial p_x}\right) \tag{1.89}$$

$$\frac{\partial\Phi}{\partial p_y} = k_0\left(\frac{\partial\phi_0}{\partial x'}\frac{\partial x'}{\partial p_y} + \frac{\partial\phi_0}{\partial y'}\frac{\partial y'}{\partial p_y}\right) - gk_0^2 f_{\text{int}}\left(\frac{\partial\phi_y}{\partial p_y} + 2x'\frac{\partial x'}{\partial p_y}\phi_x + x'^2\frac{\partial\phi_x}{\partial p_y}\right) \tag{1.90}$$

$$\frac{\partial\Phi}{\partial\delta} = k_0\left(\frac{\partial\phi_0}{\partial x'}\frac{\partial x'}{\partial\delta} + \frac{\partial\phi_0}{\partial y'}\frac{\partial y'}{\partial\delta}\right) - gk_0^2 f_{\text{int}}\left(\frac{\partial\phi_y}{\partial\delta} + 2x'\frac{\partial x'}{\partial\delta}\phi_x + x'^2\frac{\partial\phi_x}{\partial\delta}\right) \tag{1.91}$$

Expression of all other quantities needed for the calculation:

$$x' = \frac{p_x}{p_z} \tag{1.92}$$
$$\frac{\partial x'}{\partial p_x} = -\frac{p_x}{p_z^2}\frac{\partial p_z}{\partial p_x} + \frac{1}{p_z} \tag{1.93}$$
$$\frac{\partial x'}{\partial p_y} = -\frac{p_x}{p_z^2}\frac{\partial p_z}{\partial p_x} \tag{1.94}$$
$$\frac{\partial x'}{\partial \delta} = -\frac{p_x}{p_z^2}\frac{\partial p_z}{\partial \delta} \tag{1.95}$$

$$y' = \frac{p_y}{p_z} \tag{1.96}$$
$$\frac{\partial y'}{\partial p_y} = -\frac{p_y}{p_z^2}\frac{\partial p_z}{\partial p_y} \tag{1.97}$$
$$\frac{\partial y'}{\partial p_y} = -\frac{p_y}{p_z^2}\frac{\partial p_z}{\partial p_y} + \frac{1}{p_z} \tag{1.98}$$
$$\frac{\partial y'}{\partial \delta} = -\frac{p_y}{p_z^2}\frac{\partial p_z}{\partial \delta} \tag{1.99}$$

$$p_z = \sqrt{(1+\delta)^2 - p_x^2 - p_y^2} \tag{1.100}$$
$$\frac{\partial p_z}{\partial p_x} = -\frac{p_x}{p_z} = -x' \tag{1.101}$$
$$\frac{\partial p_z}{\partial p_y} = -\frac{p_y}{p_z} = -y' \tag{1.102}$$
$$\frac{\partial p_z}{\partial \delta} = \frac{1+\delta}{p_z} \tag{1.103}$$

$$\phi_x = \frac{(1+\delta)^2 - p_x^2}{p_z^3} \tag{1.104}$$
$$\frac{\partial \phi_x}{\partial p_x} = -\frac{3}{p_z^4}\frac{\partial p_z}{\partial p_x}\left((1+\delta)^2 - p_x^2\right) - 2\frac{p_x}{p_z^3} \tag{1.105}$$
$$\frac{\partial \phi_x}{\partial p_y} = -\frac{3}{p_z^4}\frac{\partial p_z}{\partial p_y}\left((1+\delta)^2 - p_x^2\right) \tag{1.106}$$
$$\frac{\partial \phi_x}{\partial \delta} = -\frac{3}{p_z^4}\frac{\partial p_z}{\partial \delta}\left((1+\delta)^2 - p_x^2\right) + 2\frac{(1+\delta)}{p_z^3} \tag{1.107}$$

$$\phi_y = \frac{(1+\delta)^2 - p_y^2}{p_z^3} \tag{1.108}$$

$$\frac{\partial \phi_y}{\partial p_x} = -\frac{3}{p_z^4}\frac{\partial p_z}{\partial p_x}\left((1+\delta)^2 - p_y^2\right) \tag{1.109}$$

$$\frac{\partial \phi_y}{\partial p_y} = -\frac{3}{p_z^4}\frac{\partial p_z}{\partial p_y}\left((1+\delta)^2 - p_y^2\right) - 2\frac{p_y}{p_z^3} \tag{1.110}$$

$$\frac{\partial \phi_x}{\partial \delta} = -\frac{3}{p_z^4}\frac{\partial p_z}{\partial \delta}\left((1+\delta)^2 - p_x^2\right) + 2\frac{(1+\delta)}{p_z^3} \tag{1.111}$$

$$\phi_0 = \frac{x'}{1+y'^2} \tag{1.112}$$

$$\frac{\partial \phi_0}{\partial x'} = \frac{1}{1+y'^2} \tag{1.113}$$

$$\frac{\partial \phi_0}{\partial y'} = -\frac{2x'y'}{(1+y'^2)^2} \tag{1.114}$$

1.5.2.5 MAD8 fringe

Again nased on: `https://cds.cern.ch/record/2857004` (eq. 37)
The map of the fringe field of a bending magnet can be written as:

$$y^f = \frac{2y}{1+\sqrt{1-2\frac{\partial \Psi}{\partial p_y}y}} \tag{1.115}$$

$$x^f = x + \frac{1}{2}\frac{\partial \Psi}{\partial p_x}y^{f2} \tag{1.116}$$

$$p_y^f = p_y - \Psi y^f \tag{1.117}$$

$$\zeta^f = \zeta + \frac{\beta_0}{\beta}\frac{1}{2}\frac{\partial \Psi}{\partial \delta}y^{f2} \tag{1.118}$$

where:

$$\Psi\left(p_x, p_y, \delta\right) = k_0 \tan^{-1}\left(\frac{x'}{1+y'^2}\right) - g k_0^2 f_{\text{int}} p_z \left(1 + x'^2\left(2 + y'^2\right)\right) \tag{1.119}$$

We define:

$$\phi_0(x', y') = \frac{x'}{1+y'^2} \tag{1.120}$$

$$\phi_1(x', y') = 1 + 2x'^2 + x'^2 y'^2 \tag{1.121}$$

so we can write

$$\Psi = k_0 \tan^{-1}\left(\phi_0\right) - g k_0^2 f_{\text{int}} p_z \phi_1 \tag{1.122}$$

from which:

$$\frac{\partial \Psi}{\partial p_x} = k_0 \frac{1}{1+\phi_0^2}\frac{\partial \phi_0}{\partial p_x} - g k_0^2 f_{\text{int}} \left(\phi_1 \frac{\partial p_z}{\partial p_x} + p_z \frac{\phi_1}{\partial p_x} \right) \tag{1.123}$$

$$\frac{\partial \Psi}{\partial p_y} = k_0 \frac{1}{1+\phi_0^2}\frac{\partial \phi_0}{\partial p_y} - g k_0^2 f_{\text{int}} \left(\phi_1 \frac{\partial p_z}{\partial p_y} + p_z \frac{\phi_1}{\partial p_y} \right) \tag{1.124}$$

$$\frac{\partial \Psi}{\partial \delta} = k_0 \frac{1}{1+\phi_0^2}\frac{\partial \phi_0}{\partial \delta} - g k_0^2 f_{\text{int}} \left(\phi_1 \frac{\partial p_z}{\partial p_y} + p_z \frac{\phi_1}{\partial \delta} \right) \tag{1.125}$$

$$\tag{1.126}$$

$$\frac{\partial \phi_{0,1}}{\partial p_x} = \frac{\partial \phi_{0,1}}{\partial x'}\frac{\partial x'}{\partial p_x} + \frac{\partial \phi_{0,1}}{\partial y'}\frac{\partial y'}{\partial p_x} \tag{1.127}$$

$$\frac{\partial \phi_{0,1}}{\partial p_y} = \frac{\partial \phi_{0,1}}{\partial x'}\frac{\partial x'}{\partial p_y} + \frac{\partial \phi_{0,1}}{\partial y'}\frac{\partial y'}{\partial p_y} \tag{1.128}$$

$$\frac{\partial \phi_{0,1}}{\partial \delta} = \frac{\partial \phi_{0,1}}{\partial x'}\frac{\partial x'}{\partial \delta} + \frac{\partial \phi_{0,1}}{\partial y'}\frac{\partial y'}{\partial \delta} \tag{1.129}$$

$$\phi_0 = \frac{x'}{1+y'^2} \tag{1.130}$$

$$\frac{\partial \phi_0}{\partial x'} = \frac{1}{1+y'^2} \tag{1.131}$$

$$\frac{\partial \phi_0}{\partial y'} = -\frac{2x'y'}{(1+y'^2)^2} \tag{1.132}$$

$$\phi_1 = 1 + 2x'^2 + x'^2 y'^2 \tag{1.133}$$

$$\frac{\partial \phi_1}{\partial x'} = 4x' + 2x'y'^2 \tag{1.134}$$

$$\frac{\partial \phi_1}{\partial y'} = 2x'^2 y' \tag{1.135}$$

1.5.3 Combined dipole quadrupole

The following vector potential in curvilinear coordinates

$$A_s = -\frac{g}{1+hx}\left(\frac{x^2}{2} - \frac{y^2}{2} + \frac{hx^3}{3} \right) \tag{1.136}$$

produce a field

$$B_x = g\left(y + \frac{hxy}{1+hx} \right) \qquad B_y = gx \tag{1.137}$$

The following vector potential in curvilinear coordinates

$$A_s = -\frac{g}{1+hx}\left(\frac{x^2}{2} - \frac{y^2}{2} + \frac{hx^3}{3} - \frac{hxy^2}{2}\right) \tag{1.138}$$

produce a field

$$B_x = gy \qquad\qquad B_y = g\left(x + \frac{hy^2}{2+2hx}\right) \tag{1.139}$$

1.5.4 Thin Multipole

The effect of a thin multipole can be approximated by the following Hamiltonian
A longitudinally uniform static magnetic field can be described by the following equations

$$B_y + iB_x = \sum_{n=1} \frac{B_n + iA_n}{r_0^{n-1}}(x+iy)^{n-1} \tag{1.140}$$

$$= B_N \sum_{n=N} \frac{b_n + ia_n}{r_0^{n-1}}(x+iy)^{n-1}. \tag{1.141}$$

The kick $\Delta\mathbf{P} = q_0 v_z \hat{z} \times (B_x\hat{x} + B_y\hat{y})$ translates into

$$\Delta p_x - i\Delta p_y = -\frac{q_0}{P_0}\chi(B_y + iB_x) \tag{1.142}$$

A thin multiple idealizes the effect of the field by taking the limit of the integration length going to zero while keeping constant the integrated strength. The Hamiltonian is:

$$H = \delta(s)\chi L\Re\left[\sum_{n=0}\frac{1}{(n+1)!}(k_n + i\hat{k}_n)(x+iy)^{n+1}\right]. \tag{1.143}$$

where

$$k_n = n!\frac{q_0}{p_0}\frac{B_{n+1}}{r_0^n} \qquad\qquad \hat{k}_n = n!\frac{q_0}{p_0}\frac{A_{n+1}}{r_0^n}. \tag{1.144}$$

The corresponding map is:

$$p_x \leftarrow p_x - \chi L\cdot\Re\left[\sum_{n=0}\frac{1}{n!}(k_n + i\hat{k}_n)(x+iy)^n\right], \tag{1.145}$$

$$p_y \leftarrow p_y + \chi L\cdot\Im\left[\sum_{n=0}\frac{1}{n!}(k_n + i\hat{k}_n)(x+iy)^n\right], \tag{1.146}$$

In case a curvature h, the vector potential become:

$$f(x,y) = \int B_x(x,y)dy \tag{1.147}$$

$$g(x,y) = \int \partial x B_x(x,y)dy \tag{1.148}$$

$$a_s(x,y) = \frac{c_1}{1+hx} + f(x,y) - \frac{\int_1^x (1+h\tilde{x})(g(\tilde{x},y)+\tilde{x}) + hf(x,y)\,d\tilde{x}}{1+hx} \tag{1.149}$$

$$\frac{\int_1^x \left(-h\tilde{x}\,(g(x,y)) - \int \mathrm{bx}^{(1,0)}(\tilde{x},y)\,dy - h\int \mathrm{bx}(\tilde{x},y)\,dy - h\tilde{x}\mathrm{by}(\tilde{x},y) - \mathrm{by}(\tilde{x},y)\right)\,d\tilde{x}}{hx+1} \tag{1.150}$$

1.5.5 Accelerating Cavity

The approximated energy gain of a particle passing through an electric field of frequency $f = \frac{k}{2\pi c}$ for which:

$$V\sin(\phi - k\tau) = \int_{-l/2}^{l/2} E_s(0,0,t,s)\,\mathrm{d}s. \tag{1.151}$$

An equivalent vector potential can be derived and normalized as

$$A_s = -\frac{V}{\omega}\cos(\phi - k\tau) \qquad\qquad V_n = \frac{q_0}{P_0 c}V \tag{1.152}$$

from which one can derive the following map

$$p_\tau \leftarrow p_\tau + \chi V_n \sin(\phi - k\tau + k\frac{s-s_0}{\beta_0}), \tag{1.153}$$

where the additional terms in the phase is added in case harmonic number is not exactly integer and the phase is unlocked phase). The new δ can be updated from the new p_τ.

1.5.6 RF-Multipole

The RF-multipole generalizes the interaction of a particle with an electromagnetic field by assuming that

$$\Delta E(x,y,\tau) = q\int_{-L/2}^{L/2} E_z(x,y,t)\,\mathrm{d}s \tag{1.154}$$

$$\Delta P_x(x,y,\tau) = q\int_{-L/2}^{L/2} E_x(x,y,t) + \beta c B_y(x,y,t)\,\mathrm{d}s \tag{1.155}$$

$$\Delta P_y(x,y,\tau) = q\int_{-L/2}^{L/2} E_y(x,y,t) - \beta c B_x(x,y,t)\,\mathrm{d}s. \tag{1.156}$$

are harmonic in x, y and periodic in τ of frequency $f = \frac{k}{2\pi c}$ such that:

$$a_s(x, y, \tau) = \Re\left[\sum_{n=1}^{N}\left(k_n \cos(\phi_n - k\tau) + i\hat{k}_n \cos(\hat{\phi}_n - k\tau)\right)(x + iy)^n\right], \tag{1.157}$$

The map then follows:

$$\Delta p_x = -\sum_{n=1}^{N}\frac{\chi}{n!}\Re\left[(k_n C_n + i\hat{k}_n\hat{C}_n)(x + iy)^{(n-1)}\right], \tag{1.158}$$

$$\Delta p_y = \sum_{n=1}^{N}\frac{\chi}{n!}\Im\left[(k_n C_n + i\hat{k}_n\hat{C}_n)(x + iy)^{(n-1)}\right], \tag{1.159}$$

$$\Delta p_\tau = -\chi k\sum_{n=1}^{N}\Re\left[(k_n S_n + ik_n\hat{S}_n)(x + iy)^n\right], \tag{1.160}$$

where

$$C_n = \cos(\phi_n - \omega\Delta t) \qquad \hat{C}_n = \cos(\hat{\phi}_n - \omega\Delta t) \tag{1.161}$$

$$S_n = \sin(\phi_n - \omega\Delta t) \qquad \hat{S}_n = \sin(\hat{\phi}_n - \omega\Delta t). \tag{1.162}$$

1.5.7 Solenoid

The derivation largely follows one by Forest [8], while the final map can be verified to be the same as the one by Wolski [9].
We can write the Hamiltonian for the solenoid as follows:

$$H = p_\zeta - \sqrt{(1+\delta)^2 - \left(p_x + \frac{b_z}{2}y\right)^2 - \left(p_y - \frac{b_z}{2}x\right)^2} \tag{1.163}$$

where we have defined the normalized quantities $b_z = B_z\frac{q_0}{P_0}$, $a_x = A_x\frac{q_0}{P_0}$, $a_y = A_y\frac{q_0}{P_0}$. This can be obtained knowing the general Hamiltonian

$$H = p_\zeta - \sqrt{(1+\delta)^2 - (p_x - a_x)^2 - (p_y - a_y)^2} - a_z, \tag{1.164}$$

we can extract the magnetic field potential and convince ourselves that H describes a magnetic field with only the longitudinal component equal to B_z, as expected of a solenoid:

$$\mathbf{A} = \begin{bmatrix} A_x \\ A_y \\ A_z \end{bmatrix} = \begin{bmatrix} -\frac{B_z}{2}y \\ \frac{B_z}{2}x \\ 0 \end{bmatrix} \implies \mathbf{B} = \nabla \times \mathbf{A} = \begin{bmatrix} \frac{\partial A_z}{\partial y} - \frac{\partial A_y}{\partial z} \\ \frac{\partial A_z}{\partial x} - \frac{\partial A_x}{\partial z} \\ \frac{\partial A_y}{\partial x} - \frac{\partial A_x}{\partial y} \end{bmatrix} = \begin{bmatrix} 0 \\ 0 \\ B_z \end{bmatrix}. \tag{1.165}$$

The Hamiltonian H can be simplified, by applying the following transformation, which should be understood as the change of reference from the general coordinate

system $\mathbf{X}$ to a new $\mathbf{X}_{\text{new}}$:

$$T := \begin{bmatrix} -\frac{1}{2} & 0 & 0 & \frac{1}{b_z} \\ 0 & 1 & \frac{1}{2}b_z & 0 \\ -\frac{1}{2} & 0 & 0 & -\frac{1}{b_z} \\ 0 & 1 & -\frac{1}{2}b_z & 0 \end{bmatrix}.$$

In particular, note that if

$$\mathbf{X} = \begin{bmatrix} x \\ p_x \\ y \\ p_y \end{bmatrix} = T^{-1}\mathbf{X}_{\text{new}} = \begin{bmatrix} -x_{\text{new}} - y_{\text{new}} \\ \frac{1}{2}(p_{x,\text{new}} + p_{y,\text{new}}) \\ \frac{1}{b_z}(p_{x,\text{new}} - p_{y,\text{new}}) \\ \frac{b_z}{2}(x_{\text{new}} - y_{\text{new}}) \end{bmatrix},$$

then we can rewrite H in terms of $\mathbf{X}_{\text{new}}$ (dropping the 'new' suffix, while keeping it in mind) as

$$K := -\sqrt{(1+\delta)^2 - p_x^2 - b_z^2 x^2}.$$

We can simplify H even further, rewriting it in terms of the following action-angle variables:

$$x := \sqrt{\frac{2J}{|b_z|}}\cos(\phi) \quad \text{and} \quad p_x := \sqrt{2|b_z|J}\sin(\phi). \tag{1.166}$$

The new Hamiltonian with respect to J is the following:

$$\begin{aligned} K = -\sqrt{(1+\delta)^2 - p_x^2 - b_z^2 x^2} = \\ -\sqrt{(1+\delta)^2 - \left(\sqrt{2|b_z|J}\sin(\phi)\right)^2 - b_z^2\sqrt{\frac{2J}{|b_z|}}\cos(\phi)^2} = \\ -\sqrt{(1+\delta)^2 - \left(\sqrt{2|b_z|J}\sin(\phi)\right)^2 - \left(\sqrt{2|b_z|J}\cos(\phi)\right)^2} = \\ -\sqrt{(1+\delta)^2 - 2|b_z|J}. \end{aligned}$$

Then, using Hamilton's equations, we can solve for ϕ:

$$\frac{d\phi}{dz} = \frac{\partial K}{\partial J} \implies \phi(z) = \phi(0) + z\frac{\partial K}{\partial J} = \phi(0) - z\frac{|b_z|}{K}.$$

Let $\omega := -b_z/K$. Keeping in mind that we are still in the realm of $\mathbf{X}_{\text{new}}$, we can compute x_{new} and y_{new} substituting the above into (1.166). Note that we can drop the modulus on b_z in both ω and the equations below, as cos is an even function, and

while sin is an odd function and the signs of $\sin(\omega z)$ and b_z will cancel out anyway.

$$x = \sqrt{\frac{2J}{|b_z|}}\cos\left(\phi(0) + \left(-z\frac{|b_z|}{K}\right)\right) =$$
$$\sqrt{\frac{2J}{|b_z|}}\cos\phi(0)\cos(\omega z) - \frac{\sqrt{2J|b_z|}}{|b_z|}\sin\phi(0)\sin\left(-z\frac{|b_z|}{K}\right) =$$
$$x_0\cos(\omega z) - \frac{p_{x,0}}{b_z}\sin(\omega z)$$

$$p_x = \sqrt{2|b_z|J}\sin\left(\phi(0) + \left(-z\frac{|b_z|}{K}\right)\right) =$$
$$\sqrt{2|b_z|J}\sin\phi(0)\cos(\omega z) + |b_z|\sqrt{\frac{2J}{|b_z|}}\cos\phi(0)\sin\left(-z\frac{|b_z|}{K}\right) =$$
$$p_{x,0}\cos(\omega z) + b_z x_0\sin(\omega z)$$

These equations give us the map for the solenoid in $\mathbf{X}_{\text{new}}$. We can write this transformation in the form of a matrix

$$R := \begin{bmatrix} \cos(\omega z) & -\frac{\sin(\omega z)}{b_z} & 0 & 0 \\ b_z\sin(\omega z) & \cos(\omega z) & 0 & 0 \\ 0 & 0 & 1 & 0 \\ 0 & 0 & 0 & 1 \end{bmatrix},$$

and therefore the whole solenoid map in $\mathbf{X}$ as follows (let $S := \sin(\omega z)$ and $C := \cos(\omega z)$):

$$M := T^{-1}RT = \begin{bmatrix} \frac{C+1}{2} & \frac{S}{b_z} & \frac{S}{2} & \frac{1-C}{b_z} \\ -\frac{b_z S}{4} & \frac{C+1}{2} & \frac{b_z(C-1)}{4} & \frac{S}{2} \\ -\frac{S}{2} & \frac{C-1}{b_z} & \frac{C+1}{2} & \frac{S}{b_z} \\ \frac{b_z(1-C)}{4} & -\frac{S}{2} & -\frac{b_z S}{4} & \frac{C+1}{2} \end{bmatrix}$$

In the tracking procedure of Xtrack (and MAD-X) the map is implemented with respect to a different quantity `sk`, which we will denote with k, and which represents half of magnetic field strength b_z: $k = \frac{b_z}{2}$. Let $s := \sin(\frac{zk}{H}) = \sin(\frac{\omega z}{2})$ and $c := \cos(\frac{\omega z}{2})$; then we can rewrite M using the trigonometric identities:

$$\cos(2\theta) = 2\cos^2\theta - 1 = 1 - 2\sin^2\theta \implies c^2 = \frac{C+1}{2} \text{ and } s^2 = \frac{1-C}{2},$$
$$\sin(2\theta) = 2\cos\theta\sin\theta \implies sc = \frac{S}{2},$$

as the following transfer matrix

$$M = \begin{bmatrix} c^2 & \frac{cs}{k} & cs & \frac{s^2}{k} \\ -kcs & c^2 & -ks^2 & cs \\ -cs & -\frac{s^2}{k} & c^2 & \frac{cs}{k} \\ ks^2 & -cs & -kcs & c^2 \end{bmatrix},$$

which, with relatively little effort, can be verified to correspond to the implementation of the tracking procedure. We have the following map (note the change in ζ is analogous to the drift):

$$\begin{aligned} x &\leftarrow (x\cos(\theta) + y\sin(\theta))\cos(\theta) + \frac{2}{b_z}\left(p_x\cos(\theta) + p_y\sin(\theta)\right)\sin(\theta) \\ p_x &\leftarrow -\frac{1}{2}(x\cos(\theta) + y\sin(\theta))b_z\sin(\theta) + \left(p_x\cos(\theta) + p_y\sin(\theta)\right)\cos(\theta) \\ y &\leftarrow (y\cos(\theta) - x\sin(\theta))\cos(\theta) + \frac{2}{b_z}\left(p_y\cos(\theta) - p_x\sin(\theta)\right)\sin(\theta) \\ p_y &\leftarrow -\frac{1}{2}(y\cos(\theta) - x\sin(\theta))b_z\sin(\theta) + \left(p_y\cos(\theta) - p_x\sin(\theta)\right)\cos(\theta) \\ \zeta &\leftarrow \zeta + L\left(1 - \frac{\beta_0}{\beta}\frac{1+\delta}{p_z}\right), \end{aligned}$$

where $p_z := \sqrt{(\delta+1)^2 - \left(\frac{b_z}{2}x - p_y\right)^2 - \left(\frac{b_z}{2}y + p_x\right)^2}$, $\theta := \frac{b_z L}{2p_z}$, and L is the length of the thick solenoid.

1.5.8 AC-dipole

The excitation amplitude of the AC-dipole is denoted by A [Tm], the excitation frequency by q_d [2π] and the phase of the excitation by ϕ. The map presented here is for a purely horizontal dipole, the map for a vertical dipole is obtained by replacing $p_x \to p_y$.
The effect of the AC-dipole is split into four stages. The turn number is denoted by n.

1. A number of free turns n_{free}, in which the AC-dipole has no effect on the motion.
2. Ramp-up of the voltage from 0 to the excitation amplitude A for $n_{\text{ramp-up}}$ turns.

$$\begin{aligned} n' &= \frac{n - n_{\text{free}}}{n_{\text{ramp-up}}} \\ p_x &\to p_x + n' \cdot \frac{A}{pc} \cdot (1+\delta)\sin\left(2\pi q_d \cdot (n - n_{\text{free}}) + \phi\right) \end{aligned}$$

3. Constant excitation amplitude for n_{flat} turns.

$$p_x \to p_x + \frac{A}{pc} \cdot (1+\delta)\sin\left(2\pi q_d \cdot (n - n_{\text{free}}) + \phi\right)$$

4. Ramp-down of the voltage from the excitation amplitude A to 0 for $n_{\text{ramp-down}}$ turns.

$$n' = \frac{n - n_{\text{free}} - n_{\text{ramp-up}} - n_{\text{flat}} - n_{\text{ramp-down}}}{n_{\text{ramp-down}}}$$

$$p_x \to p_x + n' \cdot \frac{A}{p} \cdot (1+\delta) \sin\left(2\pi q_d \cdot (n - n_{\text{free}}) + \phi\right)$$

1.5.9 Wire

For each part we define $p_z = \sqrt{(1+\delta)^2 - x'^2 - y'^2}$, using the current values for x' and y'.
Step 1. Initial backwards drift of length $L = \frac{embl}{2}$.

$$x \to x - L \cdot \frac{x'}{p_z}$$

$$y \to y - L \cdot \frac{y'}{p_z}$$

Step 2.

$$y \to y - \frac{x \cdot \sin(t_x)}{\cos\left(\arctan\left(\frac{x'}{p_z}\right) - t_x\right)} \cdot \frac{y'}{\sqrt{(1+\delta)^2 - y'^2}}$$

$$x \to x \cdot \left[\cos(t_x) - \sin(t_x) \cdot \tan\left(\arctan\left(\frac{x'}{p_z}\right) - t_x\right)\right]$$

$$x' \to \sqrt{(1+\delta)^2 - y'^2} \cdot \sin\left(\arctan\left(\frac{x'}{p_z}\right) - t_x\right)$$

$$x \to x - \frac{y \cdot \sin(t_y)}{\cos\left(\arctan\left(\frac{y'}{p_z}\right) - t_y\right)} \cdot \frac{x'}{\sqrt{(1+\delta)^2 - x'^2}}$$

$$y \to y \left[\cos(t_y) - \sin(t_y) \cdot \tan\left(\arctan\left(\frac{y'}{p_z}\right) - t_y\right)\right]$$

$$y' \to \sqrt{(1+\delta)^2 - x'^2} \sin\left(\arctan\left(\frac{y'}{p_z}\right) - t_y\right)$$

Step 3. Drift part of length $L = lin$.

$$x \to x + L \cdot \frac{x'}{p_z}$$

$$y \to y + L \cdot \frac{y'}{p_z}$$

Step 4. Here $x_i = x - r_x$ and $y = y - r_y$.

$$x' \to x' - \frac{\frac{cur \cdot 10^{-7}}{chi}}{x_i^2 + y_i^2} \cdot x_i \left[\sqrt{(lin+l)^2 + x_i^2 + y_i^2} - \sqrt{(lin-l)^2 + x_i^2 + y_i^2}\right]$$

$$y' \to y' - \frac{\frac{cur \cdot 10^{-7}}{chi}}{x_i^2 + y_i^2} \cdot y_i \left[\sqrt{(lin+l)^2 + x_i^2 + y_i^2} - \sqrt{(lin-l)^2 + x_i^2 + y_i^2}\right]$$

Step 5. Drift of length $L = leff - lin$.

$$x \to x + L\frac{x'}{p_z}$$
$$y \to y + L\frac{y'}{p_z}$$

Step 6.

$$x \to x - \frac{y \cdot \sin(-t_y)}{\cos\left(\arctan\left(\frac{y'}{p_z}\right) + t_y\right)} \cdot \frac{x'}{\sqrt{(1+\delta)^2 - x'^2}}$$
$$y \to y \cdot \left[\cos(-t_y) - \sin(-t_y) \cdot \tan\left(\arctan\left(\frac{y'}{p_z}\right) + t_y\right)\right]$$
$$y' \to \sqrt{(1+\delta)^2 - x'^2} \cdot \sin\left(\arctan\left(\frac{y'}{p_z}\right) + t_y\right)$$
$$y \to y - \frac{x \cdot \sin(-t_x)}{\cos\left(\arctan\left(\frac{x'}{p_z}\right) + t_x\right)} \cdot \frac{y'}{\sqrt{(1+\delta)^2 - y'^2}}$$
$$x \to x \left[\cos(-t_x) - \sin(-t_x) \cdot \tan\left(\arctan\left(\frac{x'}{p_z}\right) + t_x\right)\right]$$
$$x' \to \sqrt{(1+\delta)^2 - y'^2} \cdot \sin\left(\arctan\left(\frac{x'}{p_z}\right) + t_x\right)$$

Step 7. Shift.

$$x \to x + embl \cdot \tan(t_x)$$
$$y \to y + embl \cdot \frac{\tan(t_y)}{\cos(t_x)}$$

Step 8. Negative drift of length $L = \frac{embl}{2}$.

$$x \to x - L \cdot \frac{x'}{p_z}$$
$$y \to y - L \cdot \frac{y'}{p_z}$$

1.5.10 Misalignment

Misalignments of elements affects the coordinates at the entrance of an element as follows

$$x \to (x - x_s) \cdot t_c + (y - y_s) \cdot t_s$$
$$y \to -(x - x_s) \cdot t_s + (y - y_s) \cdot t_c,$$

where x_s and y_s are the displacements in the horizontal and vertical directions, respectively. t_c and t_s are the cosine and sine of the tilt angle for the element.

1.5.11 Electron Lens

1.5.11.1 Hollow electron lens - uniform annular profile

For a uniform distribution of the electron beam between R_1 and R_2, the radial kick can be described by a shape function $f(r)$ and a maximum kick strength $\theta_{\max}$:

$$\theta(r) = \frac{f(r)}{(r/R_2)} \cdot \theta_{\max} \tag{1.167}$$

with $r = \sqrt{x^2 + y^2}$ and $\theta_{\max}$ independent of r. The shape function $f(r)$ is defined as

$$f(r) = \frac{I(r)}{I_T} = \frac{2\pi}{I_T} \int_0^r r\rho(r)dr \tag{1.168}$$

where I_T is the total electron beam current, $I(r)$ is the current enclosed in a radius r and $\rho(r)$ is the electron beam density distribution.
For a uniform profile one then obtains:

$$\begin{cases} 0 & , \quad r < R_1 \\ \frac{r^2 - R_1^2}{R_2^2 - R_1^2} & , \quad R_1 \leq r < R_2 \\ 1 & , \quad R_2 \leq r \end{cases} \tag{1.169}$$

and

$$\theta_{\max} = \theta(R_2) = \frac{2LI_T(1 \pm \beta_e\beta_p)}{4\pi\epsilon_0 \left(B\rho\right)_p \beta_e\beta_p c^2} \cdot \frac{1}{R_2} \tag{1.170}$$

where L is the length of the e-lens, I_T the total electron beam current, $\beta_{e/p}$ the relativistic β of electron/proton beam, $B\rho$ the magnetic rigidity, c the speed of light and ϵ_0 the vacuum permittivity. The $\pm$-sign represents the two cases of the electron beam traveling in the direction of the proton beam $(+)$ or in the opposite direction $(-)$. For hollow electron beam collimation, electron and proton beam travel in the same direction.
The kick in (x', y') can then be expressed as (note $\frac{x}{r} = \cos(\phi)$, $\frac{y}{r} = \sin(\phi)$):

$$x' = x' - \theta_{\max} \cdot \frac{r_2}{r^2} \cdot f(r) \cdot x \tag{1.171}$$

$$y' = y' - \theta_{\max} \cdot \frac{r_2}{r^2} \cdot f(r) \cdot y \tag{1.172}$$

If the electron lens is offset by $(x_{\text{offset}}, y_{\text{offset}})$, the coordinates (x, y) are simply transfered to:

$$\tilde{x} = x + x_{\text{offset}} \tag{1.173}$$

$$\tilde{y} = y + y_{\text{offset}} \tag{1.174}$$

$$\tilde{r} = \sqrt{\tilde{x}^2 + \tilde{y}^2} \tag{1.175}$$

and the kick is then given by:

$$x' = x' - \theta_{\max} \cdot \frac{r_2}{\tilde{r}^2} \cdot f(\tilde{r}) \cdot \tilde{x} \tag{1.176}$$

$$y' = y' - \theta_{\max} \cdot \frac{r_2}{\tilde{r}^2} \cdot f(\tilde{r}) \cdot \tilde{y} \tag{1.177}$$

1.5.12 Electron Cooler

Electron cooling is a process used to reduce the momentum spread of charged particles such as ions or protons. This process involves passing the particles through a cloud of electrons that are cooler than the particles themselves. The particles lose energy as they collide with the electrons, causing them to slow down and reduce their temperature. The Parkhomchuk model is a mathematical model that describes the force acting on a particle as it passes through the electron cooler. This force is given by the equation [**?**]:

$$\mathbf{F} = -\frac{4e^4 n_{\mathrm{e}}}{m_e} \frac{\mathbf{V}}{\left(\sqrt{\mathbf{V}^2 + V_{\mathrm{eff}}^2}\right)^3} \ln\left(\frac{\rho_{\mathrm{min}} + \rho_{\mathrm{max}} + \rho_{\mathrm{L}}}{\rho_{\mathrm{min}} + \rho_{\mathrm{L}}}\right) \tag{1.178}$$

Where **F** is the force acting on the ion when the ion is within the radius of the electron beam, e is the elementary charge, n_{e} is the density of the electrons, m_e is the electron mass, and **V** is the velocity difference between the ion and the electron. V_{eff} is the effective root-mean-square velocity of motion of Larmor circles, which is influenced by both the longitudinal root-mean-square electron velocity, $\mathrm{V_l}$, and transverse drift motions, which arise due to imperfections in the magnetic field. In particular, the transverse motion is described by $\mathrm{V_{magnet}}$, which shows how the root-mean-square electron velocity is affected by the quality of the magnetic field. The magnetic field quality is given by the ratio of the perpendicular and longitudinal components of the magnetic field, where 0 indicates an ideal magnetic field quality. The expression for $\mathrm{V_{magnet}}$ depends on the magnetic field quality in the following way: $\mathrm{V_{magnet}} = \beta_0 \gamma_0 c B_{ratio}$, where B_{ratio} is the magnetic field quality. Where c is the speed of light, β_0 is the velocity of the electrons, γ_0 is the relativistic factor, and B_{ratio} is the magnetic field quality. These two parameters combine in the following way to produce the effective electron velocity:

$$\mathrm{V_{eff}} = \sqrt{\mathrm{Ve_l^2} + \mathrm{Ve_{magnet}^2}}$$

The variables ρ_{min} and ρ_{max} are the minimum and maximum impact parameters and are defined as:

$$\rho_{min} = \frac{Z r_e}{(V/c)^2}$$

where Z is the charge of the particle, r_e is the classical electron radius.

$$\rho_{max} = \frac{V}{\omega_{plasma} + \frac{1}{\tau}}$$

Where ω_{plasma} is the plasma frequency, which is given by $c\sqrt{4\pi n_e r_e}$ and τ is the time that the ion spends in the cooler. Finally, ρ_{L} is the Larmor radius of the electrons, which is given by:

$$\rho_{\mathrm{L}} = \frac{m_e \cdot Ve_{\perp}}{e \cdot B}$$

Where m_e is the mass of the electron, B is the magnetic field strength, and $Ve_{\perp}$ is the perpendicular component of the electron velocity.

1.5.12.1 Electron beam space charge

An additional effect of electron cooling that needs to be taken into consideration is the space charge of the electron beam. Moreover, the electron beam will assume a parabolic profile with respect to the radius, which is given by [**?**]:

$$\frac{\Delta E(r)}{E_0} = \frac{I r_e}{ec} \frac{\gamma + 1}{\beta_0^3 \gamma^2} \left(\frac{r}{r_0} \right)^2 \approx 1.2 \times 10^{-4} \frac{I}{\beta_0^3} \left(\frac{r}{r_{e-beam}} \right)^2 \tag{1.179}$$

Equation 1.179 says that the electrons at the edge electron beam have a larger momentum than the electrons at the center. This means that the ions at the edge of the beam pipe will reach a larger equilibrium momentum than the ions at the core because the ions will assume the momentum of the electrons.
The Xsuite electron cooler allows for the inclusion of an optional effect called "space charge neutralization," which is determined by the parameter "Neutralization space charge." A value of 0 for this parameter indicates that there is no space charge in the electron beam, while a value of 1 indicates that the electron beam will follow a parabolic profile as described in Equation 1.179.

1.5.12.2 Electron beam rotation

An additional effect is the rotation of the electron beam around the beam axis due to the magnetic field of the electron cooler. The angular velocity of the rotation is given by [**?**]:

$$\omega = \frac{\mathbf{F} \times \mathbf{B}}{er|B|^2} = \frac{I}{2\pi\epsilon_0 c r_{\text{e- beam}}^2 \beta\gamma^2 B_\parallel} \approx 60 \frac{I}{r_{\text{e-beam}}^2 \beta\gamma^2 B_\parallel} \tag{1.180}$$

The inclusion of this effect in the Xsuite electron cooler is optional and determined by the parameter "Neutralization rotation." A value of 0 indicates that there is no rotation of the electron beam, while a value of 1 indicates that the electron beam will rotate with the angular frequency described in Equation 1.180.

Chapter 2

Linear optics calculations

Optics calculation are needed to study the motion around the closed orbit. By defining z as the vector of $2k$ coordinates,

$$z = (z_1, \ldots, z_{2k})^T = (x - x_0, p_x - p_{x0}, y - y_0, p_y - p_{y0}, \tau - \tau_0, p_\tau - p_{\tau 0})^T \tag{2.1}$$

one can define linear transfer maps (e.g. $M_{1\to 2}$ that propagates coordinates between two points s_1, s_2) and the one-turn map (e.g. M_1 that combines the effects for one turn starting from s_1):

$$z(s_2) = M_{1\to 2} z(s_1) \qquad\qquad z(C + s_1) = M_1 z(s_1). \tag{2.2}$$

In the following we will describe the optics calculation based on the Ripken formalism described in [10]. A good summary is also given in the MAD8 physics manual [11].

2.1 Diagonalisation of one-turn matrix

Since the matrices derive from symplectic maps, the eigenvalue spectrum of the one-turn map M consists of $2k$ distinct eigenvalues and linearly independent eigenvectors. In addition, for the motion to be stable the eigenvalues $\lambda_k^\pm$ with eigenvectors $v_k^\pm$ have to be complex [10]:

$$M v_k^\pm = \lambda_k^\pm v_k^\pm,\ k = 1, \ldots, 3 \tag{2.3}$$

$$v_k^+ = (v_k^-)^*, \quad \lambda_k^+ = (\lambda_k^-)^*, \quad |\lambda_k^\pm| = 1 \tag{2.4}$$

As the eigenvectors are linearly independent M can be diagonalized with

$$M = V \Lambda V^{-1}, \tag{2.5}$$

where V consists of the eigenvectors and Λ of the eigenvalues:

$$V = \begin{pmatrix} v_{1,1}^+ & v_{1,1}^- & \cdots & v_{3,1}^- \\ v_{1,2}^+ & v_{1,2}^- & \cdots & v_{3,2}^- \\ \vdots & \vdots & \vdots & \vdots \end{pmatrix} \qquad \Lambda = \begin{pmatrix} \lambda_1^+ & & & \\ & \lambda_1^- & & \\ & & \ddots & \\ & & & \lambda_3^- \end{pmatrix} \tag{2.6}$$

for which $v^{\pm}_{i,j}$ is the component j of eigenvector $v^{\pm}_i$.
The same calculation can be carried out with real numbers by the following definitions:

$$v^{\pm}_k = a_k \pm i b_k, \qquad \lambda^{\pm}_k = \cos\mu_k \pm i \sin\mu_k, \qquad \mu_k, a_k, b_k \in \mathbb{R} \tag{2.7}$$

such that:

$$M = WRW^{-1} \tag{2.8}$$

with

$$R = R(\mu_k) = \begin{pmatrix} \cos\mu_1 & \sin\mu_1 & & & & \\ -\sin\mu_1 & \cos\mu_1 & & & & \\ & & \ddots & & & \\ & & & \cos\mu_3 & \sin\mu_3 & \\ & & & -\sin\mu_3 & \cos\mu_3 & \end{pmatrix}, \tag{2.9}$$

$$W = \begin{pmatrix} a_{1,1} & b_{1,1} & \cdots & a_{3,1} & b_{3,1} \\ a_{1,2} & b_{1,2} & \cdots & a_{3,2} & b_{3,2} \\ \vdots & \vdots & \vdots & \vdots & \\ a_{1,6} & b_{1,6} & \cdots & a_{3,6} & b_{3,6} \end{pmatrix} \tag{2.10}$$

Usually μ_k is written as $\mu_k = 2\pi Q_k$, where Q_k is then the tune of the mode k.

2.2 Normalisation of eigenvectors

By convention, the eigenvectors and values are normalized, sorted and rotated so that the following three conditions are fulfilled:

1. Plane 1 is associated with the horizontal, plane 2 with the vertical and plane 3 with the longitudinal plane. This is achieved by first normalizing the eigenvectors $v^{\pm}_k$ and then sorting them so that:

$$|v^{+}_{j,2j-1}| = |v^{-}_{j,2j-1}| = \max_{k=1,2,3} v_{k,j}, \quad j = 1,\ldots,3 \tag{2.11}$$

2. The eigenvectors are then rotated with a phase term ψ_k

$$v_k \to v_k \exp(i\psi_k) \tag{2.12}$$

such that

$$\text{angle}(v^{+}_{k,2k-1}) = 0 \leftrightarrow \psi_k = -\text{angle}(v^{+}_{k,2k-1}) \tag{2.13}$$

In real space, Eqn. 2.11 and 2.13 then become equivalent to:

$$|a_{j,2j-1}| = \max_{k=1,2,3} |a_{k,j}|, \qquad b_{j,2j-1} = 0, \qquad j = 1,\ldots,3 \tag{2.14}$$

This has the effect that a particle with $x = 0$ is transformed to $\tilde{x}$ in the normalized phase space.

3. The sign of $b_{k,j}$ is fixed by the symplectic condition on W

$$W^T S W = S \tag{2.15}$$

with S defined as

$$S = \begin{pmatrix} 0 & 1 & \\ -1 & 0 & \\ & & \ddots \end{pmatrix} \tag{2.16}$$

which is equivalent to:

$$\begin{aligned} &a_k^T \cdot S \cdot b_k = 1, \quad b_k^T \cdot S \cdot a_k = -1, && \text{for } k = l \\ &a_k^T \cdot S \cdot b_l = 0, && \text{for } k \neq l \\ &a_k^T \cdot S \cdot a_l = 0, \quad b_k^T \cdot S \cdot b_l = 0, && k, l = 1, \ldots, 3 \end{aligned} \tag{2.17}$$

Eqn. 2.17 yields that in phase space a_k is thus obtained by an anticlockwise rotation of b_k by $\pi/2$ and a scaling of its length with $|a_k| = \frac{1}{|b_k|}$.

2.3 Conversion to normalized coordinates

We will show in the following that in the normalized phase space the propagation of particle coordinates $z(s)$ from s_1 to s_2 is just a rotation by an angle ϕ_k in the $k = 1, \ldots, 3$ planes, while the amplitude I_k and initial phase $\phi_{k,0}$ stay constant, explicitly $z(s)$ is then given by:

$$z(s) = \sum_{k=1}^{3} \sqrt{2I_k} \left(a_k(s) \cos\left(\phi_{k,0} + \phi_k(s)\right) - b_k(s) \sin\left(\phi_{k,0} + \phi_k(s)\right) \right) \tag{2.18}$$

and

$$\begin{aligned} z(s_2) = W(s_2) R(\phi_k) W(s_1)^{-1} z(s_1), \\ \text{with } \phi_k = \phi_k(s_2) - \phi_k(s_1) \end{aligned} \tag{2.19}$$

This implies that one turn is simply a rotation by $\phi_k = 2\pi Q_k$ where Q_k is the tune of the mode k. In the transverse plane the tune ($Q_{I,II}$) is usually positive and the particles rotate clockwise, while in the longitudinal plane the tune (Q_{III}) is negative above γ_T leading to an anticlockwise rotation.
For the derivation the following steps are needed:

1. The effect of one turn on the normalized variable $\tilde{z}(s) = W^{-1}(s) z(s)$ is a rotation:

$$\tilde{z}(C + s) = W^{-1} z(s + C) \overset{\text{(Eqn.2.8)}}{=} W^{-1} W R W^{-1} z(s) = R \tilde{z}(s), \tag{2.20}$$

As M and R are symplectic also W is symplectic, and its inverse is thus given by $S^{-1}W^TS$, explicitly:

$$W^{-1} = \begin{pmatrix} b_{12} & -b_{11} & b_{14} & -b_{13} & b_{16} & -b_{15} \\ -a_{12} & a_{11} & -a_{14} & a_{13} & -a_{16} & a_{15} \\ b_{22} & -b_{21} & b_{24} & -b_{23} & b_{26} & -b_{25} \\ -a_{22} & a_{21} & -a_{24} & a_{23} & -a_{26} & a_{25} \\ b_{32} & -b_{31} & b_{34} & -b_{33} & b_{36} & -b_{35} \\ -a_{32} & a_{31} & -a_{34} & a_{33} & -a_{36} & a_{35} \end{pmatrix} \tag{2.21}$$

2. The one-turn map and W-matrix can be propagated from s_1 to s_2 by

$$M_2 = M_{1\to 2} M_1 M_{1\to 2}^{-1} \qquad\qquad W_2 = M_{1\to 2} W_1 \tag{2.22}$$

As Eqn. 2.20 represents a similarity transformation, the eigenvalues are thus independent of the position s and as the rotation matrix R consists of the eigenvalues of M, the angle of the rotation $\mu_k = 2\pi Q_k$ is thus also independent of s.

3. As Eqn. 2.8 represents a basis transformation from the standard $\mathbb{R}^2$ basis to the eigenvector basis, the vectors a_k and b_k are projected onto (Eqn. 2.17):

$$\begin{aligned} \tilde{a}_1 = W^{-1}a_1 &= -SW^TSa_1 \\ &= -S(a_1Sa_1, b_1Sa_1, \ldots, b_3Sa_1)^T = (1,0,\ldots,0) \\ \tilde{b}_1 = W^{-1}b_1 &= -SW^TSb_1 \\ &= -S(a_1Sb_1, b_1Sb_1, \ldots, b_3Sb_1)^T = (0,1,\ldots,0) \\ &\ldots \\ \tilde{b}_3 = W^{-1}b_3 &= -SW^TSb_3 \\ &= -S(a_1Sb_3, b_1Sb_3, \ldots, b_3Sb_3)^T = (0,0,\ldots,1) \end{aligned} \tag{2.23}$$

in the normalized phase space.

4. From Eqn. 2.20 it follows that the amplitude I_k and initial phase ϕ_{k0} of $\tilde{z} = W^{-1}z = (\tilde{z}_{a_1}, \tilde{z}_{b_1}, \ldots, \tilde{z}_{b_3})$

$$I_k = \frac{(\tilde{z}_{a_k})^2 + (\tilde{z}_{b_k})^2}{2}, \quad k = 1,\ldots,3 \tag{2.24}$$

$$\tan\phi_{k0} = -\frac{\tilde{z}_{b_k}}{\tilde{z}_{a_k}} \tag{2.25}$$

are constants of the motion. The initial phase is defined with a minus sign in view of the definition of the Twiss parameters, where the initial phase is then

added (and not subtracted) to the phase advance. The components of $\tilde{z}$ are then explicitly given by:

$$\tilde{z}_{a_k} = \sum_{j=1}^{3} b_{k,2j} z_{2j-1} - b_{k,2j-1} z_{2j}, \quad k = 1, \ldots, 3 \tag{2.26}$$

$$\tilde{z}_{b_k} = \sum_{j=1}^{3} a_{k,2j-1} z_{2j} - a_{k,2j} z_{2j-1}, \quad k = 1, \ldots, 3. \tag{2.27}$$

An arbitrary vector $z(s)$ can thus be written in the following form:

$$\begin{aligned} z(s) &= W(s)\tilde{z}(s) \\ &= W(s) \left(\sum_{k=1}^{3} \tilde{z}_{a_k} \tilde{a}_k + \tilde{z}_{b_k} \tilde{b}_k \right) \\ &= \sum_{k=1}^{3} \tilde{z}_{a_k} W(s) \tilde{a}_k + \tilde{z}_{b_k} W(s) \tilde{b}_k \overset{\text{Eqn. 2.23}}{=} \sum_{k=1}^{3} \tilde{z}_{a_k} a_k + \tilde{z}_{b_k} b_k \\ &\overset{\text{Eqns. 2.24,2.25}}{=} \sum_{k=1}^{3} \sqrt{2I_k} \left(a_k \cos \phi_{k0} - b_k \sin \phi_{k0} \right) \end{aligned} \tag{2.28}$$

2.4 Twiss parameters

In the following the parameter k will always be used for the mode k and the parameter $j = 1, 2, 3$ for the horizontal (x, p_x), vertical (y, p_y) and longitudinal plane (ζ, δ) in the phase space. z_{2j-1} then stands for the coordinates (x, y, ζ) and z_{2j} for $(p_{x,y}, \delta)$.
The Twiss parameters can be introduced by writing the components of the eigenvector basis $(a_k(s), b_k(s))$ as the product of two envelope functions $\sqrt{\beta_{k,j}(s)}$, $\sqrt{\gamma_{k,j}(s)}$ and phase functions $\phi_{k,j}(s)$, $\bar{\phi}_{k,j}(s) = \phi_{k,j}(s) - \arctan(1/\alpha_{k,j})$, also called Twiss parameters or lattice functions, with

$$\begin{aligned} a_{k,2j-1}(s) &= \sqrt{\beta_{k,j}(s)} \cos \phi_{k,j}(s), \\ b_{k,2j-1}(s) &= \sqrt{\beta_{k,j}(s)} \sin \phi_{k,j}(s), \; k, j = 1, \ldots, 3, \end{aligned} \tag{2.29}$$

$$\begin{aligned} a_{k,2j}(s) &= \sqrt{\gamma_{k,j}(s)} \cos \bar{\phi}_{k,j}(s), \\ b_{k,2j}(s) &= \sqrt{\gamma_{k,j}(s)} \sin \bar{\phi}_{k,j}(s), \; k, j = 1, \ldots, 3 \end{aligned} \tag{2.30}$$

where $\beta_{k,j}(s), \alpha_{k,j}(s), \gamma_{k,j}(s)$ represent the projection of the ellipse of mode k on the plane of coordinates $z_{2k-1} - z_{2k}$.
Using Eqns. 2.18, 2.29, 2.30 and $\cos(x + y) = \cos x \cos y - \sin x \sin y$, the coordinates $z(s)$ can be expressed by:

$$z_{2j-1}(s) = \sum_{k=1}^{3} \sqrt{2I_k \beta_{k,j}(s)} \cos \left(\phi_{k,j}(s) + \phi_{k,0} \right) \tag{2.31}$$

$$z_{2j}(s) = \sum_{k=1}^{3} \sqrt{2I_k \gamma_{k,j}(s)} \cos \left(\bar{\phi}_{k,j}(s) + \phi_{k,0} \right), \; j = 1, \ldots, 3 \tag{2.32}$$

Conversely the lattice functions can also be expressed by a_k and b_k with

$$\beta_{k,j}(s) = a_{k,2j-1}(s)^2 + b_{k,2j-1}(s)^2 \tag{2.33}$$
$$\alpha_{k,j}(s) = -a_{k,2j-1}(s)a_{k,2j}(s) - b_{k,2j-1}(s)b_{k,2j}(s) \tag{2.34}$$
$$\gamma_{k,j}(s) = a_{k,2j}(s)^2 + b_{k,2j}(s)^2, \tag{2.35}$$

The well known relations between the lattice functions

$$\sum_{j=1}^{3} \beta_{k,j}\phi'_{k,j} = 1 \tag{2.36}$$
$$\gamma_{k,j} = \frac{\beta_{k,j}^2\phi_{k,j}'^2 + \alpha_{k,j}^2}{\beta_{k,j}}, \text{ with} \tag{2.37}$$
$$\alpha_{k,j} := -\frac{1}{2}\beta'_{k,j} \tag{2.38}$$

can then be derived with the help of the normalization condition (Eqn. 2.17)

$$a_k^T S b_k = 1 \tag{2.39}$$

by the following steps:

1. As $x' = \frac{dx}{ds}$, $y' = \frac{dy}{ds}$ and $\delta = \frac{d\zeta}{ds}$ the following relations hold also for a_k and b_k:

$$a_{k,2j} = a'_{k,2j-1} = \frac{d}{ds}(a_{k,2j-1}), \tag{2.40}$$
$$b_{k,2j} = b'_{k,2j-1} = \frac{d}{ds}(b_{k,2j-1}),\ k,j = 1,\ldots,3 \tag{2.41}$$

2. The normalization condition Eqn. 2.17 can then be written as

$$\begin{aligned} a_k^T S b_k &= \sum_{j=1}^{3} \sqrt{\beta_{k,j}}\cos\phi_{k,j}\left(\sqrt{\beta_{k,j}}\sin\phi_{k,j}\right)' \\ &\quad - \left(\sqrt{\beta_{k,j}}\cos\phi_{k,j}\right)'\sqrt{\beta_{k,j}}\sin\phi_{k,j} \\ &= \sum_{j=1}^{3} \beta_{k,j}\phi'_{k,j} \\ &= 1 \end{aligned} \tag{2.42}$$

Note that Eqn. 2.42 yields the the following relation between the phase advance ϕ and β in 2D:

$$\phi(s) = \phi(0) + \int_{s_0}^{s} \frac{1}{\beta(\bar{s})} d\bar{s} \tag{2.43}$$

3. Using the abbreviation $\alpha_{k,j} := -\frac{1}{2}\beta_{k,j}$, one finds for each mode k and plane j

$$\sqrt{\gamma_{k,j}}\cos\phi_{k,j} = a_{k,2j} = a'_{k,2j-1} = (\sqrt{\beta_{k,j}}\cos\phi_{k,j})' \quad (1)$$

$$\sqrt{\gamma_{k,j}}\sin\phi_{k,j} = b_{k,2j} = b'_{k,2j-1} = (\sqrt{\beta_{k,j}}\sin\phi_{k,j})' \quad (2)$$

$$\overset{(1)^2+(2)^2}{\Rightarrow} \gamma_{k,j} = \frac{\beta_{k,j}^2\phi_{k,j}'^2 + \alpha_{k,j}^2}{\beta_{k,j}}, \quad k,j = 1,\ldots,3 \tag{2.44}$$

which simplifies in the 2D case to:

$$\gamma \overset{\text{Eqn. 2.42}}{=} \frac{1+\alpha^2}{\beta} \tag{2.45}$$

2.5 Transformation to normalized coordinates

The W matrix can be used to transform normalized coordinate into physical coordinates and viceversa:

$$\begin{pmatrix} x \\ p_x \\ y \\ p_y \\ \zeta \\ p_\zeta \end{pmatrix} = W \begin{pmatrix} \hat{x} \\ \hat{p}_x \\ \hat{y} \\ \hat{p}_y \\ \hat{\zeta} \\ \hat{p}_\zeta \end{pmatrix} = W \begin{pmatrix} \sqrt{\varepsilon_x}\tilde{x} \\ \sqrt{\varepsilon_x}\tilde{p}_x \\ \sqrt{\varepsilon_y}\tilde{y} \\ \sqrt{\varepsilon_y}\tilde{p}_y \\ \sqrt{\varepsilon_\zeta}\tilde{\zeta} \\ \sqrt{\varepsilon_\zeta}\tilde{p}_\zeta \end{pmatrix} \tag{2.46}$$

where

$$\begin{pmatrix} \tilde{x} & \tilde{p}_x & \tilde{y} & \tilde{p}_y & \tilde{\zeta} & \tilde{p}_\zeta \end{pmatrix} \tag{2.47}$$

are normalized coordinates in sigmas and ε_x, ε_y and ε_ζ are the geometric emittances.

2.6 Action, amplitude and emittance

We define the action associated to the three modes:

$$J_x = \frac{\hat{x}^2 + \hat{p}_x^2}{2}, \quad J_y = \frac{\hat{y}^2 + \hat{p}_y^2}{2}, \quad J_\zeta = \frac{\hat{\zeta}^2 + \hat{p}_\zeta^2}{2} \tag{2.48}$$

The corresponding amplitudes are defined such that:

$$A_x = \sqrt{\hat{x}^2 + \hat{p}_x^2} = \sqrt{2J_x}, \tag{2.49}$$

$$A_y = \sqrt{\hat{y}^2 + \hat{p}_y^2} = \sqrt{2J_y} \tag{2.50}$$

$$A_\zeta = \sqrt{\hat{\zeta}^2 + \hat{p}_\zeta^2} = \sqrt{2J_\zeta} \tag{2.51}$$

A Gaussian distribution is defined such that the density with respect to each action can be written as:

$$f(J_x) = Ke^{J_x/\varepsilon_x} \tag{2.52}$$

where the emittance ε_x can be written as:

$$\varepsilon_x =< J_x >= \int J_x f(J_x)\, dJ_x \tag{2.53}$$

2.7 Dispersion and crab dispersion

For a particle having no betatron amplitude ($\hat{x} = \hat{p}_x = \hat{y} = \hat{p}_y = 0$) we can write:

$$x = W_{15}\hat{\zeta} + W_{16}\hat{p}_\zeta \tag{2.54}$$
$$\zeta = W_{55}\hat{\zeta} + W_{56}\hat{p}_\zeta \tag{2.55}$$
$$p_\zeta = W_{65}\hat{\zeta} + W_{66}\hat{p}_\zeta \tag{2.56}$$

2.7.1 Dispersion

The dispersion is:

$$D_x^{p_\zeta} = \frac{dx}{d\delta} \quad \text{for } \zeta = 0 \tag{2.57}$$

By imposing $\zeta = 0$ in Eq. 2.55 we obtain:

$$\hat{\zeta} = -\frac{W_{56}}{W_{55}}\hat{p}_\zeta \tag{2.58}$$

We replace in Eq. 2.56:

$$\hat{p}_\zeta = \left(W_{66} - \frac{W_{65}W_{56}}{W_{55}}\right)^{-1} p_\zeta \tag{2.59}$$

From Eq. 2.58 we obtain:

$$\hat{\zeta} = -\frac{W_{56}}{W_{55}}\left(W_{66} - \frac{W_{65}W_{56}}{W_{55}}\right)^{-1} p_\zeta \tag{2.60}$$

Replacing the last two into Eq. 2.54 we obtain:

$$x = \left(W_{16} - \frac{W_{15}W_{56}}{W_{55}}\right)\left(W_{66} - \frac{W_{65}W_{56}}{W_{55}}\right)^{-1} p_\zeta \tag{2.61}$$

which gives the dispersion:

$$D_x^{p_\zeta} = \left(W_{16} - \frac{W_{15}W_{56}}{W_{55}}\right)\left(W_{66} - \frac{W_{65}W_{56}}{W_{55}}\right)^{-1} \tag{2.62}$$

A similar type of calculation can be done for the other planes, and for the transverse momentum dispersion, obtaining $D_{px}^{p_\zeta}$: which gives the dispersion:

$$D_{px}^{p_\zeta} = \left(W_{26} - \frac{W_{25}W_{56}}{W_{55}}\right)\left(W_{66} - \frac{W_{65}W_{56}}{W_{55}}\right)^{-1} \tag{2.63}$$

$$D_{y}^{p_\zeta} = \left(W_{36} - \frac{W_{35}W_{56}}{W_{55}}\right)\left(W_{66} - \frac{W_{65}W_{56}}{W_{55}}\right)^{-1} \tag{2.64}$$

$$D_{py}^{p_\zeta} = \left(W_{46} - \frac{W_{45}W_{56}}{W_{55}}\right)\left(W_{66} - \frac{W_{65}W_{56}}{W_{55}}\right)^{-1} \tag{2.65}$$

2.7.2 Crab dispersion

The crab dispersion is:

$$D_x^\zeta = \frac{dx}{dz} \quad \text{for } p_\zeta = 0 \tag{2.66}$$

By imposing $p_\zeta = 0$ in Eq. 2.56 we obtain:

$$\hat{p}_\zeta = -\frac{W_{65}}{W_{66}}\hat{\zeta} \tag{2.67}$$

We replace in Eq. 2.55:

$$\hat{\zeta} = \left(W_{55} - \frac{W_{56}W_{65}}{W_{66}}\right)^{-1}\zeta \tag{2.68}$$

From Eq. 2.67 we obtain:

$$\hat{p}_\zeta = -\frac{W_{65}}{W_{66}}\left(W_{55} - \frac{W_{56}W_{65}}{W_{66}}\right)^{-1}\zeta \tag{2.69}$$

Replacing the last two into Eq. 2.54 we obtain:

$$x = \left(W_{15} - \frac{W_{16}W_{65}}{W_{66}}\right)\left(W_{55} - \frac{W_{56}W_{65}}{W_{66}}\right)^{-1}\zeta \tag{2.70}$$

which gives the crab dispersion:

$$D_x^\zeta = \left(W_{15} - \frac{W_{16}W_{65}}{W_{66}}\right)\left(W_{55} - \frac{W_{56}W_{65}}{W_{66}}\right)^{-1} \tag{2.71}$$

A similar type of calculation can be done for the other planes, and for transverse momentum crab dispersion obtaining:

$$D_{p_x}^\zeta = \left(W_{25} - \frac{W_{26}W_{65}}{W_{66}}\right)\left(W_{55} - \frac{W_{56}W_{65}}{W_{66}}\right)^{-1} \tag{2.72}$$

$$D_{y}^\zeta = \left(W_{35} - \frac{W_{36}W_{65}}{W_{66}}\right)\left(W_{55} - \frac{W_{56}W_{65}}{W_{66}}\right)^{-1} \tag{2.73}$$

$$D_{p_y}^\zeta = \left(W_{45} - \frac{W_{46}W_{65}}{W_{66}}\right)\left(W_{55} - \frac{W_{56}W_{65}}{W_{66}}\right)^{-1} \tag{2.74}$$

2.8 Linear betatron coupling

The following is based on [12] and [13].

In the presence of betatron coupling the transverse on-momentum motion can be written as:

$$\begin{cases} x_n = A_{1,x}\cos\left[2\pi Q_1(n-1)+\phi_{1,x}\right] + A_{2,x}\cos\left[2\pi Q_2(n-1)+\phi_{2,x}\right] \\ y_n = A_{1,y}\cos\left[2\pi Q_1(n-1)+\phi_{1,y}\right] + A_{2,y}\cos\left[2\pi Q_2(n-1)+\phi_{2,y}\right] \end{cases} \tag{2.75}$$

We can define:

$$\begin{cases} r_1 = \left|A_{1,y}\right| / \left|A_{1,x}\right| \\ r_2 = \left|A_{2,x}\right| / \left|A_{2,y}\right| \end{cases} \tag{2.76}$$

$$\begin{cases} \Delta\phi_1 = \phi_{1,y} - \phi_{1,x} \\ \Delta\phi_2 = \phi_{2,x} - \phi_{2,y} \end{cases} \tag{2.77}$$

These quantities can be obtained from the normalized W matrix as:

$$\begin{cases} r_1 = \sqrt{W_{31}^2 + W_{32}^2}/W_{11} \\ r_2 = \sqrt{W_{13}^2 + W_{14}^2}/W_{33} \end{cases} \tag{2.78}$$

$$\begin{cases} \Delta\phi_{1,0} = \arctan\left(W_{32}/W_{31}\right) \\ \Delta\phi_{2,0} = \arctan\left(W_{14}/W_{13}\right) \end{cases} \tag{2.79}$$

From these we can compute the following quantities as [13]:

$$\left|C^-\right| = \frac{2\sqrt{r_1 r_2}\left|Q_1 - Q_2\right|}{(1+r_1 r_2)} \tag{2.80}$$

$$\chi(s) = \Delta\phi_{1,0}(s) \tag{2.81}$$

$$C^-(s) = \left|C^-\right| e^{i\chi(s)} \tag{2.82}$$

where Q_1 and Q_2 are the tunes of the betatron eigenmodes. Note that only the phase of $C^-(s)$ is s dependent.
It is possible to prove that C^- is related to the skew quadrupole strengths along the ring by the following relation:

$$C^- = \left|C^-\right| e^{i\chi} = \frac{1}{2\pi}\int_0^L \sqrt{\beta_x\beta_y}\,k_s\,e^{i\left[\Phi_x - \Phi_y - 2\pi\Delta\cdot s/L\right]}dl. \tag{2.83}$$

where Δ is the difference of the unperturbed fractional tunes.
To have a more robust estimate, Eq. 2.80 is evaluated at all s positions and averaged over the ring, as suggested in [14].

Chapter 3

Synchrotron radiation

We collect here some relevant properties of synchrotron radiation [15]:
We assume $B = |B_\perp|$.
Classical particle radius:

$$r_0 = Q^2 / \left(4\pi\epsilon_0 m_0 c^2\right) \tag{3.1}$$

Curvature, rigidity, field:

$$\frac{1}{\rho} = \frac{QB}{p} = \frac{QB}{m_0 c \beta\gamma} \tag{3.2}$$

Emitted power:

$$P_\mathrm{s} = \frac{2 r_0 c^3 Q^2 \beta^2 \gamma^2 B^2}{3 m_0 c^2} \tag{3.3}$$

Critical frequency:

$$\omega_\mathrm{c} = \frac{3 Q \beta^2 \gamma^2 B}{2 m_0} \tag{3.4}$$

Critical energy:

$$E_{\gamma\mathrm{c}} = \hbar\omega_\mathrm{c} = \frac{3 Q \hbar \beta^2 \gamma^2 B}{2 m_0} \tag{3.5}$$

Number of photons per unit time:

$$\dot{n}_\mathrm{s} = \frac{15\sqrt{3}}{8} \frac{P_\mathrm{s}}{E_{\gamma\mathrm{c}}} = \frac{60\sqrt{3}}{72} \frac{r_0 c Q B}{\hbar} \tag{3.6}$$

Average photon energy:

$$\langle E_\gamma \rangle = \frac{8\sqrt{3}}{45} E_{\gamma\mathrm{c}} = \frac{8\sqrt{3}}{15} \frac{Q \hbar \beta^2 \gamma^2 B}{2 m_0} \tag{3.7}$$

Photon energy variance:

$$\left\langle E_\gamma^2 \right\rangle = \frac{11}{27} E_{\gamma\mathrm{c}}^2 = \frac{11}{12} \frac{Q^2 \hbar^2 \beta^4 \gamma^4 B^2}{m_0^2} \tag{3.8}$$

$$\left\langle \dot{n}_s \Delta\delta^2 \right\rangle = \frac{\left\langle \dot{n}_s E_\gamma^2 \right\rangle}{E_0^2} = \frac{11}{12}\frac{1}{m_0^2 c^4 \gamma_0^2}\frac{Q^2\hbar^2\beta^4\gamma^4 B^2}{m_0^2}\frac{60\sqrt{3}}{72}\frac{cQB}{\hbar}\frac{Q^2}{4\pi\epsilon_0 m_0 c^2} \tag{3.9}$$

The algorithm to generate photon energies with the appropriate distribution in described in [16].

3.1 Damping from synchrotron radiation

The damping constants from synchrotron radiation can be easily obtained from magnitude of the eigenvalues of the one-turn matrix:

$$\alpha_x = -\log(|\lambda_x|) \tag{3.10}$$
$$\alpha_y = -\log(|\lambda_y|) \tag{3.11}$$
$$\alpha_\zeta = -\log(|\lambda_\zeta|) \tag{3.12}$$

The damping acts such that:

$$\frac{1}{A_x}\frac{dA_x}{dt} = -\frac{\alpha_x}{T_0} \tag{3.13}$$

where T_0 is the revolution period. From Eq. 2.49 we obtain:

$$\frac{dJ_x}{dt} = -\frac{2\alpha_x}{T_0}J_x \tag{3.14}$$

By averaging over the beam distribution we obtain:

$$\frac{d\varepsilon_x}{dt} = -\frac{2\alpha_x}{T_0}\varepsilon_x \tag{3.15}$$

3.2 Equilibrium emittance

This section is based on the approach described in [17].
To account for the kicks experienced by the particles due to quantum excitation we note that the transverse momentum change due to an energy kick in the direction of the particle motion can be written as:

$$P_{x,y}^{\text{new}} = P_{x,y}^{\text{old}}\frac{P^{\text{new}}}{P^{\text{old}}} \tag{3.16}$$

From this:

$$P_{x,y}^{\text{new}} - P_{x,y}^{\text{old}} = P_{x,y}^{\text{old}}\left(\frac{P^{\text{new}} - P^{\text{old}}}{P^{\text{old}}}\right) \tag{3.17}$$

Dividing by P_0:

$$\frac{P_{x,y}^{\text{new}} - P_{x,y}^{\text{old}}}{P_0} = \frac{P_{x,y}^{\text{old}}}{P_0}\left(\frac{P^{\text{new}} - P^{\text{old}}}{P_0}\right)\frac{P_0}{P^{\text{old}}} \tag{3.18}$$

Using the accelerator coordinates definitions (Eqs. 1.13 and 1.14), we obtain:

$$\Delta p_{x,y} = \frac{p_{x,y}}{1+\delta}\Delta\delta \tag{3.19}$$

The corresponding change in normalized coordinates can be computed from Eq. 3.20:

$$\begin{pmatrix} \Delta\tilde{x} \\ \Delta\tilde{p}_x \\ \Delta\tilde{y} \\ \Delta\tilde{p}_y \\ \Delta\tilde{\zeta} \\ \Delta\tilde{p}_\zeta \end{pmatrix} = W^{-1} \begin{pmatrix} 0 \\ \frac{p_x}{1+\delta}\Delta\delta \\ 0 \\ \frac{p_y}{1+\delta}\Delta\delta \\ 0 \\ \Delta\delta \end{pmatrix} \tag{3.20}$$

Using the Eq. 2.21 we obtain:

$$\Delta\hat{x} = \mathcal{K}_x\Delta\delta \tag{3.21}$$
$$\Delta\hat{p}_x = \mathcal{K}_{p_x}\Delta\delta \tag{3.22}$$
$$\Delta\hat{y} = \mathcal{K}_y\Delta\delta \tag{3.23}$$
$$\Delta\hat{p}_y = \mathcal{K}_{p_y}\Delta\delta \tag{3.24}$$
$$\Delta\hat{\zeta} = \mathcal{K}_\zeta\Delta\delta \tag{3.25}$$
$$\Delta\hat{p}_\zeta = \mathcal{K}_{p_\zeta}\Delta\delta \tag{3.26}$$

where:

$$\mathcal{K}_x = \left(\frac{a_{11}p_x + a_{13}p_y}{1+\delta} + a_{15}\right) \tag{3.27}$$
$$\mathcal{K}_{p_x} = \left(\frac{b_{11}p_x + b_{13}p_y}{1+\delta} + b_{15}\right) \tag{3.28}$$
$$\mathcal{K}_y = \left(\frac{a_{21}p_x + a_{23}p_y}{1+\delta} + a_{25}\right) \tag{3.29}$$
$$\mathcal{K}_{p_y} = \left(\frac{b_{21}p_x + b_{23}p_y}{1+\delta} + b_{25}\right) \tag{3.30}$$
$$\mathcal{K}_\zeta = \left(\frac{a_{31}p_x + a_{33}p_y}{1+\delta} + a_{35}\right) \tag{3.31}$$
$$\mathcal{K}_{p_\zeta} = \left(\frac{b_{31}p_x + b_{33}p_y}{1+\delta} + b_{35}\right) \tag{3.32}$$

The change in action (see Eq. 2.48) associated to the first mode, due to the emission of

a photon can be written as:

$$\Delta J_x = \frac{1}{2}\left[(\hat{x}+\Delta\hat{x})^2\,(\hat{p}_x+\Delta\hat{p}_x)^2 - \hat{x}^2 - \hat{p}_x^2\right] \tag{3.33}$$

$$= \frac{1}{2}\left[\Delta\hat{x}^2 + \Delta\hat{p}_x^2 + 2\hat{x}\Delta\hat{x} + 2\hat{p}_x\Delta\hat{p}_x\right] \tag{3.34}$$

Averaging over all particles in the beam we obtain:

$$\Delta\varepsilon_x = <\Delta J_x> = \frac{1}{2}\left(<\Delta\hat{x}^2> + <\Delta\hat{p}_x^2>\right) \tag{3.35}$$

Using Eqs. 3.21 and 3.22 we obtain:

$$\Delta\varepsilon_x = <\Delta J_x> = \frac{1}{2}\left(\mathcal{K}_x^2 + \mathcal{K}_{p_x}^2\right) <\Delta\delta^2> \tag{3.36}$$

Assuming that the kicks are uncorrelated we can obtain the emittance growth rate from quantum excitation integrating over a full turn:

$$\left(\frac{d\varepsilon_x}{dt}\right)_{\text{quant}} = \frac{1}{2T_0c}\int_0^C \left(\mathcal{K}_x^2 + \mathcal{K}_{p_x}^2\right) <\dot{N}\Delta\delta^2>\, ds \tag{3.37}$$

where $\dot{N}$ is the photon emission rate (number of photons per unit time), T_0 is the revolution period, C is the circumference.
By summing Eqs. 3.15 and 3.37 we obtain the total instantaneous growth rate:

$$\frac{d\varepsilon_x}{dt} = \left(\frac{d\varepsilon_x}{dt}\right)_{\text{damp}} + \left(\frac{d\varepsilon_x}{dt}\right)_{\text{quant}} = -\frac{2\alpha_x}{T_0}\varepsilon_x + \frac{1}{2T_0c}\int_0^C \left(\mathcal{K}_x^2 + \mathcal{K}_{p_x}^2\right) <\dot{N}\Delta\delta^2>\, ds \tag{3.38}$$

By imposing the derivative to be zero we obtain the value of the equilibrium emittance:

$$\varepsilon_x = \frac{1}{4\alpha_x c}\int_0^C \left(\mathcal{K}_x^2 + \mathcal{K}_{p_x}^2\right) <\dot{N}\Delta\delta^2>\, ds \tag{3.39}$$

In the ultra-relativistic approximation:

$$<\dot{N}\Delta\delta^2> = \frac{<\dot{N}(\Delta E)^2>}{E_0^2} \tag{3.40}$$

Chapter 4

Synchrotron motion

We collect here some relevant properties and quantities of the longitudinal particle motion.
Definition of momentum compaction factor:

$$\alpha_c = \frac{\Delta C/C}{\delta} \tag{4.1}$$

Slip factor:

$$\eta = -\frac{\Delta f/f_0}{\delta} = \alpha_c - \frac{1}{\gamma_0^2} = \frac{1}{\gamma_t^2} - \frac{1}{\gamma_0^2} \tag{4.2}$$

(positive above transition)
Slippage over a single turn:

$$\Delta\zeta = -\beta_0 c\Delta T = -\beta_0 c(T - T_0) = -\beta_0 c\left(\frac{1}{f} - \frac{1}{f_0}\right) \tag{4.3}$$

$$= -\frac{\beta_0 c}{f_0}\left(\frac{1}{1+\Delta f/f_0} - 1\right) \simeq \frac{\beta_0 c}{f_0}\frac{\Delta f}{f_0} = -\eta\frac{\beta_0 c}{f_0}\delta = -\eta C\delta \tag{4.4}$$

RF kick

$$\Delta E = qV_{RF}\sin\left(2\pi h_{RF} f_0 t + \phi_{RF}\right) \tag{4.5}$$

$$= qV_{RF}\sin\left(-2\pi h_{RF}\frac{\zeta}{C} + \phi_{RF}\right) \tag{4.6}$$

$$= qV_{RF}\sin\left(-2\pi f_{RF}\frac{\zeta}{\beta_0 c} + \phi_{RF}\right) \tag{4.7}$$

from which:

$$\Delta p_\zeta = \frac{\Delta E}{\beta_0^2 E_0} = \frac{qV_{RF}}{\beta_0^2 E_0}\sin\left(-2\pi f_{RF}\frac{\zeta}{\beta_0 c} + \phi_{RF}\right) \tag{4.8}$$

4.1 Linearized motion

We expand around the fixed point ζ_0:

$$\Delta p_\zeta \approx \frac{qV_{RF}}{\beta_0^2 E_0} \sin\left(-2\pi f_{RF}\frac{\zeta_0}{\beta_0 c} + \phi_{RF}\right) - \frac{2\pi q f_{RF} V_{RF}}{\beta_0^3 E_0 c}(\zeta - \zeta_0)\cos\left(-2\pi f_{RF}\frac{\zeta_0}{\beta_0 c} + \phi_{RF}\right) \tag{4.9}$$

We call synchronous phase:

$$\phi_s = -2\pi f_{RF}\frac{\zeta_0}{\beta_0 c} + \phi_{RF} \tag{4.10}$$

And we call

$$\hat{\zeta} = \zeta - \zeta_0 \tag{4.11}$$

obtaining:

$$\Delta p_\zeta \approx \frac{qV_{RF}}{\beta_0^2 E_0}\sin\phi_s - \frac{2\pi q f_{RF} V_{RF}}{\beta_0^3 E_0 c}\hat{\zeta}\cos\phi_s \tag{4.12}$$

We assume that that the energy deviation of the stable fixed point is zero:

$$\Delta p_\zeta \approx -\frac{2\pi q f_{RF} V_{RF}}{\beta_0^3 E_0 c}\cos\phi_s\hat{\zeta} \tag{4.13}$$

4.2 Smooth approximation

Assuming that the slippage and the energy kicks are uniformly distributed along the ring we have:

$$\frac{dp_\zeta}{ds} = \frac{\Delta p_\zeta}{C} = -\frac{2\pi q V_{RF}}{\beta_0^3 C E_0 c}\cos\phi_s\hat{\zeta} \tag{4.14}$$

$$\frac{d\hat{\zeta}}{ds} = \frac{\Delta\zeta}{C} = -\eta p_\zeta \tag{4.15}$$

where we have used the approximation:

$$\delta \ll 1 \Rightarrow \delta \simeq p_\zeta \tag{4.16}$$

We derive the second equation and replace the first:

$$\frac{d^2\hat{\zeta}}{ds^2} - \frac{2\pi q\eta f_{RF} V_{RF}}{\beta_0^3 C E_0 c}\cos\phi_s\hat{\zeta} = 0 \tag{4.17}$$

The motion is stable if

$$\eta\cos\phi_s < 0 \tag{4.18}$$

In that case the solution is in the form:

$$\hat{\zeta}(s) = A \sin\left(\sqrt{-\frac{2\pi q\eta f_{RF} V_{RF}}{\beta_0^3 C E_0 c}\cos\phi_s}\, s + B\right) = A\sin\left(2\pi Q_s s/C + B\right) \tag{4.19}$$

where the synchrotron tune is given by:

$$Q_s = \sqrt{-\frac{2\pi q\eta f_{RF} V_{RF}}{\beta_0^3 C E_0 c}\cos\phi_s}\,\frac{C}{2\pi} = \sqrt{-\frac{q\eta f_{RF} C V_{RF}}{2\pi\beta_0^3 E_0 c}\cos\phi_s} \tag{4.20}$$

We replace

$$f_{RF} = \frac{h_{RF}\beta_0 c}{C} \tag{4.21}$$

obtaining:

$$Q_s = \sqrt{-\frac{q\eta h_{RF} V_{RF}}{2\pi\beta_0^2 E_0}\cos\phi_s} \tag{4.22}$$

The solution can be written as:

$$\hat{\zeta}(s) = \hat{\zeta}_A \cos\left(2\pi Q_s s/C\right) + B\sin\left(2\pi Q_s s/C\right) \tag{4.23}$$

Replacing in Eq. 4.15:

$$p_\zeta = -\frac{2\pi Q_s}{\eta C}\left(-\zeta_A \sin\left(2\pi Q_s s/C\right) + B\cos\left(2\pi Q_s s/C\right)\right) \tag{4.24}$$

Replacing $s = 0$:

$$p_{\zeta_A} = -\frac{2\pi Q_s}{\eta C} B \tag{4.25}$$

from which:

$$B = -\frac{\eta C}{2\pi Q_s} p_{\zeta_A} = -\beta_\zeta p_{\zeta_A} \tag{4.26}$$

where we have defined:

$$\beta_\zeta = \frac{\eta C}{2\pi Q_s} \tag{4.27}$$

Replacing

$$\hat{\zeta}(s) = \hat{\zeta}_A \cos\left(2\pi Q_s \frac{s}{C}\right) - p_{\zeta_A}\beta_\zeta \sin\left(2\pi Q_s \frac{s}{C}\right) \tag{4.28}$$

$$p_\zeta(s) = \frac{\hat{\zeta}_A}{\beta_\zeta}\sin\left(2\pi Q_s \frac{s}{C}\right) + p_{\zeta_A}\cos\left(2\pi Q_s \frac{s}{C}\right) \tag{4.29}$$

For the kick-drift mode we want to rewrite the Eq. 4.13:

$$\Delta p_\zeta = -\frac{2\pi q f_{RF} V_{RF}}{\beta_0^3 E_0 c}\cos\phi_s \hat{\zeta} \tag{4.30}$$

4.3 Hamiltonian of the synchrotron motion

In this section we use the time in the laboratory frame as independent variable as done in the PyHEADTAIL longitudinal treatment. In this section we also include the effect of a reference momentum change of ΔP_0 per turn.
We assume small energy deviations, hence we can consider the coordinates (ζ, δ) to be canonically conjugate ($\delta \ll 1 \Rightarrow \delta \simeq p_\zeta$).
The longitudinal motion can be described by the following Hamiltonian:

$$H(\zeta,\delta) = -\frac{1}{2}\eta\beta_0 c\delta^2 + \frac{\beta_0 c}{C}\frac{\Delta P_0}{P_0}\zeta - \frac{q_0}{P_0}\sum_i \frac{1}{2\pi h_i} V_i \cos\left(-2\pi h_i \frac{\zeta}{C} + \phi_i\right) \tag{4.31}$$

This can be proven using Hamilton's equations:

$$\frac{d\zeta}{dt} = \frac{\partial H}{\partial \delta} = -\eta\beta_0 c\delta \tag{4.32}$$

$$\frac{d\delta}{dt} = -\frac{\partial H}{\partial \zeta} = -\frac{\beta_0 c}{C}\frac{\Delta P_0}{P_0} + \frac{q_0}{P_0 C}\sum_i V_i \sin\left(-2\pi h_i \frac{\zeta}{C} + \phi_i\right) \tag{4.33}$$

The coordinate change over one revolution is:

$$\Delta\zeta = \frac{d\zeta}{dt}\frac{C}{\beta_0 c} = -\eta C\delta \tag{4.34}$$

$$\Delta\delta = \frac{d\delta}{dt}\frac{C}{\beta_0 c} = -\frac{\Delta P_0}{P_0} + \frac{q_0}{\beta_0 c P_0}\sum_i V_i \sin\left(-2\pi h_i \frac{\zeta}{C} + \phi_i\right) \tag{4.35}$$

which are consistent with those found in Sec. 4.

4.3.1 Fixed points

The fixed points can be found by imposing $\Delta\zeta = 0$ and $\Delta\delta = 0$. If only a single harmonic is present a closed solution can be found:

$$-\frac{\Delta P_0}{P_0} + \frac{q_0}{\beta_0 c P_0} V_{\mathrm{RF}} \sin\left(-2\pi h_{\mathrm{RF}} \frac{\zeta}{C} + \phi_i\right) = 0 \tag{4.36}$$

We want to get an explicit expression for ζ:

$$\frac{\Delta P_0 \beta_0 c}{q_0 V_{\mathrm{RF}}} = \sin\left(-2\pi h_{\mathrm{RF}} \frac{\zeta}{C} + \phi_i\right) \tag{4.37}$$

There are two families of solutions:

$$\arcsin\left(\frac{\Delta P_0 \beta_0 c}{q_0 V_{\mathrm{RF}}}\right) + 2n\pi = -2\pi h_{\mathrm{RF}} \frac{\zeta}{C} + \phi_{\mathrm{RF}} \tag{4.38}$$

$$\pi - \arcsin\left(\frac{\Delta P_0 \beta_0 c}{q_0 V_{\mathrm{RF}}}\right) + 2n\pi = -2\pi h_{\mathrm{RF}} \frac{\zeta}{C} + \phi_{\mathrm{RF}} \tag{4.39}$$

where n is an integer number. Depending on the sign of η Only one family of fixed points is stable.

We solve for ζ:

$$\zeta = \frac{C}{2\pi h_{\mathrm{RF}}} \left(\phi_{\mathrm{RF}} - \arcsin\left(\frac{\Delta P_0 \beta_0 c}{q_0 V_{\mathrm{RF}}} \right) + 2n\pi \right) \tag{4.40}$$

$$\zeta = \frac{C}{2\pi h_{\mathrm{RF}}} \left(\phi_{\mathrm{RF}} + \pi + \arcsin\left(\frac{\Delta P_0 \beta_0 c}{q_0 V_{\mathrm{RF}}} \right) + 2n\pi \right) \tag{4.41}$$

It is possible to set ϕ_{RF} to place a fixed point of either family in $\zeta = 0$:

$$\phi_{\mathrm{RF}} = \arcsin\left(\frac{\Delta P_0 \beta_0 c}{q_0 V_{\mathrm{RF}}} \right) \tag{4.42}$$

$$\phi_{\mathrm{RF}} = \pi - \arcsin\left(\frac{\Delta P_0 \beta_0 c}{q_0 V_{\mathrm{RF}}} \right) \tag{4.43}$$

It can be shown that, to have a stable fixed point in $\zeta = 0$ one needs to use Eq. 4.42 when $\eta < 0$ (below transition) and Eq. 4.43 when $\eta > 0$ (below transition).

Chapter 5

Spin tracking and polarization

5.1 Spin tracking

This section is based on [18, 19].
The spin precession for a particle traveling in a magnetic field $\boldsymbol{B}$ can be written in term of the precession angular velocity:

$$\boldsymbol{\Omega}_{\mathrm{BMT}} = -\frac{1}{B\rho_{\mathrm{part}}}\left[(1+a\gamma)\boldsymbol{B}_{\perp} + (1+a)\boldsymbol{B}_{\parallel}\right] \tag{5.1}$$

where a is the anomalous magnetic moment and $\boldsymbol{B}_{\parallel}$ and $\boldsymbol{B}_{\perp}$ are referred to the velocity of the particle.
The precession angle for a particle traveling a path length ℓ is given by:

$$\phi = |\boldsymbol{\Omega}|\ell \tag{5.2}$$

We call:

$$\boldsymbol{\omega} = \frac{\boldsymbol{\Omega}}{|\boldsymbol{\Omega}|} \tag{5.3}$$

and we define:

$$t_0 = \cos\left(\frac{\phi}{2}\right) \tag{5.4}$$

$$t_x = \omega_x \sin\left(\frac{\phi}{2}\right) \tag{5.5}$$

$$t_y = \omega_y \sin\left(\frac{\phi}{2}\right) \tag{5.6}$$

$$t_s = \omega_z \sin\left(\frac{\phi}{2}\right) \tag{5.7}$$

The spin vector of the particle is transformed by the following rotation matrix:

$$M = \begin{bmatrix} (t_0^2+t_x^2)-(t_s^2+t_y^2) & 2(t_x t_y - t_0 t_s) & 2(t_x t_s + t_0 t_y) \\ 2(t_x t_y + t_0 t_s) & (t_0^2+t_y^2)-(t_x^2+t_s^2) & 2(t_s t_y - t_0 t_x) \\ 2(t_x t_s - t_0 t_y) & 2(t_s t_y + t_0 t_x) & (t_0^2+t_s^2)-(t_x^2+t_y^2) \end{bmatrix} \tag{5.8}$$

5.2 Linear transport matrix including spin

The coordinate vector including the spin is defined as:

$$\boldsymbol{z} = \begin{pmatrix} x \\ p_x \\ y \\ p_y \\ \zeta \\ \delta \\ s_x \\ s_y \\ s_z \end{pmatrix} \quad \text{We call } \boldsymbol{z}_{\text{orb}} = \begin{pmatrix} x \\ p_x \\ y \\ p_y \\ \zeta \\ \delta \end{pmatrix}, \quad \boldsymbol{z}_{\text{spin}} = \begin{pmatrix} s_x \\ s_y \\ s_z \end{pmatrix} \tag{5.9}$$

The corresponding 9D transport matrix can be written as

$$\mathbf{R} = \begin{pmatrix} \mathbf{R}_{\text{orb}} & 0 \\ \mathbf{D} & \mathbf{A} \end{pmatrix} \tag{5.10}$$

We call $\boldsymbol{e}_1, \ldots, \boldsymbol{e}_9$ the eigenvectors and $\lambda_1, \ldots, \lambda_9$ the eigenvalues so that

$$\mathbf{R}\boldsymbol{e}_i = \lambda_i \boldsymbol{e}_i \tag{5.11}$$

From the definition of eigenvectors (doing the matrix product in blocks), we can write:

$$\mathbf{R}_{\text{orb}}\, \boldsymbol{e}_{i,\text{orb}} = \lambda_i \boldsymbol{e}_{i,\text{orb}} \tag{5.12}$$

$$\mathbf{D}\, \boldsymbol{e}_{i,\text{orb}} + \mathbf{A}\, \boldsymbol{e}_{i,\text{spin}} = \lambda_i \boldsymbol{e}_{i,\text{spin}} \tag{5.13}$$

From this:

$$\mathbf{D}\, \boldsymbol{e}_{i,\text{orb}} = (\lambda_i \boldsymbol{I} - \mathbf{A})\, \boldsymbol{e}_{i,\text{spin}} \tag{5.14}$$

$$\boldsymbol{e}_{i,\text{spin}} = (\lambda_i \boldsymbol{I} - \mathbf{A})^{-1}\, \mathbf{D}\, \boldsymbol{e}_{i,\text{orb}} \tag{5.15}$$

5.3 Invariant Spin Field - first order computation

This section is based on [20].
We expand the Invariant Spin Field [18] function to first order

$$\boldsymbol{n}(\boldsymbol{z}_{\text{orb}}) = \boldsymbol{n}_0 + \mathbf{N}\left(\boldsymbol{z}_{\text{orb}} - \boldsymbol{z}_{\text{orb}}^{\text{CO}}\right) \tag{5.16}$$

In the following we drop all the constant terms so we simply write $\boldsymbol{n}(\boldsymbol{z}_{\text{orb}}) = \mathbf{N}\boldsymbol{z}_{\text{orb}}$.
We now call $\boldsymbol{z}_1^{\text{spin}}$ the ISF at $\boldsymbol{z}_1^{\text{orb}}$, i.e.

$$\boldsymbol{z}_1^{\text{spin}} = \mathbf{N}\boldsymbol{z}_1^{\text{orb}} \tag{5.17}$$

We call z_2 the coordinate after one revolution. By definition of the ISF, the spin part of z_2 is the ISF at z_2^{orb}, i.e.

$$z_2^{\text{spin}} = \mathbf{N} z_2^{\text{orb}} \tag{5.18}$$

We know from the structure of the one-turn matrix:

$$z_2^{\text{orb}} = \mathbf{R}_{\text{orb}} z_1^{\text{orb}} \tag{5.19}$$

$$z_2^{\text{spin}} = \mathbf{D} z_1^{\text{orb}} + \mathbf{A} z_1^{\text{spin}} \tag{5.20}$$

Combining, Eqs. 5.18, 5.19 and 5.20, we obtain:

$$\mathbf{N}\mathbf{R}_{\text{orb}} z_1^{\text{orb}} = \mathbf{D} z_1^{\text{orb}} + \mathbf{A}\mathbf{N} z_1^{\text{orb}} \tag{5.21}$$

We specialize it for the case $z_1^{\text{orb}} = e_1^{\text{orb}}$ obtaining:

$$\lambda_1 \mathbf{N} e_1^{\text{orb}} = \mathbf{D} e_1^{\text{orb}} + \mathbf{A}\mathbf{N} e_1^{\text{orb}} \tag{5.22}$$

From Eq. 5.12, we botain:

$$\mathbf{D} e_1^{\text{orb}} = \lambda_1 e_1^{\text{spin}} - \mathbf{A} e_1^{\text{spin}} \tag{5.23}$$

Replacing into Eq. 5.12, we obtain:

$$(\lambda_1 \mathbf{I} - \mathbf{A})\mathbf{N} e_1^{\text{orb}} = (\lambda_1 \mathbf{I} - \mathbf{A}) e_1^{\text{spin}} \tag{5.24}$$

If $(\lambda_1 \mathbf{I} - \mathbf{A})$ is not singular:

$$\mathbf{N} e_1^{\text{orb}} = e_1^{\text{spin}} \tag{5.25}$$

Combining this result for the six orbital eigenvectors:

$$\begin{pmatrix} \mathbf{N} e_1^{\text{orb}} & \cdots & \mathbf{N} e_6^{\text{orb}} \end{pmatrix} = \begin{pmatrix} e_1^{\text{spin}} & \cdots & e_6^{\text{spin}} \end{pmatrix} \tag{5.26}$$

In matrix form:

$$\mathbf{N}\mathbf{E}^{\text{orb}} = \mathbf{E}^{\text{spin}} \quad \Rightarrow \quad \mathbf{N} = \mathbf{E}^{\text{spin}} \left(\mathbf{E}^{\text{orb}} \right)^{-1} \tag{5.27}$$

We note that the last column of the matrix $\boldsymbol{N}$ provides the derivative $\frac{d\boldsymbol{n}}{d\delta}$ which is relevant for the computation of equilibrium polarization.

5.4 Equilibrium polarization and polarization time

This section is based on [20, 21, 22, 19, 23, 24].
In the presence of photon emission, the polarization of the beam evolves following the equation:

$$P(t) = P(0) e^{-\frac{t}{\tau_{\text{tot}}}} + P_{\text{eq}} \left(1 - e^{-\frac{t}{\tau_{\text{tot}}}} \right) \tag{5.28}$$

The equilibrium polarization and the buildup time can be computed as:

$$P_{\text{eq}} = \frac{8}{5\sqrt{3}} \frac{\alpha_-}{\alpha_+} \tag{5.29}$$

$$\tau_{\text{tot}}^{-1} = \frac{5\sqrt{3}}{8}\frac{r_e \hbar \gamma^5}{m_e} \cdot \alpha_+ \tag{5.30}$$

where, truncating to the first order the dependece of the ISF on the phase space coordinates, we have:

$$\alpha_+ \simeq \frac{1}{C}\oint \frac{ds}{|\rho(s)|^3}\left[1 - \frac{2}{9}(\boldsymbol{n_0}\cdot\hat{\boldsymbol{i}}_v)^2 + \frac{11}{18}\left|\frac{\partial \boldsymbol{n}}{\partial \delta}\right|^2\right]_s \tag{5.31}$$

$$\alpha_- \simeq \frac{1}{C}\oint \frac{ds}{|\rho(s)|^3}\left[\hat{\boldsymbol{i}}_B \cdot (\boldsymbol{n}_0 - \frac{\partial \boldsymbol{n}}{\partial \gamma})\right]_s \tag{5.32}$$

The buildup time can be decompoesed in two terms:

$$\tau_{\text{tot}}^{-1} = \tau_{\text{pol}}^{-1} + \tau_{\text{depol}}^{-1} \tag{5.33}$$

where:

$$\tau_{\text{pol}}^{-1} = \frac{5\sqrt{3}}{8}\frac{r_e \hbar \gamma^5}{m_e}\frac{1}{C}\oint \frac{ds}{|\rho(s)|^3}\left[1 - \frac{2}{9}(\boldsymbol{n_0}\cdot\hat{\boldsymbol{i}}_v)^2\right]_s \tag{5.34}$$

$$\tau_{\text{depol}}^{-1} = \frac{5\sqrt{3}}{8}\frac{r_e \hbar \gamma^5}{m_e}\frac{1}{C}\oint \frac{ds}{|\rho(s)|^3}\left[\frac{11}{18}\left|\frac{\partial \boldsymbol{n}}{\partial \delta}\right|^2\right]_s \tag{5.35}$$

5.5 Monte Carlo method for equilibrium polarization

This section is based on [22, 25].
We can define:

$$P_\infty = \frac{8}{5\sqrt{3}}\frac{\oint \frac{ds}{|\rho(s)|^3}\left[\hat{\boldsymbol{i}}_B \cdot (\boldsymbol{n}_0)\right]_s}{\oint \frac{ds}{|\rho(s)|^3}\left[1 - \frac{2}{9}(\boldsymbol{n_0}\cdot\hat{\boldsymbol{i}}_v)^2\right]_s} \tag{5.36}$$

The equilibrium polarization and the buildup rate can be written as follows:

$$P_{\text{eq}} = P_\infty \frac{1}{1 + \frac{\tau_{\text{pol}}}{\tau_{\text{depol}}}} \tag{5.37}$$

$$\tau_{\text{tot}}^{-1} = \tau_{\text{pol}}^{-1} + \tau_{\text{depol}}^{-1} \tag{5.38}$$

The term τ_{depol} can be evalated using particle tracking, accounting for quantum excitation from synchrotron radiation. Unlike the approach used in the previous section, this method accounts for the non-linear dependence of the ISF on the phase space coordinates. Using τ_{depol} we can get from Eqs. 5.37 and 5.38 estimates for P_{eq} and τ_{tot} that include non linear effects.

Chapter 6

Coasting beams

In coasting beams different particles have different revolution frequencies, depending on their momentum, particles perform a different number of turns in a given time.
If in the line we have collective elements which need to measure the beam distribution at a certain location s and at a given time t, we need to ensure that all particles present a s at the instant t are present at the element.
We define for each particle and for any couple of positions $s_1 < s_2$:

$$\hat{\beta}(s_1, s_2) = \frac{1}{c} \frac{s_2 - s_1}{t(s_2) - t(s_1)} \tag{6.1}$$

We choose an auxiliary value β_{sim} such that at all times:

$$\hat{\beta}(s_1, s_2) < \beta_{\text{sim}} \quad \text{for all particles and any } s_1, s_2 \tag{6.2}$$

$$\hat{\beta}(s_1, s_2) > \frac{\beta_{\text{sim}}}{2} \quad \text{for all particles and any } s_1, s_2 \tag{6.3}$$

From β_{sim} we define an auxiliary time interval ΔT as:

$$\Delta T = \frac{L}{\beta_{\text{sim}} c} \tag{6.4}$$

At each "turn" n we want to simulate at any collective element the time frame $F_n(s)$ given by:

$$F_n(s) = \left[T_n(s) - \frac{\Delta T}{2}, T_n(s) + \frac{\Delta T}{2} \right] \tag{6.5}$$

where:

$$T_n(s) = n\Delta T + \frac{s}{\beta_{\text{sim}} c} \tag{6.6}$$

We can see that intervals are contiguous, hence at any locations over N turns we are simulating a time interval of length $N\Delta T$.
From Eq 6.6 we can simply derive the following relations, which will be useful in the following:

$$T_{n+1}(s) - T_n(s) = \Delta T \tag{6.7}$$

$$T_n(s_2) - T_n(s_1) = \frac{s_2 - s_1}{\beta_{\text{sim}} c} \tag{6.8}$$

We also note that the condition $t(s) \in F_n(s)$ can be rewritten as:

$$-\frac{\Delta T}{2} < t - n\Delta T - \frac{s}{\beta_{\text{sim}} c} < \frac{\Delta T}{2} \tag{6.9}$$

We can prove the following propositions (see Sec. 6.3):

Proposition 1: If the time $t_k(s_1)$ defining the k-th arrival of a particle at location s_1 falls in the frame $F_n(s_1)$, then the particle arrives at location $s_2 > s_1$ either in the frame $F_n(s_2)$ or in the following frame $F_{n+1}(s_2)$. In symbols:

$$t_k(s_1) \in F_n(s_1) \Rightarrow t_k(s_2) \in F_n(s_2) \cup F_{n+1}(s_2) \quad \text{for any } s_1 < s_2 \tag{6.10}$$

Proposition 2: If the time $t_k(s_2)$ defining the k-th arrival of a particle at location s_2 falls in the frame $F_n(s_2)$, then the time of $(k+1)$-th arrival at any location $s_1 < s_2$ falls in the frame $F_{n+1}(s_1)$ or in the following frame $F_{n+1}(s_1)$. In symbols:

$$t_k(s_2) \in F_n(s_2) \Rightarrow t_{k+1}(s_1) \in F_{n+1}(s_1) \cup F_{n+2}(s_1) \quad \text{for any } s_1 < s_2 \tag{6.11}$$

Proposition 3: If the time $t_k(L)$ defining the k-th arrival of a particle at the end of the line falls in the frame $F_n(L)$, than the time $t_{k+1}(0) = t_k(L)$ of the $(k+1)$-th arrival of the particle at $s = 0$ falls in the interval $F_{n+1}(0)$. In symbols:

$$t_k(L) \in F_n(L) \Rightarrow t_{k+1}(0) \in F_{n+1}(0) \tag{6.12}$$

6.1 ζ definition and update

For the tracking of coasting beams we define the longitudinal coordinate ζ as:

$$\zeta = s - \beta_0 c(t - n\Delta T) \tag{6.13}$$

where s is the distance from the start of the line for the present turn, t is the absolute time since the start of the simulation, n is the index of the present simulated time frame.
We can write t in terms of ζ as:

$$t = \frac{s}{\beta_0 c} - \frac{\zeta}{\beta_0 c} + n\Delta T \tag{6.14}$$

With this definition the ζ coordinate needs to be updated each time the particle passes at the start of the line since across the $s = 0$ we can write:

$$\zeta^- = L - \beta_0 c(t - n\Delta T) \tag{6.15}$$

$$\zeta^+ = 0 - \beta_0 c(t - (n+1)\Delta T) \tag{6.16}$$

where t is the time at which the particle passes zero (which is the same in both equations).

Combining the two equations we can write:

$$\zeta^+ = \zeta^- - (L - \beta_0 c \Delta T) \tag{6.17}$$

In standard simulations for bunched beams the simulated frame is $\Delta T = L/(\beta_0 c)$, hence the ζ coordinate is continuous.
For coasting beams ΔT is given by Eq. 6.4, hence the ζ needs to be updated at each turn using:

$$\boxed{\zeta^+ = \zeta^- - L\left(1 - \frac{\beta_0}{\beta_{\text{sim}}}\right)} \tag{6.18}$$

We want to translate the condition Eq. 6.9 into a condition on ζ. Replacing Eq. 6.14 into Eq. 6.9 we obtain:

$$-\frac{\Delta T}{2} < \left(\frac{s}{\beta_0 c} - \frac{\zeta}{\beta_0 c} + n\Delta T\right) - n\Delta T - \frac{s}{\beta_{\text{sim}} c} < \frac{\Delta T}{2} \tag{6.19}$$

We change signs:

$$\frac{\Delta T}{2} > -\frac{s}{\beta_0 c} + \frac{\zeta}{\beta_0 c} + \frac{s}{\beta_{\text{sim}} c} > -\frac{\Delta T}{2} \tag{6.20}$$

We rearrange:

$$-\frac{\Delta T}{2} < -\frac{s}{\beta_0 c} + \frac{\zeta}{\beta_0 c} + \frac{s}{\beta_{\text{sim}} c} < \frac{\Delta T}{2} \tag{6.21}$$

$$-\beta_0 c \frac{\Delta T}{2} < \zeta - s\left(1 - \frac{\beta_0}{\beta_{\text{sim}}}\right) < \beta_0 c \frac{\Delta T}{2} \tag{6.22}$$

from which we can write:

$$\boxed{t \in F_n(s) \quad \Leftrightarrow \quad -\frac{\Delta\zeta}{2} < \zeta - s\left(1 - \frac{\beta_0}{\beta_{\text{sim}}}\right) < \frac{\Delta\zeta}{2}} \tag{6.23}$$

where we have defined:

$$\boxed{\Delta\zeta = \beta_0 c \Delta T = \frac{\beta_0}{\beta_{\text{sim}}} L} \tag{6.24}$$

6.2 Handling particles jumping to the following frame

From Proposition 1 we know that during tracking particles will either stay in the present frame or "jump" to the following one.
From Eqs. 6.5 and 6.23, we know that the jump occurs when:

$$t > T_n(s) + \frac{\Delta T}{2} \;\Leftrightarrow\; \zeta < -\frac{\Delta\zeta}{2} + s\left(1 - \frac{\beta_0}{\beta_{\text{sim}}}\right) \tag{6.25}$$

When this condition is met, the particle tracking needs to be paused for the remainder of the frame n (based on Proposition 1 it cannot go back to frame n) and, based on Proposition 2, its tracking needs to be resumed from the same location where the

tracking was paused when tracking the following frame. As the frame index is increased, ζ needs to be updated to preserve the time of arrival:

$$\zeta_{\text{before jump}} = s - \beta_0 c\,(t - n\Delta T) \tag{6.26}$$

$$\zeta_{\text{after jump}} = s - \beta_0 c\,(t - (n+1)\Delta T) \tag{6.27}$$

from which we obtain:

$$\boxed{\zeta_{\text{after jump}} = \zeta_{\text{before jump}} + \beta_0 c \Delta T = \zeta_{\text{before jump}} + \Delta\zeta} \tag{6.28}$$

6.3 Proofs

We notice that from Eqs. 6.2 and 6.3 we can write

$$\hat{\beta} < \beta_{\text{sim}} \quad \Rightarrow \quad \frac{1}{\hat{\beta}} > \frac{1}{\beta_{\text{sim}}} \quad \Rightarrow \quad \left(\frac{1}{\hat{\beta}} - \frac{1}{\beta_{\text{sim}}}\right) > 0 \tag{6.29}$$

$$\hat{\beta} > \frac{\beta_{\text{sim}}}{2} \quad \Rightarrow \quad \frac{1}{\hat{\beta}} < \frac{2}{\beta_{\text{sim}}} \quad \Rightarrow \quad \left(\frac{1}{\hat{\beta}} - \frac{1}{\beta_{\text{sim}}}\right) < \frac{1}{\beta_{\text{sim}}} \tag{6.30}$$

Combining the two we obtain

$$0 < \left(\frac{1}{\hat{\beta}} - \frac{1}{\beta_{\text{sim}}}\right) < \frac{1}{\beta_{\text{sim}}} \tag{6.31}$$

Proof of proposition 1

By definition of $\hat{\beta}$ we can write:

$$t_k(s_2) = t_k(s_1) + \frac{s_2 - s_1}{\hat{\beta} c} \tag{6.32}$$

By the hypothesis:

$$t_k(s_1) > T_n(s_1) - \frac{\Delta T}{2} \tag{6.33}$$

hence:

$$t_k(s_2) > T_n(s_1) - \frac{\Delta T}{2} + \frac{s_2 - s_1}{\hat{\beta} c} \tag{6.34}$$

Using Eq. 6.8 we can write:

$$t_k(s_2) > T_n(s_2) - \frac{s_2 - s_1}{\beta_{\text{sim}} c} - \frac{\Delta T}{2} + \frac{s_2 - s_1}{\hat{\beta} c} \tag{6.35}$$

Rearranging:

$$t_k(s_2) > T_n(s_2) - \frac{\Delta T}{2} + \frac{s_2 - s_1}{c}\left(\frac{1}{\hat{\beta}(s)} - \frac{1}{\beta_{\text{sim}}}\right) \tag{6.36}$$

Using Eq. 6.31 and the fact that by hypotheses that $s_2 > s_1$, we know that the last term is positive. Therefore we can write:

$$t_k(s_2) > T_n(s_2) - \frac{\Delta T}{2} \tag{6.37}$$

Similarly from the hypothesis we know:

$$t_k(s_1) < T_n(s_1) + \frac{\Delta T}{2} \tag{6.38}$$

From Eq. 6.32 we can write:

$$t_k(s_2) < T_n(s_1) + \frac{\Delta T}{2} + \frac{s_2 - s_1}{\hat{\beta} c} \tag{6.39}$$

Again, using Eq. 6.8 we obtain:

$$t_k(s_2) < T_n(s_2) - \frac{s_2 - s_1}{\beta_{\text{sim}} c} - \frac{\Delta T}{2} + \frac{s_2 - s_1}{\hat{\beta} c} \tag{6.40}$$

Rearranging:

$$t_k(s_2) < T_n(s_2) + \frac{\Delta T}{2} + \frac{s_2 - s_1}{c} \left(\frac{1}{\hat{\beta}(s)} - \frac{1}{\beta_{\text{sim}}} \right) \tag{6.41}$$

Using Eq. 6.31 we obtain:

$$t_k(s_2) < T_n(s_2) + \frac{\Delta T}{2} + \frac{s_2 - s_1}{\beta_{\text{sim}} c} \tag{6.42}$$

Using the fact that $s_2 - s_1 < L$ and Eq. 6.4 we can write:

$$\frac{s_2 - s_1}{\beta_{\text{sim}} c} < \frac{L}{\beta_{\text{sim}} c} = \Delta T \tag{6.43}$$

Replacing in Eq. 6.42 we obtain:

$$t_k(s_2) < T_n(s_2) + \frac{\Delta T}{2} + \Delta T \tag{6.44}$$

Using Eq. 6.7 we obtain:

$$t_k(s_2) < T_{n+1}(s_2) + \frac{\Delta T}{2} \tag{6.45}$$

Combining Eq. 6.37 and 6.37 we obtain:

$$T_n(s_2) - \frac{\Delta T}{2} < t_k(s_2) < T_{n+1}(s_2) + \frac{\Delta T}{2} \tag{6.46}$$

which is what we wanted to prove.

Proof of proposition 2

From the hypothesis:

$$t_k(s_2) > T_n(s_2) - \frac{\Delta T}{2} \tag{6.47}$$

As $L > s_2$, using Proposition 1 we can write:

$$t_k(L) > T_n(L) - \frac{\Delta T}{2} \tag{6.48}$$

Using Proposition 3 we can write:

$$t_{k+1}(0) > T_{n+1}(0) - \frac{\Delta T}{2} \tag{6.49}$$

Using the fact that $s1 > 0$, we can apply again Proposition 1, obtaining:

$$t_{k+1}(s1) > T_{n+1}(1) - \frac{\Delta T}{2} \tag{6.50}$$

which is what we wanted to prove.

Proof of proposition 3

By definition:

$$t_{k+1}(0) = t_k(L) \tag{6.51}$$

We know that $t_k(L) \in F_n(L)$ hence, from Eq. 6.5 we can write:

$$t_{k+1}(0) > T_n(L) - \frac{\Delta T}{2} \tag{6.52}$$

From Eq. 6.6 we obtain:

$$t_{k+1}(0) > n\Delta T - \frac{\Delta T}{2} + \frac{L}{\beta_{\text{sim}} c} \tag{6.53}$$

from Eq. 6.4 we get:

$$t_{k+1}(0) > (n+1)\Delta T - \frac{\Delta T}{2} \tag{6.54}$$

and from Eq. 6.6 (with $s = 0$) we obtain:

$$t_{k+1}(0) > T_{n+1}(0) - \frac{\Delta T}{2} \tag{6.55}$$

which is what we wanted to prove.

Chapter 7

Space charge and beam-beam forces

7.1 Fields generated by a bunch of particles

We assume that the bunch travels rigidly along s with velocity $\beta_0 c$:

$$\rho\left(x,y,s,t\right) = \rho_0\left(x,y,s-\beta_0 ct\right) \tag{7.1}$$
$$\mathbf{J}\left(x,y,s,t\right) = \beta_0 c\,\rho_0\left(x,y,s-\beta_0 ct\right)\hat{\mathbf{i}}_s \tag{7.2}$$

We define an auxiliary variable ζ as the position along the bunch:

$$\zeta = s - \beta_0 ct\,. \tag{7.3}$$

We call K the lab reference frame in which we have defined all equations above, and we introduce a boosted frame K' moving rigidly with the reference particle. The coordinates in the two systems are related by a Lorentz transformation [**?**]:

$$ct' = \gamma_0\left(ct - \beta_0 s\right) \tag{7.4}$$
$$x' = x \tag{7.5}$$
$$y' = y \tag{7.6}$$
$$s' = \gamma_0\left(s - \beta_0 ct\right) = \gamma_0\zeta \tag{7.7}$$

The corresponding inverse transformation is:

$$ct = \gamma_0\left(ct' + \beta_0 s'\right) \tag{7.8}$$
$$x = x' \tag{7.9}$$
$$y = y' \tag{7.10}$$
$$s = \gamma_0\left(s' + \beta_0 ct'\right) \tag{7.11}$$

The quantities $\left(c\rho, J_x, J_y, J_s\right)$ form a Lorentz 4-vector and therefore they are transformed between K and K' by relationships similar to the Eqs. 7.4-7.6 [**?**]:

$$c\rho'\left(\mathbf{r'},t'\right) = \gamma_0\left[c\rho\left(\mathbf{r}\left(\mathbf{r'},t'\right),t\left(\mathbf{r'},t'\right)\right) - \beta_0 J_s\left(\mathbf{r}\left(\mathbf{r'},t'\right),t\left(\mathbf{r'},t'\right)\right)\right] \tag{7.12}$$
$$J_s'\left(\mathbf{r'},t'\right) = \gamma_0\left[J_s\left(\mathbf{r}\left(\mathbf{r'},t'\right),t\left(\mathbf{r'},t'\right)\right) - \beta_0 c\rho\left(\mathbf{r}\left(\mathbf{r'},t'\right),t\left(\mathbf{r'},t'\right)\right)\right] \tag{7.13}$$

where the transformations $\mathbf{r}\left(\mathbf{r'}, t'\right)$ and $t\left(\mathbf{r'}, t'\right)$ are defined by Eqs. 7.8 and 7.11 respectively. The transverse components J_x and J_y of the current vector are invariant for our transformation, and are anyhow zero in our case.
Using Eq. 7.2 these become:

$$\rho'\left(\mathbf{r'}, t'\right) = \frac{1}{\gamma_0}\rho\left(\mathbf{r}\left(\mathbf{r'}, t'\right), t\left(\mathbf{r'}, t'\right)\right) \tag{7.14}$$

$$J'_s\left(\mathbf{r'}, t'\right) = 0 \tag{7.15}$$

Using Eqs. 7.1 and 7.8-7.10, we obtain:

$$\rho\left(x', y', s(s', t'), t(s', t')\right) = \rho_0\left(x', y', s(s', t') - \beta_0 c\, t(s', t')\right) \tag{7.16}$$

From Eq. 7.7 we get:

$$s(s', t') - \beta_0 c\, t(s', t') = \frac{s'}{\gamma_0} \tag{7.17}$$

where the coordinate t' has disappeared.
We can therefore write:

$$\rho'\left(x', y', s', t'\right) = \frac{1}{\gamma_0}\rho_0\left(x', y', \frac{s'}{\gamma_0}\right) \tag{7.18}$$

The electric potential in the bunch frame is solution of Poisson's equation:

$$\frac{\partial^2\phi'}{\partial x'^2} + \frac{\partial^2\phi'}{\partial y'^2} + \frac{\partial^2\phi'}{\partial s'^2} = -\frac{\rho'(x', y', s')}{\varepsilon_0} \tag{7.19}$$

From Eq. 7.18 we can write:

$$\frac{\partial^2\phi'}{\partial x'^2} + \frac{\partial^2\phi'}{\partial y'^2} + \frac{\partial^2\phi'}{\partial s'^2} = -\frac{1}{\gamma_0\varepsilon_0}\rho_0\left(x', y', \frac{s'}{\gamma_0}\right) \tag{7.20}$$

We now make the substitution:

$$\zeta = \frac{s'}{\gamma_0} \tag{7.21}$$

obtained from Eq. 7.7, which allows to rewrite Eq. 7.20 as:

$$\frac{\partial^2\phi'}{\partial x^2} + \frac{\partial^2\phi'}{\partial y^2} + \frac{1}{\gamma_0^2}\frac{\partial^2\phi'}{\partial \zeta^2} = -\frac{1}{\gamma_0\varepsilon_0}\rho_0\left(x, y, \zeta\right) \tag{7.22}$$

Here we have dropped the "'" sign from x and y as these coordinates are unaffected by the Lorentz boost.
The quantities $\left(\frac{\phi}{c}, A_x, A_y, A_s\right)$ form a Lorentz 4-vector, so we can write:

$$\phi = \gamma_0\left(\phi' + \beta_0 c A'_s\right) \tag{7.23}$$

$$A_s = A'_s + \beta_0\frac{\phi'}{c} \tag{7.24}$$

In the bunch frame the charges are at rest therefore $A'_x = A'_y = A'_s = 0$ therefore:

$$\phi = \gamma_0 \phi' \tag{7.25}$$

$$A_s = \beta_0 \frac{\phi'}{c} = \frac{\beta_0}{\gamma_0 c}\phi \tag{7.26}$$

Combining Eq. 7.25 with Eq. 7.22 we obtain the equation in ϕ:

$$\boxed{\frac{\partial^2 \phi}{\partial x^2} + \frac{\partial^2 \phi}{\partial y^2} + \frac{1}{\gamma_0^2}\frac{\partial^2 \phi}{\partial \zeta^2} = -\frac{1}{\varepsilon_0}\rho_0\left(x, y, \zeta\right)} \tag{7.27}$$

7.1.1 2.5D approximation

For large enough values of γ_0, Eq. 7.22 can be approximated by:

$$\boxed{\frac{\partial^2 \phi}{\partial x^2} + \frac{\partial^2 \phi}{\partial y^2} = -\frac{1}{\varepsilon_0}\rho_0\left(x, y, \zeta\right)} \tag{7.28}$$

which means that we can solve a simple 2D problem for each beam slice (identified by its coordinate ζ).

7.1.2 Modulated 2D

Often the beam distribution can be factorized as:

$$\rho_0(x, y, \zeta) = q_0 \lambda_0(\zeta) \rho_\perp(x, y) \tag{7.29}$$

where:

$$\int \rho_\perp(x, y)\, dx\, dy = 1 \tag{7.30}$$

and $\lambda_0(z)$ is therefore the bunch line density.
For a bunched beam:

$$\int \lambda_0(z)\, dz = N \tag{7.31}$$

where N is the bunch population.
In this case the potential can be factorized as:

$$\phi(x, y, \zeta) = q_0 \lambda(\zeta) \phi_\perp(x, y) \tag{7.32}$$

where $\phi_\perp(x, y)$ is the solution of the following 2D Poisson equation:

$$\frac{\partial^2 \phi_\perp}{\partial x^2} + \frac{\partial^2 \phi_\perp}{\partial y^2} = -\frac{1}{\varepsilon_0}\rho_\perp\left(x, y\right) \tag{7.33}$$

7.2 Lorentz force

We now compute the Lorentz force on the particles moving in the longitudinal directions, including particles of the bunch itself (space charge forces) and particles of a colliding bunch moving in the opposite directions (beam-beam forces). The angles of such test particles are neglected as done in the usual thin-lens approximation. Therefore the velocity of a test particle can be written as:

$$\mathbf{v} = \beta c\, \hat{\mathbf{i}}_s \tag{7.34}$$

The Lorenz force can be written as:

$$\begin{aligned} \mathbf{F} &= q\left(-\nabla\phi - \frac{\partial \mathbf{A}}{\partial t} + \beta c\, \hat{\mathbf{i}}_s \times (\nabla \times \mathbf{A})\right) \\ &= q\left(-\nabla\phi - \frac{\beta_0}{\gamma_0 c}\frac{\partial \phi}{\partial t}\hat{\mathbf{i}}_s + \beta c\, \hat{\mathbf{i}}_s \times (\nabla \times \mathbf{A})\right) \end{aligned} \tag{7.35}$$

We compute the vector product:

$$\begin{aligned} \hat{\mathbf{i}}_s \times (\nabla \times \mathbf{A}) &= \left(\frac{\partial A_s}{\partial x} - \frac{\partial A_x}{\partial s}\right)\hat{\mathbf{i}}_x + \left(\frac{\partial A_s}{\partial y} - \frac{\partial A_y}{\partial s}\right)\hat{\mathbf{i}}_y \\ &= \left(\frac{\partial A_s}{\partial x} - \frac{\partial A_x}{\partial s}\right)\hat{\mathbf{i}}_x + \left(\frac{\partial A_s}{\partial y} - \frac{\partial A_y}{\partial s}\right)\hat{\mathbf{i}}_y + \underbrace{\left(\frac{\partial A_s}{\partial s} - \frac{\partial A_s}{\partial s}\right)}_{=0}\hat{\mathbf{i}}_s \\ &= \nabla A_s - \frac{\partial \mathbf{A}}{\partial s} \end{aligned} \tag{7.36}$$

We replace:

$$\mathbf{F} = q\left(-\nabla\phi - \frac{\beta_0}{\gamma_0 c}\frac{\partial \phi}{\partial t}\hat{\mathbf{i}}_s + \beta\beta_0\nabla\phi - \frac{\beta\beta_0}{\gamma_0}\frac{\partial \phi}{\partial s}\hat{\mathbf{i}}_s\right) \tag{7.37}$$

The potentials will have the same form as the sources (this can be shown explicitly using the Lorentz transformations):

$$\phi(x, y, s, t) = \phi\left(x, y, t - \frac{s}{\beta_0 c}\right) \tag{7.38}$$

For a function in this form we can write:

$$\frac{\partial \phi}{\partial s} = \frac{\partial}{\partial \zeta} = -\frac{1}{\beta_0 c}\frac{\partial \phi}{\partial t} \tag{7.39}$$

obtaining:

$$\mathbf{F} = q\left(-\nabla\phi + \frac{\beta_0^2}{\gamma_0}\frac{\partial \phi}{\partial \zeta}\hat{\mathbf{i}}_s + \beta\beta_0\nabla\phi - \frac{\beta\beta_0}{\gamma_0}\frac{\partial \phi}{\partial \zeta}\hat{\mathbf{i}}_s\right) \tag{7.40}$$

Reorganizing:

$$\mathbf{F} = -q(1 - \beta\beta_0)\nabla\phi - \frac{\beta_0(\beta - \beta_0)}{\gamma_0}\frac{\partial \phi}{\partial \zeta}\hat{\mathbf{i}}_s \tag{7.41}$$

Writing the dependencies explicitly:

$$F_x(x,y,\zeta(t)) = -q(1-\beta\beta_0)\frac{\partial\phi}{\partial x}(x,y,\zeta(t)) \tag{7.42}$$

$$F_y(x,y,\zeta(t)) = -q(1-\beta\beta_0)\frac{\partial\phi}{\partial y}(x,y,\zeta(t)) \tag{7.43}$$

$$F_z(x,y,\zeta(t)) = -q\left(1-\beta\beta_0-\frac{\beta_0(\beta-\beta_0)}{\gamma_0}\right)\frac{\partial\phi}{\partial\zeta}(x,y,\zeta(t)) \tag{7.44}$$

where $\zeta(t)$ is the position of the particle within the bunch.

7.3 Space charge

Over the single interaction we neglect the particle slippage[1]:

$$\beta = \beta_0 \tag{7.45}$$

$$\zeta(t) = \zeta \tag{7.46}$$

This gives the following simplification of Eqs. (7.42) - (7.44):

$$F_x(x,y,\zeta) = -q(1-\beta_0^2)\frac{\partial\phi}{\partial x}(x,y,\zeta) \tag{7.47}$$

$$F_y(x,y,\zeta) = -q(1-\beta_0^2)\frac{\partial\phi}{\partial y}(x,y,\zeta) \tag{7.48}$$

$$F_z(x,y,\zeta) = -q(1-\beta_0^2)\frac{\partial\phi}{\partial\zeta}(x,y,\zeta) \tag{7.49}$$

In this way the force over the single interaction becomes independent on time and therefore we can compute the kicks simply as:

$$\Delta\mathbf{P} = \frac{L}{\beta_0 c}\mathbf{F} \tag{7.50}$$

where L is the portion of the machine on which we want to compute the e-cloud interaction.
The kicks on the normalized momenta can be expressed as (recalling that $P_0 = m_0\beta_0\gamma_0 c$):

$$\boxed{\Delta p_x = \frac{m_0}{m}\frac{\Delta P_x}{P_0} = -\frac{qL(1-\beta_0^2)}{m\gamma_0\beta_0^2c^2}\frac{\partial\phi}{\partial x}(x,y,\zeta)} \tag{7.51}$$

$$\boxed{\Delta p_y = \frac{m_0}{m}\frac{\Delta P_y}{P_0} = -\frac{qL(1-\beta_0^2)}{m\gamma_0\beta_0^2c^2}\frac{\partial\phi}{\partial y}(x,y,\zeta)} \tag{7.52}$$

$$\boxed{\Delta\delta \simeq \Delta p_z = \frac{m_0}{m}\frac{\Delta P_z}{P_0} = -\frac{qL(1-\beta_0^2)}{m\gamma_0\beta_0^2c^2}\frac{\partial\phi}{\partial\zeta}(x,y,\zeta)} \tag{7.53}$$

[1] In any case one would need to take into account also the dispersion in order to have the right slippage.

If the beam includes particles of different species (tracking of fragments), note that here q and m refer to the individual particle while m_0 is the mass of the reference particle.
In the modulated 2D case (see Sec. 7.1.2 and in particular Eq. 7.32), the kick can be expressed as:

$$\boxed{\Delta p_x = \frac{m_0}{m}\frac{\Delta P_x}{P_0} = -\frac{qq_0L(1-\beta_0^2)}{m\gamma_0\beta_0^2c^2}\,\lambda_0(\zeta)\,\frac{\partial\phi_\perp}{\partial x}(x,y)} \tag{7.54}$$

$$\boxed{\Delta p_y = \frac{m_0}{m}\frac{\Delta P_y}{P_0} = -\frac{qq_0L(1-\beta_0^2)}{m\gamma_0\beta_0^2c^2}\,\lambda_0(\zeta)\,\frac{\partial\phi_\perp}{\partial y}(x,y)} \tag{7.55}$$

$$\boxed{\Delta\delta \simeq \Delta p_z = \frac{m_0}{m}\frac{\Delta P_z}{P_0} = -\frac{qq_0L(1-\beta_0^2)}{m\gamma_0\beta_0^2c^2}\,\frac{d\lambda_0}{d\zeta}(\zeta)\,\phi_\perp(x,y)} \tag{7.56}$$

In some cases, for example in the case of transversely Gaussian beams, an analytic closed form exists for the quantities $\frac{\partial\phi_\perp}{\partial x}$ and $\frac{\partial\phi_\perp}{\partial y}$ but not for the potential $\phi\ \perp$ itself. In those cases, in order to compute the longitudinal kick, it is possible to obtain a function $\phi_\perp(x,y)$ generating the same transverse kicks by computing numerically the integral:

$$\phi_\perp(x,y) = \int_{(0,0)}^{(x,y)} \left(\frac{\partial\phi_\perp}{\partial x}\hat{\mathbf{i}}_x + \frac{\partial\phi_\perp}{\partial y}\hat{\mathbf{i}}_y\right)\cdot d\mathbf{r}' \tag{7.57}$$

7.4 Beam-beam interaction (4D model)

We consider a test particle moving in the opposite direction with velocity:

$$\mathbf{v}_W = -\beta_{0W}c\,\hat{\mathbf{i}}_s \tag{7.58}$$

$$s_W(t) = -\beta_{0W}ct \tag{7.59}$$

Equations (7.42) - (7.44) become:

$$F_x(x,y,\zeta_W(t)) = -q(1+\beta_{0W}\beta_{0s})\frac{\partial\phi}{\partial x}(x,y,\zeta_W(t)) \tag{7.60}$$

$$F_y(x,y,\zeta_W(t)) = -q(1+\beta_{0W}\beta_{0S})\frac{\partial\phi}{\partial y}(x,y,\zeta_W(t)) \tag{7.61}$$

$$F_z(x,y,\zeta_W(t)) = -q\left(1+\beta_{0W}\beta_{0S} - \frac{\beta_{0S}(\beta_{0W}+\beta_{0S})}{\gamma_0}\right)\frac{\partial\phi}{\partial\zeta}(x,y,\zeta_W(t)) \tag{7.62}$$

where we have used the the subscript S (strong) for the bunch generating the fields, and the subscript W (weak) for the test particle.
$\zeta_W(t)$ is the position of the test particle within the bunch generating the fields:

$$\zeta_W(t) = s_W(t) - \beta_{0S}ct = -(\beta_{0W}+\beta_{0S})ct \tag{7.63}$$

In modulated-2D case (Eq. 7.32), Eqs. (7.60) - (7.61) become:

$$F_x(x,y,\zeta_W(t)) = -qq_{0S}(1+\beta_{0W}\beta_{0s})\lambda_{0S}(\zeta_W(t))\frac{\partial\phi_\perp}{\partial x}(x,y) \tag{7.64}$$

$$F_y(x,y,\zeta_W(t)) = -qq_{0S}(1+\beta_{0W}\beta_{0s})\lambda_{0S}(\zeta_W(t))\frac{\partial\phi_\perp}{\partial y}(x,y) \tag{7.65}$$

$$F_z(x,y,\zeta_W(t)) = -qq_{0S}\left(1+\beta_{0W}\beta_{0S}-\frac{\beta_{0S}(\beta_{0W}+\beta_{0S})}{\gamma_0}\right)\frac{d\lambda_{0S}}{d\zeta}(\zeta_W(t))\phi_\perp(x,y) \tag{7.66}$$

The change in momentum for the test particle is given by:

$$\Delta\mathbf{P} = \int_{-\infty}^{+\infty}\mathbf{F}(t)\,dt \tag{7.67}$$

Therefore:

$$\Delta P_x(x,y,\zeta_W(t)) = -qq_{0S}N_S(1+\beta_{0W}\beta_{0s})\frac{\partial\phi_\perp}{\partial x}(x,y)\int_{-\infty}^{+\infty}\lambda_{0S}(\zeta_W(t))\,dt \tag{7.68}$$

$$\Delta P_y(x,y,\zeta_W(t)) = -qq_{0S}N_S(1+\beta_{0W}\beta_{0s})\frac{\partial\phi_\perp}{\partial y}(x,y)\int_{-\infty}^{+\infty}\lambda_{0S}(\zeta_W(t))\,dt \tag{7.69}$$

$$\Delta P_z(x,y,\zeta_W(t)) = -qq_{0S}\left(1+\beta_{0W}\beta_{0S}-\frac{\beta_{0S}(\beta_{0W}+\beta_{0S})}{\gamma_0}\right)\phi_\perp(x,y)\int_{-\infty}^{+\infty}\frac{d\lambda_{0S}}{d\zeta}(\zeta_W(t))\,dt \tag{7.70}$$

Using Eq. (7.63) and Eq. (7.31) we can write:

$$\int_{-\infty}^{+\infty}\lambda_{0S}(\zeta_W(t))\,dt = \frac{1}{(\beta_{0W}+\beta_{0S})c}\int_{-\infty}^{+\infty}\lambda_{0S}(\zeta)\,d\zeta = \frac{N_S}{(\beta_{0W}+\beta_{0S})c} \tag{7.71}$$

Similarly, for a bunched beam:

$$\int_{-\infty}^{+\infty}\frac{d\lambda_{0S}}{d\zeta}(\zeta_W(t))\,dt = \frac{1}{(\beta_{0W}+\beta_{0S})c}\int_{-\infty}^{+\infty}\frac{d\lambda_{0S}}{d\zeta}\,d\zeta = \frac{\lambda_{0S}(+\infty)-\lambda_{0S}(-\infty)}{(\beta_{0W}+\beta_{0S})c} = 0 \tag{7.72}$$

From which we can write:

$$\boxed{\Delta p_x = \frac{m_0}{m}\frac{\Delta P_x}{P_0} = -\frac{qq_{0S}N_S}{m\beta_{0W}\gamma_{0W}c^2}\frac{(1+\beta_{0W}\beta_{0s})}{(\beta_{0W}+\beta_{0S})}\frac{\partial\phi_\perp}{\partial x}(x,y)} \tag{7.73}$$

$$\boxed{\Delta p_y = \frac{m_0}{m}\frac{\Delta P_y}{P_0} = -\frac{qq_{0S}N_S}{m\beta_{0W}\gamma_{0W}c^2}\frac{(1+\beta_{0W}\beta_{0s})}{(\beta_{0W}+\beta_{0S})}\frac{\partial\phi_\perp}{\partial y}(x,y)} \tag{7.74}$$

$$\boxed{\Delta p_z = \frac{m_0}{m}\frac{\Delta P_z}{P_0} = 0} \tag{7.75}$$

7.5 Longitudinal profiles

7.5.1 Gaussian profile

The profile is in the form:

$$\lambda_0(z) = \frac{N}{\sqrt{2\pi}\sigma}e^{-\frac{(z-z_0)^2}{2\sigma^2}} \tag{7.76}$$

7.5.2 q-Gaussian

The profile is in the form:

$$\lambda_0(z) = \frac{N\sqrt{\beta}}{C_q} e_q\left(-\beta(z-z_0)^2\right) \tag{7.77}$$

where e_q is the q-exponential function:

$$e_q(x) = [1+(1-q)x]_+^{\frac{1}{1-q}} \tag{7.78}$$

C_q is a normalization factor dependent on q alone:

$$C_q = \frac{\sqrt{\pi}\Gamma\left(\frac{3-q}{2(q-1)}\right)}{\sqrt{q-1}\Gamma\left(\frac{1}{q-1}\right)} \tag{7.79}$$

The parameter beta defines the standard deviation of the distribution:

$$\sigma = \sqrt{\frac{1}{\beta(5-3q)}} \iff \beta = \frac{1}{\sigma^2(5-3q)} \tag{7.80}$$

These expressions are valid for values of the parameter q is the range of interest:

$$1 < q < \frac{5}{3} \tag{7.81}$$

In general the q-Gaussian is defined outside this range, but for smaller values it has a limited support (not of interest) and for larger values has a not defined standard deviation.

7.6 Beam-beam interaction (6D model, Hirata method)

This chapter describes in detail the numerical method used for the simulation of beam-beam interactions in the weak-strong framework using the "Synchro Beam Mapping" approach [26, 27]. This allows correctly modeling the coupling introduced by beam-beam between the longitudinal and transverse planes. The goal of this document is in particular to provide in a compact, complete and self-consistent manner, the set of equations that are needed for the implementation in a numerical code. Complementary information can be found in [28], including graphical representations of the procedure presented in this note and several validation tests.
The effect of a "crossing angle" in an arbitrary "crossing plane" with respect to the assigned reference frame is taken into account with a suitable coordinate transformation following the approach described in [26, 6]. The employed description of the strong beam allows the correct inclusion of the hour-glass effect as well as the linear coupling at the interaction point, following the treatment presented in [6].
If not differently stated in an explicit way in the following, all coordinates are given in the reference system defined by the closed orbit of the weak beam, which is traveling

with positive speed along the s direction. The Interaction Point (IP) is located at s=0 and the crossing plane is defined by as the angle that the strong beam forms with the s-axis. In the presence of an offset between the beams (separation), the orientation of the reference system is defined by the closed orbit of the weak beam and the system is centered at the IP location as defined for the strong beam. Therefore the strong beam passes always through the origin of the reference frame.

7.6.1 Direct Lorentz boost (for the weak beam)

We want to transform the coordinates by moving to a Lorentz boosted frame in which the collision is head-on (i.e. $p_x = p_y = 0$ for the strong beam and for the reference particle of the weak beam). We call ϕ the half crossing angle and α the angle that the crossing plane makes with respect to the $x - z$ plane. For this purpose, we perform a transformation which actually includes four operations (more details can be found in Appendix 7.6.6.1 and in [28, 6]):

- Transform the accelerator positions and momenta into Cartesian coordinates (which can then be Lorentz boosted);
- Rotate particle coordinates to the "barycentric" reference frame;
- Perform the Lorentz boost;
- Drift all the particles back to $s = 0$ (as not all particles with $s = 0$ are fixed points of the transformation, and we are tracking with respect to s and not with respect to time).

We name the original accelerator coordinates (as defined in the SixTrack Physics Manual [29]):

$$\left(x, p_x, y, p_y, \sigma, \delta\right) \tag{7.82}$$

and the transformed coordinates:

$$\left(x^*, p_x^*, y^*, p_y^*, \sigma^*, \delta^*\right) \tag{7.83}$$

We start by computing the drift Hamiltonian in the original coordinates (we are doing a Lorentz transformation, therefore constants matter as we are assuming that h is the total energy of the particle):

$$h = \delta + 1 - \sqrt{(1+\delta)^2 - p_x^2 - p_y^2} \tag{7.84}$$

We transform the momenta:

$$p_x^* = \frac{p_x}{\cos\phi} - h\cos\alpha\frac{\tan\phi}{\cos\phi} \tag{7.85}$$

$$p_y^* = \frac{p_y}{\cos\phi} - h\sin\alpha\frac{\tan\phi}{\cos\phi} \tag{7.86}$$

$$\delta^* = \delta - p_x\cos\alpha\tan\phi - p_y\sin\alpha\tan\phi + h\tan^2\phi \tag{7.87}$$

In order to calculate the angles in the transformed frame, we evaluate:

$$p_z^* = \sqrt{(1+\delta^*)^2 - p_x^{*2} - p_y^{*2}} \tag{7.88}$$

We can now evaluate the following derivatives of the transformed Hamiltonian (from Hamilton's equations it can be easily seen that these are the angles in the boosted frame):

$$h_x^* = \frac{\partial h^*}{\partial p_x^*} = \frac{p_x^*}{p_z^*} \tag{7.89}$$

$$h_y^* = \frac{\partial h^*}{\partial p_y^*} = \frac{p_y^*}{p_z^*} \tag{7.90}$$

$$h_\sigma^* = \frac{\partial h^*}{\partial \delta} = 1 - \frac{\delta^* + 1}{p_z^*} \tag{7.91}$$

These can be used to build the following matrix:

$$L = \begin{pmatrix} (1 + h_x^* \cos\alpha \sin\phi) & h_x^* \sin\alpha \sin\phi & \cos\alpha \tan\phi \\ h_y^* \cos\alpha \sin\phi & \left(1 + h_y^* \sin\alpha \sin\phi\right) & \sin\alpha \tan\phi \\ h_\sigma^* \cos\alpha \sin\phi & h_\sigma^* \sin\alpha \sin\phi & \frac{1}{\cos\phi} \end{pmatrix} \tag{7.92}$$

which can then be used to transform the test-particle positions:

$$\begin{pmatrix} x^* \\ y^* \\ \sigma^* \end{pmatrix} = L \begin{pmatrix} x \\ y \\ \sigma \end{pmatrix} \tag{7.93}$$

7.6.2 Synchro-beam mapping

Following the approach introduced in [26], the strong beam is sliced along z. A common approach is to use constant-charge slices (see Appendix 7.6.6.2). For each particle in the weak beam and for each slice in the strong beam we perform the following.

We identify the position of the Collision Point (CP):

$$S = \frac{\sigma^* - \sigma_{\mathrm{sl}}^*}{2} \tag{7.94}$$

Here σ^* is defined in the reference system of the weak beam ($\sigma^* > 0$ for particles at the head of the weak bunch) while σ_{sl}^* is defined in the reference system of the strong beam ($\sigma_{\mathrm{sl}}^* > 0$ for particles at the head of the strong bunch). S is the coordinate of the collision point in the reference system of the weak beam (from Eq. 7.94, we can see that particles at the head of the weak bunch, collide with particles at the tail of the strong bunch at $S > 0$).

N.B. Here we are making an approximation since we are assuming that particles are moving at the speed of light along z independently on their angles. This means that the presented approach works only for small particle angles. It is for this reason that we need to Lorentz boost to get rid of the crossing angle and we cannot just move to the reference of the strong beam using a rotation (in this case the weak beam would have large angles).

We now evaluate the transverse position of the particle at the CP, with respect to the centroid of the slice, taking into account the particle angles :

$$\overline{x}^* = x^* + p_x^* S - (x_{\mathrm{sl}}^* - p_{x,\mathrm{sl}}^* S) \tag{7.95}$$

$$\overline{y}^* = y^* + p_y^* S - (y_{\mathrm{sl}}^* - p_{y,\mathrm{sl}}^* S) \tag{7.96}$$

Here x_{sl}^*, y_{sl}^*, $p_{x,\mathrm{sl}}^*$ and $p_{y,\mathrm{sl}}^*$ are defined in the coordinate system of the weak beam. The momenta of the strong slice appear with a negative sign since in the weak frame the strong slice is travelling "backwards".

7.6.3 Propagation of the strong beam to the collision point

The distribution of the strong beam in the transverse phase-space can be written using the Σ-matrix [9]:

$$f(\eta) = f_0 e^{-\eta^{\mathrm{T}} \Sigma^{-1} \eta} \tag{7.97}$$

where:

$$\eta = \begin{pmatrix} x \\ p_x \\ y \\ p_y \end{pmatrix} \tag{7.98}$$

Points having same phase space density lie on hyper-elliptic manifolds defined by the equation:

$$\eta^{\mathrm{T}} \Sigma^{-1} \eta = \text{const.} \tag{7.99}$$

Further considerations on the Σ-matrix can be found in Appendix 7.6.6.3.

We transform the Σ-matrix at the Interaction Point to take into account the Lorentz

Boost:

$$\Sigma_{11}^{*0} = \Sigma_{11}^{0} \tag{7.100}$$
$$\Sigma_{12}^{*0} = \Sigma_{12}^{0} / \cos\phi \tag{7.101}$$
$$\Sigma_{13}^{*0} = \Sigma_{13}^{0} \tag{7.102}$$
$$\Sigma_{14}^{*0} = \Sigma_{14}^{0} / \cos\phi \tag{7.103}$$
$$\Sigma_{22}^{*0} = \Sigma_{22}^{0} / \cos^2\phi \tag{7.104}$$
$$\Sigma_{23}^{*0} = \Sigma_{23}^{0} / \cos\phi \tag{7.105}$$
$$\Sigma_{24}^{*0} = \Sigma_{24}^{0} / \cos^2\phi \tag{7.106}$$
$$\Sigma_{33}^{*0} = \Sigma_{33}^{0} \tag{7.107}$$
$$\Sigma_{34}^{*0} = \Sigma_{34}^{0} / \cos\phi \tag{7.108}$$
$$\Sigma_{44}^{*0} = \Sigma_{44}^{0} / \cos^2\phi \tag{7.109}$$
$$\tag{7.110}$$

We transport the position part of the boosted Σ-matrix to the CP (here we are taking into account hourglass effect, assuming that we are in a drift space):

$$\Sigma_{11}^{*} = \Sigma_{11}^{*0} + 2\Sigma_{12}^{*0} S + \Sigma_{22}^{*0} S^2 \tag{7.111}$$
$$\Sigma_{33}^{*} = \Sigma_{33}^{*0} + 2\Sigma_{34}^{*0} S + \Sigma_{44}^{*0} S^2 \tag{7.112}$$
$$\Sigma_{13}^{*} = \Sigma_{13}^{*0} + \left(\Sigma_{14}^{*0} + \Sigma_{23}^{*0}\right) S + \Sigma_{24}^{*0} S^2 \tag{7.113}$$

The Σ-matrix is given in the reference system of the weak beam.
For singular cases we will also need to transport the other terms:

$$\Sigma_{12}^{*} = \Sigma_{12}^{*0} + \Sigma_{22}^{*0} S \tag{7.114}$$
$$\Sigma_{14}^{*} = \Sigma_{14}^{*0} + \Sigma_{24}^{*0} S \tag{7.115}$$
$$\Sigma_{22}^{*} = \Sigma_{22}^{*0} \tag{7.116}$$
$$\Sigma_{23}^{*} = \Sigma_{23}^{*0} + \Sigma_{24}^{*0} S \tag{7.117}$$
$$\Sigma_{24}^{*} = \Sigma_{24}^{*0} \tag{7.118}$$
$$\Sigma_{34}^{*} = \Sigma_{34}^{*0} + \Sigma_{44}^{*0} S \tag{7.119}$$
$$\Sigma_{44}^{*} = \Sigma_{44}^{*0} \tag{7.120}$$

We introduce the following three auxiliary quantities:

$$R\left(S\right) = \Sigma_{11}^{*} - \Sigma_{33}^{*} \tag{7.121}$$
$$W\left(S\right) = \Sigma_{11}^{*} + \Sigma_{33}^{*} \tag{7.122}$$
$$T\left(S\right) = R^2 + 4{\Sigma_{13}^{*}}^2 \tag{7.123}$$

The following derivatives will be needed in the following:

$$\frac{\partial R}{\partial S} = 2\left(\Sigma_{12}^0 - \Sigma_{34}^0\right) + 2S\left(\Sigma_{22}^0 - \Sigma_{44}^0\right) \tag{7.124}$$

$$\frac{\partial W}{\partial S} = 2\left(\Sigma_{12}^0 + \Sigma_{34}^0\right) + 2S\left(\Sigma_{22}^0 + \Sigma_{44}^0\right) \tag{7.125}$$

$$\frac{\partial \Sigma_{13}^*}{\partial S} = \Sigma_{14}^0 + \Sigma_{23}^0 + 2\Sigma_{24}^0 S \tag{7.126}$$

$$\frac{\partial T}{\partial S} = 2R\frac{\partial R}{\partial S} + 8\Sigma_{13}^*\frac{\partial \Sigma_{13}^*}{\partial S} \tag{7.127}$$

We will now compute, at the location of the CP, the coupling angle θ, defining a reference frame in which the beam is decoupled. We will call $\hat{x}$ and $\hat{y}$ the coordinates in the decoupled frame and $\hat{\Sigma}_{11}^*$, $\hat{\Sigma}_{33}^*$ the corresponding squared beam sizes. The angle θ is defined as the angle between the $\hat{x}$-axis and the x-axis.
These quantities can be found by diagonalizing the $x-y$ block of the Σ-matrix. We will make determination choices (Eqs. 7.130, 7.133 and 7.137) so that the set $(\theta, \hat{\Sigma}_{11}^*, \hat{\Sigma}_{33}^*)$ is uniquely defined and the coupling angle θ lies in the interval:

$$-\frac{\pi}{4} < \theta < \frac{\pi}{4} \tag{7.128}$$

Different cases need to be treated separately:

Case T>0, $\left|\Sigma_{13}^*\right|$>0

We evaluate the coupling angle at the position of the CP in the boosted frame:

$$\cos 2\theta = \mathrm{sgn}\left(\Sigma_{11}^* - \Sigma_{33}^*\right)\frac{\Sigma_{11}^* - \Sigma_{33}^*}{\sqrt{\left(\Sigma_{11}^* - \Sigma_{33}^*\right)^2 + 4{\Sigma_{13}^*}^2}} \tag{7.129}$$

Or more synthetically:

$$\cos 2\theta = \mathrm{sgn}(R)\frac{R}{\sqrt{T}} \tag{7.130}$$

In the following we will need also the derivative of this quantity:

$$\frac{\partial}{\partial S}\left[\cos 2\theta\right] = \mathrm{sgn}(R)\left(\frac{\partial R}{\partial S}\frac{1}{\sqrt{T}} - \frac{R}{2\left(\sqrt{T}\right)^3}\frac{\partial T}{\partial S}\right) \tag{7.131}$$

It can be proved that [6]:

$$\cos\theta = \sqrt{\frac{1}{2}\left(1 + \cos 2\theta\right)} \tag{7.132}$$

$$\sin\theta = \mathrm{sgn}(R)\mathrm{sgn}(\Sigma_{13}^*)\sqrt{\frac{1}{2}\left(1 - \cos 2\theta\right)} \tag{7.133}$$

The corresponding derivatives are given by (see Eq. 2.64 in [**?**]):

$$\frac{\partial}{\partial S}\cos\theta = \frac{1}{4\cos\theta}\frac{\partial}{\partial S}\cos 2\theta \tag{7.134}$$

$$\frac{\partial}{\partial S}\sin\theta = -\frac{1}{4\sin\theta}\frac{\partial}{\partial S}\cos 2\theta \tag{7.135}$$

The squared beam sizes in the rotated (un-coupled) boosted frame are given by:

$$\hat{\Sigma}^*_{11} = \frac{1}{2}\left[(\Sigma^*_{11}+\Sigma^*_{33}) + \mathrm{sgn}\,(\Sigma^*_{11}-\Sigma^*_{33})\sqrt{(\Sigma^*_{11}-\Sigma^*_{33})^2 + 4{\Sigma^*_{13}}^2}\right] \tag{7.136}$$

$$\hat{\Sigma}^*_{33} = \frac{1}{2}\left[(\Sigma^*_{11}+\Sigma^*_{33}) - \mathrm{sgn}\,(\Sigma^*_{11}-\Sigma^*_{33})\sqrt{(\Sigma^*_{11}-\Sigma^*_{33})^2 + 4{\Sigma^*_{13}}^2}\right] \tag{7.137}$$

Equation 7.137 can be written in a compact form as:

$$\hat{\Sigma}^*_{11} = \frac{1}{2}\left(W + \mathrm{sgn}(R)\sqrt{T}\right) \tag{7.138}$$

$$\hat{\Sigma}^*_{33} = \frac{1}{2}\left(W - \mathrm{sgn}(R)\sqrt{T}\right) \tag{7.139}$$

The corresponding derivatives, which will be needed in the following, are given by:

$$\frac{\partial}{\partial S}\left[\hat{\Sigma}^*_{11}\right] = \frac{1}{2}\left(\frac{\partial W}{\partial S} + \mathrm{sgn}(R)\frac{1}{2\sqrt{T}}\frac{\partial T}{\partial S}\right) \tag{7.140}$$

$$\frac{\partial}{\partial S}\left[\hat{\Sigma}^*_{33}\right] = \frac{1}{2}\left(\frac{\partial W}{\partial S} - \mathrm{sgn}(R)\frac{1}{2\sqrt{T}}\frac{\partial T}{\partial S}\right) \tag{7.141}$$

Case T>0, $\left|\Sigma^*_{13}\right|$=0:

The treatment of the previous case is still applicable with the exception of Eq. 7.135 in which the denominator becomes zero. This happens when Σ^*_{13}=0, which implies $\sqrt{T} = |R|$ and therefore $\cos 2\theta = 1$. The case $T = 0$ will be treated separately later, therefore here we can assume $|R| > 0$. We can expand with respect to Σ^*_{13}/R obtaining:

$$\cos 2\theta = \frac{|R|}{\sqrt{R^2 + 4{\Sigma^*_{13}}^2}} = \frac{1}{\sqrt{1+4\frac{{\Sigma^*_{13}}^2}{R^2}}} \simeq \frac{1}{1+2\frac{{\Sigma^*_{13}}^2}{R^2}} \simeq 1 - 2\frac{{\Sigma^*_{13}}^2}{R^2} \tag{7.142}$$

Replacing these result in Eq. 7.133 we obtain:

$$\sin\theta = \mathrm{sgn}(R)\mathrm{sgn}(\Sigma^*_{13})\frac{\left|\Sigma^*_{13}\right|}{|R|} = \frac{\Sigma^*_{13}}{R} \tag{7.143}$$

We call S_0 the location at which $\Sigma^*_{13} = 0$. At this location we define the auxiliary quantities:

$$c = \Sigma^*_{14} + \Sigma^*_{23} \tag{7.144}$$

$$d = \Sigma^*_{24} \tag{7.145}$$

We introduce $\Delta S = S - S_0$ and we can write using Eqs. 7.111–7.113:

$$\Sigma_{13}^* = c\Delta S + d\Delta S^2 \tag{7.146}$$

By taking the derivative of Eq. 7.143 and using Eq. 7.146 we obtain:

$$\frac{\partial}{\partial S}\sin\theta = \frac{1}{R^2}\left[(c + 2d\Delta S)\,R\; - \frac{\partial R}{\partial S}\left(c\Delta S + d\Delta S^2\right)\right] \tag{7.147}$$

In the implementation we need only the value for ΔS=0, which is simply given by:

$$\frac{\partial}{\partial S}\sin\theta = \frac{c}{R} \tag{7.148}$$

Case T=0, $|c|$>0

Special care has to be taken at sections S_0 at which $\Sigma_{11}^* = \Sigma_{33}^*$ and $\Sigma_{13}^* = 0$ as Eqs. 7.130 and 7.141 cannot be evaluated directly. Also in this case we define:

$$\Delta S = S - S_0 \tag{7.149}$$

At the location of the apparent singularity (ΔS=0) we define the auxiliary quantities:

$$a = \Sigma_{12}^* - \Sigma_{34}^* \tag{7.150}$$
$$b = \Sigma_{22}^* - \Sigma_{44}^* \tag{7.151}$$
$$c = \Sigma_{14}^* + \Sigma_{23}^* \tag{7.152}$$
$$d = \Sigma_{24}^* \tag{7.153}$$

and therefore, using Eqs. 7.111–7.113, we can write:

$$R = 2a\Delta S + b\Delta S^2 \tag{7.154}$$
$$\Sigma_{13}^* = c\Delta S + d\Delta S^2 \tag{7.155}$$

With these definitions the function T (defined by Eq. 7.123) can be expanded around $\Delta S = 0$ (using the Eqs. 7.111, 7.112, 7.113):

$$T = \Delta S^2\left[(2a + b\Delta S)^2 + 4\,(c + d\Delta S)^2\right] \tag{7.156}$$

Replacing Eq. 7.156 in Eq. 7.130 allows removing the apparent singularity:

$$\cos 2\theta = \frac{|2a + b\Delta S|}{\sqrt{(2a + b\Delta S)^2 + 4\,(c + d\Delta S)^2}} \tag{7.157}$$

This can be derived obtaining:

$$\frac{\partial}{\partial S}\left[\cos 2\theta\right] = \mathrm{sgn}(2a + b\Delta S)\left[\frac{b}{\sqrt{(2a + b\Delta S)^2 + 4\,(c + d\Delta S)^2}}\right.$$
$$\left. - \frac{(2a + b\Delta S)(2ab + b^2\Delta s + 4cd + 4d^2\Delta S)}{\left(\sqrt{(2a + b\Delta S)^2 + 4\,(c + d\Delta S)^2}\right)^3}\right] \tag{7.158}$$

Similarly, replacing Eq. 7.156 in Eq. 7.139 we obtain:

$$\hat{\Sigma}^*_{11} = \frac{W}{2} + \frac{1}{2}\mathrm{sgn}\left(2a\Delta S + b\Delta S^2\right)|\Delta S|\sqrt{(2a+b\Delta S)^2 + 4\,(c+d\Delta S)^2} \tag{7.159}$$

$$\hat{\Sigma}^*_{33} = \frac{W}{2} - \frac{1}{2}\mathrm{sgn}\left(2a\Delta S + b\Delta S^2\right)|\Delta S|\sqrt{(2a+b\Delta S)^2 + 4\,(c+d\Delta S)^2} \tag{7.160}$$

This can be derived obtaining:

$$\frac{\partial}{\partial S}\left[\hat{\Sigma}^*_{11}\right] = \frac{1}{2}\frac{\partial W}{\partial S} + \frac{1}{2}\mathrm{sgn}\left(2a\Delta S + b\Delta S^2\right)\mathrm{sgn}(\Delta S)\left[\sqrt{(2a+b\Delta S)^2 + 4\,(c+d\Delta S)^2} + \frac{\Delta S\left(2ab + b^2\Delta s + 4cd + 4d^2\Delta S\right)}{\sqrt{(2a+b\Delta S)^2 + 4\,(c+d\Delta S)^2}}\right] \tag{7.161}$$

$$\frac{\partial}{\partial S}\left[\hat{\Sigma}^*_{33}\right] = \frac{1}{2}\frac{\partial W}{\partial S} - \frac{1}{2}\mathrm{sgn}\left(2a\Delta S + b\Delta S^2\right)\mathrm{sgn}(\Delta S)\left[\sqrt{(2a+b\Delta S)^2 + 4\,(c+d\Delta S)^2} + \frac{\Delta S\left(2ab + b^2\Delta s + 4cd + 4d^2\Delta S\right)}{\sqrt{(2a+b\Delta S)^2 + 4\,(c+d\Delta S)^2}}\right] \tag{7.162}$$

In the implementation only the values at ΔS=0 are needed. For this case the obtained results above can be simplified as:

$$\cos 2\theta = \frac{|2a|}{2\sqrt{a^2+c^2}} \tag{7.163}$$

$$\frac{\partial}{\partial S}\left[\cos 2\theta\right] = \mathrm{sgn}(2a)\left[\frac{b}{2\sqrt{a^2+c^2}} - \frac{a(ab+2cd)}{2\left(\sqrt{a^2+c^2}\right)^3}\right] \tag{7.164}$$

$$\hat{\Sigma}^*_{11} = \frac{W}{2} \tag{7.165}$$

$$\hat{\Sigma}^*_{33} = \frac{W}{2} \tag{7.166}$$

$$\frac{\partial}{\partial S}\left[\hat{\Sigma}^*_{11}\right] = \frac{1}{2}\frac{\partial W}{\partial S} + \mathrm{sgn}(2a)\sqrt{a^2+c^2} \tag{7.167}$$

$$\frac{\partial}{\partial S}\left[\hat{\Sigma}^*_{33}\right] = \frac{1}{2}\frac{\partial W}{\partial S} - \mathrm{sgn}(2a)\sqrt{a^2+c^2} \tag{7.168}$$

Eqs. 7.133 and 7.135 can still be used to evaluate $\sin\theta$ and $\cos\theta$ and the corresponding derivatives, once we assume that $\mathrm{sgn}(0) = 1$ and noticing from Eqs. 7.154 and 7.155 that for small ΔS:

$$\mathrm{sgn}(R)\mathrm{sgn}(\Sigma^*_{13}) = \mathrm{sgn}(a)\mathrm{sgn}(c) \tag{7.169}$$

Case T=0, c=0, $|a|$>0

The treatment of the previous case is still applicable with the exception of Eq. 7.135 in which the denominator becomes zero.
For this case we can write (from Eq. 7.157) around the point where this condition is verified:

$$\cos 2\theta = \frac{1}{\sqrt{1+\frac{4d^2\Delta S^2}{(2a+b\Delta S)^2}}} \simeq 1 - \frac{2d^2\Delta S^2}{(2a+b\Delta S)^2} \tag{7.170}$$

We notice from Eqs. 7.154 and 7.155 that for small ΔS:

$$\mathrm{sgn}(R)\mathrm{sgn}(\Sigma_{13}^*) = \mathrm{sgn}(a)\mathrm{sgn}(d)\mathrm{sgn}(\Delta S) \tag{7.171}$$

Replacing Eq. 7.170 and 7.171 into in Eq. 7.133 we obtain:

$$\sin\theta = \frac{d\Delta S}{2a}\left|1 - \frac{b\Delta S}{2a}\right| \tag{7.172}$$

which can be derived in $\Delta S = 0$ obtaining:

$$\frac{\partial}{\partial S}\sin\theta = \frac{d}{2a} \tag{7.173}$$

The case in which also $d = 0$ is (or is equivalent to) the uncoupled case as Σ_{13}^* is zero for all S.

Case T=0, c=0, a=0

Around the apparently singular point we can write:

$$R = b\Delta S^2 \tag{7.174}$$

$$\Sigma_{13}^* = d\Delta S^2 \tag{7.175}$$

Therefore:

$$T = S^4\left(b^2 + 4d^2\right) \tag{7.176}$$

and:

$$\cos 2\theta = \frac{|b|}{\sqrt{b^2+4d^2}} \tag{7.177}$$

which is a constant. Eqs. 7.133 and 7.135 can still be used to evaluate $\sin\theta$ and $\cos\theta$ while the corresponding derivatives vanish:
This can be derived obtaining:

$$\frac{\partial}{\partial S}\cos\theta = 0 \tag{7.178}$$

$$\frac{\partial}{\partial S}\sin\theta = 0 \tag{7.179}$$

Replacing $a = c = 0$ into Eq 7.160 we obtain:

$$\hat{\Sigma}^*_{11} = \frac{W}{2} + \frac{1}{2}\mathrm{sgn}(b)\Delta S^2\sqrt{b^2+4d^2} \tag{7.180}$$

$$\hat{\Sigma}^*_{33} = \frac{W}{2} - \frac{1}{2}\mathrm{sgn}(b)\Delta S^2\sqrt{b^2+4d^2} \tag{7.181}$$

and:

$$\frac{\partial}{\partial S}\left[\hat{\Sigma}^*_{11}\right] = \frac{1}{2}\frac{\partial W}{\partial S} \tag{7.182}$$

$$\frac{\partial}{\partial S}\left[\hat{\Sigma}^*_{33}\right] = \frac{1}{2}\frac{\partial W}{\partial S} \tag{7.183}$$

The case in which also $d = 0$ is (or is equivalent to the uncoupled case) as Σ^*_{13} is zero for all S.

7.6.4 Forces and kicks on weak beam particles

The positions of the weak beam particle in the un-coupled boosted frame are given by:

$$\hat{\bar{x}}^* = \bar{x}^*\cos\theta + \bar{y}^*\sin\theta \tag{7.184}$$

$$\hat{\bar{y}}^* = -\bar{x}^*\sin\theta + \bar{y}^*\cos\theta \tag{7.185}$$

In the following we will also need to evaluate:

$$\frac{\partial}{\partial S}\left[\hat{\bar{x}}^*\left(\theta(S)\right)\right] = \frac{\partial \bar{x}^*}{\partial S}\cos\theta + \bar{x}^*\frac{\partial}{\partial S}\left[\cos\theta\right] + \frac{\partial \bar{y}^*}{\partial S}\sin\theta + \bar{y}^*\frac{\partial}{\partial S}\left[\sin\theta\right] \tag{7.186}$$

$$\frac{\partial}{\partial S}\left[\hat{\bar{y}}^*\left(\theta(S)\right)\right] = -\frac{\partial \bar{x}^*}{\partial S}\sin\theta - \bar{x}^*\frac{\partial}{\partial S}\left[\sin\theta\right] + \frac{\partial \bar{y}^*}{\partial S}\cos\theta + \bar{y}^*\frac{\partial}{\partial S}\left[\cos\theta\right] \tag{7.187}$$

In this boosted, rotated and re-centered frame, closed formulas exist to evaluate the following quantities:

$$\hat{F}^*_x = -K_{sl}\frac{\partial \hat{U}^*}{\partial \hat{\bar{x}}^*}\left(\hat{\bar{x}}^*, \hat{\bar{y}}^*, \hat{\Sigma}^*_{11}, \hat{\Sigma}^*_{33}\right) \tag{7.188}$$

$$\hat{F}^*_y = -K_{sl}\frac{\partial \hat{U}^*}{\partial \hat{\bar{y}}^*}\left(\hat{\bar{x}}^*, \hat{\bar{y}}^*, \hat{\Sigma}^*_{11}, \hat{\Sigma}^*_{33}\right) \tag{7.189}$$

$$\hat{G}^*_x = -K_{sl}\frac{\partial \hat{U}^*}{\partial \hat{\Sigma}^*_{11}}\left(\hat{\bar{x}}^*, \hat{\bar{y}}^*, \hat{\Sigma}^*_{11}, \hat{\Sigma}^*_{33}\right) \tag{7.190}$$

$$\hat{G}^*_y = -K_{sl}\frac{\partial \hat{U}^*}{\partial \hat{\Sigma}^*_{33}}\left(\hat{\bar{x}}^*, \hat{\bar{y}}^*, \hat{\Sigma}^*_{33}, \hat{\Sigma}^*_{33}\right) \tag{7.191}$$

where $\hat{U}^*$ is the electric potential associated to the normalized transverse distribution and:

$$K_{sl} = \frac{N_{sl}q_{sl}q_0}{P_0 c} \tag{7.192}$$

where N_{sl} is the number of particles in the strong-beam slice, q_{sl} and q_0 are the particle charges for the strong and weak beam respectively, P_0 is the reference momentum of the weak beam.

The minus sign in the Eqs. 7.188-7.191 comes from the definition of electric potential, i.e. $E = -\nabla U$.

For a bi-Gaussian beam (elliptic) [26]:

$$\hat{f}_x^* = -\frac{\partial \hat{U}^*}{\partial \hat{\bar{x}}^*} = \frac{1}{2\epsilon_0\sqrt{2\pi\left(\hat{\Sigma}_{11}^* - \hat{\Sigma}_{33}^*\right)}}\mathrm{Im}\left[w\left(\frac{\hat{\bar{x}}^* + i\hat{\bar{y}}^*}{\sqrt{2\left(\hat{\Sigma}_{11}^* - \hat{\Sigma}_{33}^*\right)}}\right)\right. \\ \left. - \exp\left(-\frac{(\hat{\bar{x}}^*)^2}{2\hat{\Sigma}_{11}^*} - \frac{(\hat{\bar{y}}^*)^2}{2\hat{\Sigma}_{33}^*}\right) w\left(\frac{\hat{\bar{x}}^*\sqrt{\frac{\hat{\Sigma}_{33}^*}{\hat{\Sigma}_{11}^*}} + i\hat{\bar{y}}^*\sqrt{\frac{\hat{\Sigma}_{11}^*}{\hat{\Sigma}_{33}^*}}}{\sqrt{2\left(\hat{\Sigma}_{11}^* - \hat{\Sigma}_{33}^*\right)}}\right)\right] \quad (7.193)$$

$$\hat{f}_y^* = -\frac{\partial \hat{U}^*}{\partial \hat{\bar{x}}^*} = \frac{1}{2\epsilon_0\sqrt{2\pi\left(\hat{\Sigma}_{11}^* - \hat{\Sigma}_{33}^*\right)}}\mathrm{Re}\left[w\left(\frac{\hat{\bar{x}}^* + i\hat{\bar{y}}^*}{\sqrt{2\left(\hat{\Sigma}_{11}^* - \hat{\Sigma}_{33}^*\right)}}\right)\right. \\ \left. - \exp\left(-\frac{(\hat{\bar{x}}^*)^2}{2\hat{\Sigma}_{11}^*} - \frac{(\hat{\bar{y}}^*)^2}{2\hat{\Sigma}_{33}^*}\right) w\left(\frac{\hat{\bar{x}}^*\sqrt{\frac{\hat{\Sigma}_{33}^*}{\hat{\Sigma}_{11}^*}} + i\hat{\bar{y}}^*\sqrt{\frac{\hat{\Sigma}_{11}^*}{\hat{\Sigma}_{33}^*}}}{\sqrt{2\left(\hat{\Sigma}_{11}^* - \hat{\Sigma}_{33}^*\right)}}\right)\right] \quad (7.194)$$

$$\hat{g}_x^* = -\frac{\partial \hat{U}^*}{\partial \hat{\Sigma}_{11}^*} = -\frac{1}{2\left(\hat{\Sigma}_{11}^* - \hat{\Sigma}_{33}^*\right)}\left\{\hat{\bar{x}}^*\hat{E}_x^* + \hat{\bar{y}}^*\hat{E}_y^* + \frac{1}{2\pi\epsilon_0}\left[\sqrt{\frac{\hat{\Sigma}_{33}^*}{\hat{\Sigma}_{11}^*}}\exp\left(-\frac{(\hat{\bar{x}}^*)^2}{2\hat{\Sigma}_{11}^*} - \frac{(\hat{\bar{y}}^*)^2}{2\hat{\Sigma}_{33}^*}\right) - 1\right]\right\} \quad (7.195)$$

$$\hat{g}_y^* = -\frac{\partial \hat{U}^*}{\partial \hat{\Sigma}_{33}^*} = \frac{1}{2\left(\hat{\Sigma}_{11}^* - \hat{\Sigma}_{33}^*\right)}\left\{\hat{\bar{x}}^*\hat{E}_x^* + \hat{\bar{y}}^*\hat{E}_y^* + \frac{1}{2\pi\epsilon_0}\left[\sqrt{\frac{\hat{\Sigma}_{11}^*}{\hat{\Sigma}_{33}^*}}\exp\left(-\frac{(\hat{\bar{x}}^*)^2}{2\hat{\Sigma}_{11}^*} - \frac{(\hat{\bar{y}}^*)^2}{2\hat{\Sigma}_{33}^*}\right) - 1\right]\right\} \quad (7.196)$$

where w is the Faddeeva function.

For a round beam, i.e. $\hat{\Sigma}^*_{11} = \hat{\Sigma}^*_{33} = \hat{\Sigma}^*$:

$$\hat{f}^*_x = -\frac{\partial \hat{U}^*}{\partial \hat{\bar{x}}^*} = \frac{1}{2\pi\epsilon_0}\left[1 - \exp\left(-\frac{(\hat{\bar{x}}^*)^2 + (\hat{\bar{y}}^*)^2}{2\hat{\Sigma}^*}\right)\right]\frac{x}{(\hat{\bar{x}}^*)^2 + (\hat{\bar{y}}^*)^2} \tag{7.197}$$

$$\hat{f}^*_y = -\frac{\partial \hat{U}^*}{\partial \hat{\bar{x}}^*} = \frac{1}{2\pi\epsilon_0}\left[1 - \exp\left(-\frac{(\hat{\bar{x}}^*)^2 + (\hat{\bar{y}}^*)^2}{2\hat{\Sigma}^*}\right)\right]\frac{y}{(\hat{\bar{x}}^*)^2 + (\hat{\bar{y}}^*)^2} \tag{7.198}$$

$$\hat{g}^*_x = -\frac{\partial \hat{U}^*}{\partial \hat{\Sigma}^*_{11}} = \frac{1}{2\left[(\hat{\bar{x}}^*)^2 + (\hat{\bar{y}}^*)^2\right]}\left[\hat{\bar{y}}^*\hat{E}^*_y - \hat{\bar{x}}^*\hat{E}^*_x + \frac{1}{2\pi\epsilon_0}\frac{\left(\hat{\bar{x}}^*\right)^2}{\hat{\Sigma}^*}\exp\left(-\frac{(\hat{\bar{x}}^*)^2 + (\hat{\bar{y}}^*)^2}{2\hat{\Sigma}^*}\right)\right] \tag{7.199}$$

$$\hat{g}^*_y = -\frac{\partial \hat{U}^*}{\partial \hat{\Sigma}^*_{33}} = \frac{1}{2\left[(\hat{\bar{x}}^*)^2 + (\hat{\bar{y}}^*)^2\right]}\left[\hat{\bar{x}}^*\hat{E}^*_x - \hat{\bar{y}}^*\hat{E}^*_y + \frac{1}{2\pi\epsilon_0}\frac{\left(\hat{\bar{y}}^*\right)^2}{\hat{\Sigma}^*}\exp\left(-\frac{(\hat{\bar{x}}^*)^2 + (\hat{\bar{y}}^*)^2}{2\hat{\Sigma}^*}\right)\right] \tag{7.200}$$

We have used lower-case symbols to indicate that the factor given by Eq. 7.192 is not yet applied.

The transverse kicks in the coupled (but still boosted) reference frame are given by:

$$F^*_x = \hat{F}^*_x\cos\theta - \hat{F}^*_y\sin\theta \tag{7.201}$$

$$F^*_y = \hat{F}^*_x\sin\theta + \hat{F}^*_y\cos\theta \tag{7.202}$$

To compute the longitudinal kick we notice from Eq. 7.94 that:

$$\frac{\partial}{\partial z} = \frac{1}{2}\frac{\partial}{\partial S} \tag{7.203}$$

Therefore:

$$F^*_z = \frac{1}{2}\frac{\partial}{\partial S}\left[\hat{U}^*\left(\hat{\bar{x}}^*\left(\theta(S)\right), \hat{\bar{y}}^*\left(\theta(S)\right), \hat{\Sigma}^*_{11}(S), \hat{\Sigma}^*_{33}(S)\right)\right] \tag{7.204}$$

This can be rewritten as:

$$F^*_z = \frac{1}{2}\left(\hat{F}^*_x\frac{\partial}{\partial S}\left[\hat{\bar{x}}^*\left(\theta(S)\right)\right] + \hat{F}^*_y\frac{\partial}{\partial S}\left[\hat{\bar{y}}^*\left(\theta(S)\right)\right] + \hat{G}^*_x\frac{\partial}{\partial S}\left[\hat{\Sigma}^*_{11}(S)\right] + \hat{G}^*_y\frac{\partial}{\partial S}\left[\hat{\Sigma}^*_{33}(S)\right]\right) \tag{7.205}$$

where all the terms have been evaluated before.
The quantities evaluated so far can be used to compute the effect of the beam-beam interaction on the particles coordinates and momenta [26]:

$$x^*_{new} = x^* - SF^*_x \tag{7.206}$$

$$p^*_{x,new} = p^*_x + F^*_x \tag{7.207}$$

$$y^*_{new} = y^* - SF^*_y \tag{7.208}$$

$$p^*_{y,new} = p^*_y + F^*_y \tag{7.209}$$

$$z^*_{new} = z^* \tag{7.210}$$

$$\delta^*_{new} = \delta^* + F^*_z + \frac{1}{2}\left[F^*_x\left(p^*_x + \frac{1}{2}F^*_x + p^*_{x,\mathrm{sl}}\right) + F^*_y\left(p^*_y + \frac{1}{2}F^*_y + p^*_{y,\mathrm{sl}}\right)\right] \tag{7.211}$$

The physical meaning of the different terms in these equations is illustrated in [28].

7.6.5 Inverse Lorentz boost (for the weak beam)

Now we need to go back to the accelerator coordinates by undoing the transformation described in Sec. 7.6.1.
As before we evaluate:

$$p_z^* = \sqrt{(1+\delta^*)^2 - p_x^{*2} - p_y^{*2}} \tag{7.212}$$

and then:

$$h_x^* = \frac{p_x^*}{p_z^*} \tag{7.213}$$

$$h_y^* = \frac{p_y^*}{p_z^*} \tag{7.214}$$

$$h_\sigma^* = 1 - \frac{\delta^*+1}{p_z^*} \tag{7.215}$$

We invert the matrix (7.92) using Cramer's rule:

$$\mathrm{Det}\,(L) = \frac{1}{\cos\phi} + \left(h_x^*\cos\alpha + h_y^*\sin\alpha - h_\sigma^*\sin\phi\right)\tan\phi \tag{7.216}$$

$$L^{\mathrm{inv}} = \frac{1}{\mathrm{Det}\,(L)} \times \begin{pmatrix} \left(\frac{1}{\cos\phi} + \sin\alpha\tan\phi\left(h_y^* - h_\sigma^*\sin\alpha\sin\phi\right)\right) & \sin\alpha\tan\phi\left(h_\sigma^*\cos\alpha\sin\phi - h_x^*\right) & -\tan\phi\left(\cos\alpha - h_x^*\sin^2\alpha\sin\phi + h_y^*\cos\alpha\sin\alpha\sin\phi\right) \\ \cos\alpha\tan\phi\left(-h_y^* + h_\sigma^*\sin\alpha\sin\phi\right) & \left(\frac{1}{\cos\phi} + \cos\alpha\tan\phi\left(h_x^* - h_\sigma^*\cos\alpha\sin\phi\right)\right) & -\tan\phi\left(\sin\alpha - h_y^*\cos^2\alpha\sin\phi + h_x^*\cos\alpha\sin\alpha\sin\phi\right) \\ -h_\sigma^*\cos\alpha\sin\phi & -h_\sigma^*\sin\alpha\sin\phi & \left(1 + h_x^*\cos\alpha\sin\phi + h_y^*\sin\alpha\sin\phi\right) \end{pmatrix} \tag{7.217}$$

This can be used to transform the positions:

$$\begin{pmatrix} x \\ y \\ \sigma \end{pmatrix} = L^{\mathrm{inv}} \begin{pmatrix} x^* \\ y^* \\ \sigma^* \end{pmatrix} \tag{7.218}$$

The Hamiltonian can be transformed with a re-scaling:

$$h = h^*\cos^2\phi = \left(\delta^* + 1 - \sqrt{(1+\delta^*)^2 - p_x^{*2} - p_y^{*2}}\right)\cos^2\phi \tag{7.219}$$

This can be used to transform the transverse momenta (inverting Eqs. 7.85 and following):

$$p_x = p_x^*\cos\phi + h\cos\alpha\tan\phi \tag{7.220}$$

$$p_y = p_y^*\cos\phi + h\sin\alpha\tan\phi \tag{7.221}$$

The longitudinal momentum can be calculated using directly Eq. 7.87:

$$\delta = \delta^* + p_x\cos\alpha\tan\phi + p_y\sin\alpha\tan\phi - h\tan^2\phi \tag{7.222}$$

7.6.6 Additional material

7.6.6.1 Detailed explanation of "the boost" transformation

The reference frame transformation used in Sec. 7.6.1 can be written as [26, 6]:

$$\begin{pmatrix} \sigma^* \\ x^* \\ s^* \\ y^* \end{pmatrix} = A^{-1} {R_{\mathrm{CP}}}^{-1} L_{\mathrm{boost}} R_{\mathrm{CA}} R_{\mathrm{CP}} A \begin{pmatrix} \sigma \\ x \\ s \\ y \end{pmatrix} \tag{7.223}$$

Here A is the matrix transforming the accelerator coordinates (Courant-Snyder) to Cartesian coordinates:

$$\begin{pmatrix} ct \\ X \\ Z \\ Y \end{pmatrix} = A \begin{pmatrix} \sigma \\ x \\ s \\ y \end{pmatrix} = \begin{pmatrix} -1 & 0 & 1 & 0 \\ 0 & 1 & 0 & 0 \\ 0 & 0 & 1 & 0 \\ 0 & 0 & 0 & 1 \end{pmatrix} \begin{pmatrix} \sigma \\ x \\ s \\ y \end{pmatrix} \tag{7.224}$$

R_{CP} is a rotation matrix bringing the crossing plane to the $X - Z$ plane:

$$R_{\mathrm{CP}} = \begin{pmatrix} 1 & 0 & 1 & 0 \\ 0 & \cos\alpha & 0 & \sin\alpha \\ 0 & 0 & 1 & 0 \\ 0 & -\sin\alpha & 0 & \cos\alpha \end{pmatrix} \tag{7.225}$$

R_{CA} is a rotation matrix moving to the barycentric reference frame (in which the two beams are symmetric with respect to the s-axis):

$$R_{\mathrm{CA}} = \begin{pmatrix} 1 & 0 & 0 & 0 \\ 0 & \cos\phi & \sin\phi & 0 \\ 0 & -\sin\phi & \cos\phi & 0 \\ 0 & 0 & 0 & 1 \end{pmatrix} \tag{7.226}$$

L_{boost} is the matrix defining a Lorentz boost in the direction of the rotated X-axis:

$$L_{\mathrm{boost}} = \begin{pmatrix} 1/\cos\phi & -\tan\phi & 0 & 0 \\ -\tan\phi & 1/\cos\phi & 0 & 0 \\ 0 & 0 & 1 & 0 \\ 0 & 0 & 0 & 1 \end{pmatrix} \tag{7.227}$$

The momenta are transformed similarly [6]:

$$\begin{pmatrix} \delta^* \\ p_x^* \\ h^* \\ p_y^* \end{pmatrix} = B^{-1} {R_{\mathrm{CP}}}^{-1} L_{\mathrm{boost}} R_{\mathrm{CA}} R_{\mathrm{CP}} B \begin{pmatrix} \delta \\ p_x \\ h \\ p_y \end{pmatrix} \tag{7.228}$$

where the transformation from accelerator to Cartesian coordinates given by:

$$\begin{pmatrix} E/c - p_0 \\ P_x \\ P_z - p_0 \\ P_y \end{pmatrix} = p_0 \begin{pmatrix} 1 & 0 & 0 & 0 \\ 0 & 1 & 0 & 0 \\ 0 & 0 & -1 & 0 \\ 0 & 0 & 0 & 1 \end{pmatrix} \begin{pmatrix} \delta \\ p_x \\ h \\ p_y \end{pmatrix} \tag{7.229}$$

As explaned in Sec.7.6.1 not all particles with $s = 0$ are fixed points of the transformation, therefore a drift back to s=0 needs to be performed as we are tracking w.r.t. s and not w.r.t. time. The net effect of the transformation is to move from the reference frame of the weak beam to the boosted barycentric frame.

7.6.6.2 Constant charge slicing

We consider a Gaussian longitudinal bunch distribution:

$$\lambda(z) = \frac{1}{\sigma_z \sqrt{2\pi}} e^{-\frac{z^2}{2\sigma_z^2}} \tag{7.230}$$

We introduce the cumulative distribution function:

$$Q(z) = \int_{-\infty}^{z} \lambda(z')dz' = \frac{1}{2} + \frac{1}{2}\mathrm{erf}\left(\frac{z}{\sqrt{2}\sigma_z}\right) \tag{7.231}$$

We define longitudinal cuts z_n^{cut} such that the bunch is sliced in N sections having the same charge:

$$Q(z_n^{\mathrm{cut}}) = \frac{n}{N} \tag{7.232}$$

Replacing 7.232 in 7.231 we obtain:

$$z_n^{\mathrm{cut}} = \sqrt{2}\sigma_z \mathrm{erf}^{-1}\left(\frac{2n}{N} - 1\right) \tag{7.233}$$

For each slice we need to find the longitudinal centroid position. For generic slice having edges z_1 and z_2 the centroid position can be written as:

$$z^{centroid} = \frac{1}{Q(z_2) - Q(z_1)} \int_{z_1}^{z_2} z\lambda(z)dz = \frac{\sigma_z}{\sqrt{2\pi}\left(Q(z_2) - Q(z_1)\right)} \left(e^{-\frac{z_1^2}{2\sigma_z^2}} - e^{-\frac{z_2^2}{2\sigma_z^2}}\right) \tag{7.234}$$

7.6.6.3 Considerations on the Σ-matrix description

Given the reduced Σ-matrix of the beam (including only position terms, no momenta):

$$\Sigma = \begin{pmatrix} \Sigma_{11} & \Sigma_{13} \\ \Sigma_{13} & \Sigma_{33} \end{pmatrix} \tag{7.235}$$

the distribution for a Gaussian beam can be written as:

$$\rho(\mathbf{x}) = \rho_0 e^{-\mathbf{x}^{\mathrm{T}}\Sigma^{-1}\mathbf{x}} \tag{7.236}$$

Points having same density lie con ellipses defined by the equation:

$$\mathbf{x}^{\mathrm{T}}\Sigma^{-1}\mathbf{x} = \text{const.} \tag{7.237}$$

As Σ is symmetric, it can be diagonalized:

$$\Sigma = \mathbf{V}\mathbf{W}\mathbf{V}^{T} \tag{7.238}$$

where the matrix **V** has in its columns the eigenvectors of Σ and **W** is a diagonal matrix with the corresponding eigenvalues:

$$W = \begin{pmatrix} \hat{\Sigma}_{11} & 0 \\ 0 & \hat{\Sigma}_{33} \end{pmatrix} \tag{7.239}$$

V is a unitary matrix (eigenvectors are ortho-normal):

$$\mathbf{V}\mathbf{V}^{T} = \mathbf{I} \Rightarrow \mathbf{V}^{-1} = \mathbf{V}^{T} \tag{7.240}$$

V can be used to transform coordinates from the initial frame to the de-coupled frame: where $\hat{\mathbf{x}}$ are the coordinates in the decoupled frame, i.e. the projections of of **x** on the eigenvectors:

$$\hat{\mathbf{x}} = \mathbf{V}^{T}\mathbf{x} \tag{7.241}$$

Combining Eqs. 7.238 and 7.240 we can write:

$$\Sigma^{-1} = \mathbf{V}\mathbf{W}^{-1}\mathbf{V}^{T} \tag{7.242}$$

This can be replaced in Eq. 7.237, re-writing the equation of the ellipse as:

$$\mathbf{x}^{\mathrm{T}}\mathbf{V}\mathbf{W}^{-1}\mathbf{V}^{T}\mathbf{x} = \text{const.} \tag{7.243}$$

Using Eq. 7.241 we obtain the equation of the ellipse in the reference system of the eigenvectors:

$$\hat{\mathbf{x}}^{\mathrm{T}}\mathbf{W}^{-1}\hat{\mathbf{x}} = \text{const.} \tag{7.244}$$

which can be rewritten in the familiar form:

$$\frac{\hat{x}^2}{\hat{\Sigma}_{11}} + \frac{\hat{y}^2}{\hat{\Sigma}_{33}} = \text{const.} \tag{7.245}$$

Once the Σ-matrix is assigned, the one-sigma ellipse can be drawn by the following procedure:

- We diagonalize Σ and we generate an auxiliary matrix defined as:

$$\mathbf{A} = \mathbf{V}\sqrt{\mathbf{W}}\mathbf{V}^T \tag{7.246}$$

- We generate a set of points in the unitary circle

$$\mathbf{z} = \begin{bmatrix} \cos t \\ \sin t \end{bmatrix} \tag{7.247}$$

- We apply $\mathbf{A}$ to t to generate points on the one-sigma ellipse:

$$\mathbf{x}_{1\sigma} = \mathbf{A}\mathbf{z} \tag{7.248}$$

This can be verified as follows:

$$\begin{aligned} {\mathbf{x}_{1\sigma}}^{\mathrm{T}}\Sigma^{-1}\mathbf{x}_{1\sigma} &= \mathbf{z}^{\mathrm{T}}\mathbf{A}^{\mathrm{T}}\Sigma^{-1}\mathbf{A}\mathbf{z} = \mathbf{z}^{\mathrm{T}}(\mathbf{V}\sqrt{\mathbf{W}}\mathbf{V})(\mathbf{V}^T\mathbf{W}^{-1}\mathbf{V}^T)(\mathbf{V}\sqrt{\mathbf{W}}\mathbf{V}^T)\mathbf{z} \\ &= \mathbf{z}^{\mathrm{T}}\mathbf{V}\sqrt{\mathbf{W}}\mathbf{W}^{-1}\sqrt{\mathbf{W}}\mathbf{V}^T\mathbf{z} = \mathbf{z}^{\mathrm{T}}\mathbf{V}\mathbf{V}^T\mathbf{z} = \mathbf{z}^{\mathrm{T}}\mathbf{z} = 1 \end{aligned} \tag{7.249}$$

7.7 Beam-beam interaction (6d model, Particle In Cell)

To simulate self-consistently the interaction between two bunches of particles, it is possible to use the Particle In Cell method. The computation is done in a boosted reference frame in which the bunches move mainly along s as illustrated in the previous section.
For this purpose, as for space charge simulations, we define a uniform 3D grid with grid sizes Δx, Δy, $\Delta\zeta$. We note that each value of ζ corresponds to a different time of arrival at the Interaction Point (IP):

$$\zeta = s_{\mathrm{IP}} - \beta_0 c t \;\Leftrightarrow\; t = \frac{s_{\mathrm{IP}} - \zeta}{\beta_0 c} \tag{7.250}$$

We simulate the interaction in discrete time intervals corresponding to the passage of the different slices. The duration of each interval is

$$\Delta t = \frac{\Delta\zeta}{\beta_0 c} \tag{7.251}$$

We call t_i the time at which the i-th slice is passing at the IP. The is is related to the ζ_i coordinate of the slice by the relation

$$t_i = \frac{s_{\mathrm{IP}} - \zeta_i}{\beta_0 c} \tag{7.252}$$

7.7.1 Propagation of particles during the interaction

From the conventional tracking using s as independent variable we get for all particles the coordinates at the IP, which we call x_{IP}, $p_{\mathrm{x\,IP}}$, y_{IP}, $p_{\mathrm{y\,IP}}$, $zeta_{\mathrm{IP}} = s_{\mathrm{y\,IP}} - \beta_0 c t_{\mathrm{IP}}$, where t_{IP} is the time of arrival of the particle at the IP. Assuming the motion is in a drift space, for each time step, we propagate the particles from the IP to their positions at the time t_i:

$$x\left(t_i\right) = x_{\mathrm{IP}} + \beta_x c\left(t_i - t_{\mathrm{IP}}\right) = x_{\mathrm{IP}} + \beta_x c\left(\frac{s_{\mathrm{IP}} - \zeta_i}{\beta_0 c} - \frac{s_{\mathrm{IP}} - \zeta_{\mathrm{IP}}}{\beta_0 c}\right) \tag{7.253}$$

Using the fact that:

$$p_x = \frac{P_x}{P_0} = \frac{m_0 \gamma \beta_x c}{m_0 \gamma_0 \beta_0 c} = \frac{\gamma \beta_x}{\gamma_0 \beta_0} \tag{7.254}$$

we can write:

$$x\left(t_i\right) = x_{\mathrm{IP}} + p_x \frac{\gamma_0}{\gamma}\left(\zeta_{\mathrm{IP}} - \zeta_i\right) \tag{7.255}$$

With the coordinates of the propagated particles we can solve a Poisson problem having as source the 3D particle distribution at time t_i. Using the fact that the bunches are elongated and relativistic, we can solve the 2D Poisson equation instead of the full 3D problem. This procedure needs to be performed for the two colliding bunches.

7.7.2 Time relation between the two beams

For a particle of beam 1 having longitudinal coordinate $\zeta_{\mathrm{IP}}^{\mathrm{B1}}$ we want to know the longitudinal coordinate $\zeta_{\mathrm{IP}}^{\mathrm{B2}}$ corresponding to the section of beam 2 crossing the particle at time t_i.
We assume that the reference systems of the two beams are antiparallel and coincident in transverse:

$$s^{\mathrm{B2}} - s_{\mathrm{IP}}^{\mathrm{B2}} = -\left(s^{\mathrm{B1}} - s_{\mathrm{IP}}^{\mathrm{B1}}\right) \tag{7.256}$$

$$x^{\mathrm{B2}} = -x^{\mathrm{B1}} \tag{7.257}$$

$$y^{\mathrm{B2}} = +x^{\mathrm{B1}} \tag{7.258}$$

Similarly as done in Sec. 7.7.1, we can write the s position at the time t_i for the particles of beam 1 and beam 2:

$$s^{\mathrm{B1}}\left(t_i\right) = s_{\mathrm{IP}}^{\mathrm{B1}} + \frac{\beta_s^{\mathrm{B1}}}{\beta_0^{\mathrm{B1}}}\left(\zeta_{\mathrm{IP}}^{\mathrm{B1}} - \zeta_i^{\mathrm{B1}}\right) \tag{7.259}$$

$$s^{\mathrm{B2}}\left(t_i\right) = s_{\mathrm{IP}}^{\mathrm{B2}} + \frac{\beta_s^{\mathrm{B2}}}{\beta_0^{\mathrm{B2}}}\left(\zeta_{\mathrm{IP}}^{\mathrm{B2}} - \zeta_i^{\mathrm{B2}}\right) \tag{7.260}$$

To find particles that are at the same s at time t_i we replace Eqs. 7.259-7.260 in we obtain:

$$\zeta_{\mathrm{IP}}^{\mathrm{B2}} = \zeta_i^{\mathrm{B2}} - \frac{\beta_s^{\mathrm{B1}}}{\beta_0^{\mathrm{B1}}}\frac{\beta_0^{\mathrm{B2}}}{\beta_s^{\mathrm{B2}}}\left(\zeta_{\mathrm{IP}}^{\mathrm{B1}} - \zeta_i^{\mathrm{B1}}\right) \tag{7.261}$$

This relation can be used to probe the field map generated by the other bunch at the position of each particle.

7.7.3 Computation of the kick

The transverse kick at each time step can be written as:

$$\Delta p_x^{\mathrm{B1}} = \frac{\Delta P_x^{\mathrm{B1}}}{P_0^{\mathrm{B1}}} = \frac{F_x \Delta t}{P_0^{\mathrm{B1}}} \tag{7.262}$$

Using Eqs. 7.42 and 7.251, taking onto account that the beams move in opposite directions, we obtain:

$$\Delta p_x^{\mathrm{B1}} = -\frac{q\Delta\zeta^{\mathrm{B1}}}{m_0^{\mathrm{B1}}\gamma_0^{\mathrm{B1}}(\beta_0^{\mathrm{B1}})^2c^2}\left(1+\beta^{\mathrm{B1}}\beta^{\mathrm{B2}}\right)\frac{\partial\phi^{\mathrm{B2}}}{\partial x}(x,y,\zeta^{\mathrm{B2}}) \tag{7.263}$$

7.8 Configuration of beam-beam lenses for tracking simulations (weak-strong)

The effects of the non-linear forces introduced by beam-beam interactions in the Large Hadron Collider (LHC) are studied with tracking simulations using, for example, the SixTrack and sixtracklib codes [29, 30]. In these simulations the beam-beam interactions are modeled by a set of "thin" non-linear lenses around the collision points. "6D beam-beam lenses" based on Hirata's synchro-beam method [26, 31, 28] are used to model the Head-On (HO) interactions at the for interaction points (IPs) while simpler "4D lenses" are used to model parasitic Long-Range encounters [32].
This document describes a method to configure the beam-beam lenses in tracking simulations based on the model of the accelerator, which has been recently developed as an evolution of existing tools in MAD-X scripting language [33][2]
In particular, in Sec. 7.8.1, we discuss how to reconstruct the absolute position of the two beams with respect to the lab frame using the twiss and survey tables; in Sec. 7.8.2 we discuss how to compute the separation between the two beams; in Sec. 7.8.3 we describe how to identify the crossing plane and crossing angle; in Sec. 7.8.6 we describe how to configure the anticlockwise beam (conventionally called beam 4) from the MAD-X model based on two clockwise-oriented sequences; in Sec. 7.8.7 we introduce the effect of crab cavities on the beam-beam configuration.

7.8.1 Identification of the beam position and direction

The position and orientation of the beams at a certain machine element can be obtained from MAD-X combining the information from the survey and twiss tables.
We assume that:

- The sequences start from an element at which the reference trajectories of the two beams are known to be parallel;

[2]The authors would like to acknowledge all the colleagues who have contributed to the development of the MAD-X tools for the configuration of tracking simulations, on which the present work is largely based, and have provided important input and support, in particular G. Arduini, J. Barranco Garcia, R. De Maria, S. Fartoukh, M. Giovannozzi, S. Kostoglou, E. Métral, Y. Papaphippou, D. Pellegrini, T. Pieloni and F. Van Der Veken.

- Both beams (B1 and B2) have the same orientation (clockwise);
- Markers or beam-beam lenses are installed at the s-locations of the beam-beam interactions.

The survey provides the coordinates in the lab frame of the two beams:

$$\mathbf{P}^{\mathrm{su}} = \begin{pmatrix} x^{\mathrm{su}} \\ y^{\mathrm{su}} \\ s^{\mathrm{su}} \end{pmatrix} \tag{7.264}$$

and the corresponding set of angles $(\theta^{\mathrm{su}}, \phi^{\mathrm{su}}, \psi^{\mathrm{su}})$ defining the orientation of the local reference system used by the twiss [34]. The origin and the orientation of the lab frame are defined by the the first element in the sequence.
The components of the unit vectors defining the local reference frame with respect to the lab frame can be obtained from the following relationship:

$$\begin{aligned} &(\hat{\mathbf{e}}_x, \hat{\mathbf{e}}_y, \hat{\mathbf{e}}_s) = \\ &\begin{pmatrix} \cos\theta^{\mathrm{su}} & 0 & \sin\theta^{\mathrm{su}} \\ 0 & 1 & 0 \\ -\sin\theta^{\mathrm{su}} & 0 & \cos\theta^{\mathrm{su}} \end{pmatrix} \times \begin{pmatrix} 1 & 0 & 0 \\ 0 & \cos\phi^{\mathrm{su}} & \sin\phi^{\mathrm{su}} \\ 0 & -\sin\phi^{\mathrm{su}} & \cos\phi^{\mathrm{su}} \end{pmatrix} \times \begin{pmatrix} \cos\psi^{\mathrm{su}} & -\sin\psi^{\mathrm{su}} & 0 \\ \sin\psi^{\mathrm{su}} & \cos\psi^{\mathrm{su}} & 0 \\ 0 & 0 & 1 \end{pmatrix}. \end{aligned} \tag{7.265}$$

The MAD-X twiss provides the transverse position of the beam in the local reference frame $(x^{\mathrm{tw}}, y^{\mathrm{tw}})$, so that the absolute position of the beam in the lab frame can written as

$$\mathbf{P} = \mathbf{P}^{\mathrm{su}} + x^{\mathrm{tw}}\hat{\mathbf{e}}_x + y^{\mathrm{tw}}\hat{\mathbf{e}}_y\,. \tag{7.266}$$

At the beam-beam locations the local reference frames for the two beams are assumed to be aligned. This is not strictly the case in the regions between the separation-recombination magnets (D1 and D2), but also in that case that case the existing small divergence can be considered negligible. The beam-beam module of pymask checks the conditions:

$$||\hat{\mathbf{e}}_x^{\mathrm{b1}} - \hat{\mathbf{e}}_x^{\mathrm{b2}}|| \ll 1\,, \tag{7.267}$$

$$||\hat{\mathbf{e}}_y^{\mathrm{b1}} - \hat{\mathbf{e}}_y^{\mathrm{b2}}|| \ll 1\,. \tag{7.268}$$

Therefore we will simply define:

$$\hat{\mathbf{e}}_x = \hat{\mathbf{e}}_x^{\mathrm{b1}} = \hat{\mathbf{e}}_x^{\mathrm{b2}}\,, \tag{7.269}$$

$$\hat{\mathbf{e}}_y = \hat{\mathbf{e}}_y^{\mathrm{b1}} = \hat{\mathbf{e}}_y^{\mathrm{b2}}\,. \tag{7.270}$$

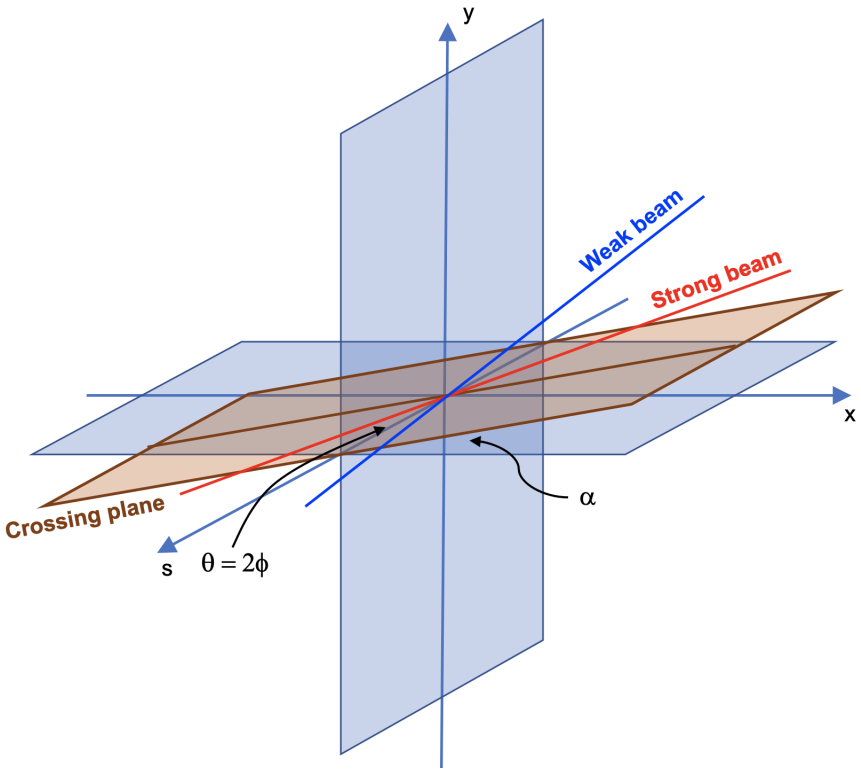

Figure 7.1: Schematic illustration of the crossing plane.

7.8.2 Computation of beam-beam separations

The beam-beam separations are defined as the transverse coordinates of the strong beam with respect to the weak beam. They can be computed as:

$$\Delta x = \hat{\mathbf{e}}_x \cdot \left(\mathbf{P}^S - \mathbf{P}^W\right) , \tag{7.271}$$

$$\Delta y = \hat{\mathbf{e}}_y \cdot \left(\mathbf{P}^S - \mathbf{P}^W\right) , \tag{7.272}$$

where the superscripts identify the weak (W) and the strong (S) beam.
Typically the accuracy of the survey table is insufficient to computed the separations correctly, especially for elements that are too far from the first element in the sequence, due to accumulation of errors along the sequence. A correction can be computed looking as the apparent displacement of the closest Interaction Point (IP) between the two surveys, as the IPs are supposed to coincide.

7.8.3 Crossing plane and crossing angle

At the beam-beam encounters the local reference frames for the two beams share the same orientation. Therefore the elevation angle α of the crossing plane and the crossing angle θ can be computed in the local reference frame, as will be illustrated in the following.

7.8.4 The crossing plane

The directions defined by the local trajectories of the two beams are identified by the unit vectors

$$\hat{\mathbf{p}}^W = \left(p_x^W, p_y^W, p_s^W\right) , \tag{7.273}$$

$$\hat{\mathbf{p}}^S = \left(p_x^S, p_y^S, p_s^S\right) , \tag{7.274}$$

containing the angles of the closed orbit obtained from the twiss of the two beams. The plane defined by these two directions is called Crossing Plane (XP), as illustrated in Fig. 7.1, and its equation is given by:

$$\mathbf{v}_{\mathrm{XP}}(w_1, w_2) = w_1 \hat{\mathbf{p}}^W + w_2 \hat{\mathbf{p}}^S \, . \tag{7.275}$$

The line defined by the intersection of the crossing plane and the transverse plane identified by the unit vectors $\hat{\mathbf{e}}_x$ and $\hat{\mathbf{e}}_y$ is given by the condition:

$$\mathbf{v}_{\mathrm{XP}}(w_1, w_2) \cdot \hat{\mathbf{e}}_s = 0 \, . \tag{7.276}$$

Replacing Eq. (7.275) into Eq. (7.276) we obtain:

$$w_1 p_s^W + w_2 p_s^S = 0 \, , \tag{7.277}$$

and replacing this condition in Eq. (7.275) we obtain the equation of the intersection line

$$\mathbf{v}_{\mathrm{T}}(w_1) = w_1 \left(\hat{\mathbf{p}}^W - \frac{p_s^W}{p_s^S} \hat{\mathbf{p}}^S \right) . \tag{7.278}$$

The elevation angle α of the intersection line with respect to the local x-direction ($\hat{\mathbf{e}}_x$) can be written as:

$$\alpha = \arctan \frac{\mathbf{v}_{\mathrm{T}} \cdot \hat{\mathbf{e}}_y}{\mathbf{v}_{\mathrm{T}} \cdot \hat{\mathbf{e}}_x} \, . \tag{7.279}$$

Using Eq. (7.278) we obtain:

$$\alpha = \arctan \frac{\left(p_y^W - \frac{p_s^W}{p_s^S} p_y^S \right)}{\left(p_x^W - \frac{p_s^W}{p_s^S} p_x^S \right)} . \tag{7.280}$$

In the paraxial approximation ($p_s^S \simeq p_s^W \simeq 1$) this simply becomes:

$$\alpha = \arctan \frac{\Delta p_y}{\Delta p_x} , \tag{7.281}$$

where we have defined:

$$\Delta p_x = p_x^W - p_x^S \, , \tag{7.282}$$

$$\Delta p_y = p_y^W - p_y^S \, . \tag{7.283}$$

In the legacy beam-beam macros as well as in the configuration pymask tool, the following logic is implemented

$$\alpha = \begin{cases} \arctan\left(\dfrac{\Delta p_y}{\Delta p_x}\right) & \text{if } |\Delta p_x| \geq |\Delta p_y| \\ \dfrac{\pi}{2} - \arctan\left(\dfrac{\Delta p_x}{\Delta p_y}\right) & \text{if } |\Delta p_x| < |\Delta p_y| \end{cases}, \tag{7.284}$$

for which α is limited to the range:

$$-\frac{\pi}{4} \leq \alpha \leq \frac{3}{4}\pi\,. \tag{7.285}$$

In particular, for a purely horizontal crossing we have $\alpha = 0$ and for a purely vertical crossing we have $\alpha = \frac{\pi}{2}$.

7.8.5 The crossing angle

The crossing angle θ between the two beams can be found from the relation:

$$\cos\theta = \hat{\mathbf{p}}^W \cdot \hat{\mathbf{p}}^S\,. \tag{7.286}$$

The half crossing angle

$$\phi = \frac{\theta}{2} \tag{7.287}$$

is often used instead of θ.
In the paraxial approximation

$$p_x \ll 1\,, \tag{7.288}$$
$$p_y \ll 1\,, \tag{7.289}$$
$$\tag{7.290}$$

the scalar product in Eq. (7.286) can be rewritten as

$$\begin{aligned} \hat{\mathbf{p}}^W \cdot \hat{\mathbf{p}}^S &= p_x^W p_x^S + p_y^W p_y^S + p_s^W p_s^S \\ &= p_x^W p_x^S + p_y^W p_y^S + \sqrt{1 - \left(p_x^W\right)^2 - \left(p_y^W\right)^2}\sqrt{1 - \left(p_x^S\right)^2 - \left(p_y^S\right)^2} \\ &\simeq p_x^W p_x^S + p_y^W p_y^S + \left(1 - \frac{\left(p_x^W\right)^2}{2} - \frac{\left(p_y^W\right)^2}{2}\right)\left(1 - \frac{\left(p_x^S\right)^2}{2} - \frac{\left(p_y^S\right)^2}{2}\right) \\ &\simeq p_x^W p_x^S + p_y^W p_y^S + 1 - \frac{\left(p_x^W\right)^2}{2} - \frac{\left(p_y^W\right)^2}{2} - \frac{\left(p_x^S\right)^2}{2} - \frac{\left(p_y^S\right)^2}{2}, \end{aligned} \tag{7.291}$$

which can be written in compact form as:

$$\hat{\mathbf{p}}^W \cdot \hat{\mathbf{p}}^S \simeq 1 - \frac{\left(p_x^W - p_x^S\right)^2 + \left(p_y^W - p_y^S\right)^2}{2}. \tag{7.292}$$

For small crossing angle we can write:

$$\cos\theta \simeq 1 - \frac{\theta^2}{2}. \tag{7.293}$$

Replacing Eqs. (7.292) and (7.293) into Eq. (7.286) we obtain

$$|\theta| = \sqrt{\Delta p_x^2 + \Delta p_y^2}\,. \tag{7.294}$$

The sign of θ is defined positive when the weak beam needs to rotate in the clockwise sense in the crossing plane in order to be brought on the strong beam. This corresponds to the following sign choices:

	$\lvert\Delta p_x\rvert > \lvert\Delta p_y\rvert$	$\lvert\Delta p_x\rvert < \lvert\Delta p_y\rvert$
$\Delta p_x \geq 0$, $\Delta p_y \geq 0$	$\theta > 0$	$\theta > 0$
$\Delta p_x < 0$, $\Delta p_y \geq 0$	$\theta < 0$	$\theta > 0$
$\Delta p_x < 0$, $\Delta p_y < 0$	$\theta < 0$	$\theta < 0$
$\Delta p_x \geq 0$, $\Delta p_y < 0$	$\theta > 0$	$\theta < 0$

which are consistent with the sign convention used in LHC operation.

7.8.6 Transformations for the counterclockwise beam (B4)

The typically used MAD-X model of the LHC consists of two sequences both having clockwise (CW) orientation, conventionally called Beam 1 and Beam 2. To perform tracking simulations of the anticlockwise (ACW) beam, an anticlockwise sequence needs to be generated, which is conventionally called Beam 4. The beam-beam lenses in the Beam 4 sequence can be configured based on the beam-beam lenses defined in Beam 2, taking into account that the two are related by the following change of coordinates:

$$x^{\mathrm{ACW}} = -x^{\mathrm{CW}}, \tag{7.295}$$
$$y^{\mathrm{ACW}} = +y^{\mathrm{CW}}, \tag{7.296}$$
$$s^{\mathrm{ACW}} = -s^{\mathrm{CW}}. \tag{7.297}$$

The corresponding transformation for the transverse momenta is:

$$p_x^{\mathrm{ACW}} = +p_x^{\mathrm{CW}}, \tag{7.298}$$
$$p_y^{\mathrm{ACW}} = -p_y^{\mathrm{CW}}. \tag{7.299}$$

This can be easily seen from the fact that:

$$p_x \simeq \frac{dx}{ds}, \tag{7.300}$$
$$p_y \simeq \frac{dy}{ds}. \tag{7.301}$$

Additionally, from Eqs. (7.295) - (7.299) it is possible to derive the following relations to transform the Σ-matrix [31] of the strong beam:

$$\Sigma_{11}^{\mathrm{ACW}} = +\Sigma_{11}^{\mathrm{CW}}\,, \tag{7.302}$$
$$\Sigma_{12}^{\mathrm{ACW}} = -\Sigma_{12}^{\mathrm{CW}}\,, \tag{7.303}$$
$$\Sigma_{13}^{\mathrm{ACW}} = -\Sigma_{13}^{\mathrm{CW}}\,, \tag{7.304}$$
$$\Sigma_{14}^{\mathrm{ACW}} = +\Sigma_{14}^{\mathrm{CW}}\,, \tag{7.305}$$
$$\Sigma_{22}^{\mathrm{ACW}} = +\Sigma_{22}^{\mathrm{CW}}\,, \tag{7.306}$$
$$\Sigma_{23}^{\mathrm{ACW}} = +\Sigma_{23}^{\mathrm{CW}}\,, \tag{7.307}$$
$$\Sigma_{24}^{\mathrm{ACW}} = -\Sigma_{24}^{\mathrm{CW}}\,, \tag{7.308}$$
$$\Sigma_{33}^{\mathrm{ACW}} = +\Sigma_{33}^{\mathrm{CW}}\,, \tag{7.309}$$
$$\Sigma_{34}^{\mathrm{ACW}} = -\Sigma_{34}^{\mathrm{CW}}\,, \tag{7.310}$$
$$\Sigma_{44}^{\mathrm{ACW}} = +\Sigma_{44}^{\mathrm{CW}}\,. \tag{7.311}$$
$$\tag{7.312}$$

7.8.7 Crab crossing

To discuss the effect of crab cavities, we define along the bunches of Beam 1 and Beam 2 (sharing the same s coordinate as in the MAD-X model), the longitudinal coordinates z_1 and z_2, oriented like s.
Assuming that the slices with $z_1 = z_2 = 0$ collide at s=0, the collision point (CP) for two generic slices z_1 and z_2 is at the location:

$$s_{\mathrm{CP}} = \frac{z_1 + z_2}{2}\,. \tag{7.313}$$

In the absence of crab crossing, the transverse position of the two beams is independent from z:

$$x_1 = +\phi s\,, \tag{7.314}$$
$$x_2 = -\phi s\,. \tag{7.315}$$

Ideal crab cavities, in the linear approximation, introduce a z-dependent orbit correction such that:

$$x_1(s) = +\phi s + \phi_c z_1\,, \tag{7.316}$$
$$x_2(s) = -\phi s - \phi_c z_2\,, \tag{7.317}$$

where ϕ_c is the crabbing angle and we assume, without loss of generality, horizontal crabbing plane.
The separation of the two slices at their collision point is obtained replacing (7.313) into (7.316) and (7.317):

$$\Delta x(s_{\mathrm{CP}}) = x_2(s_{\mathrm{CP}}) - x_1(s_{\mathrm{CP}}) = -(\phi + \phi_c)(z_1 + z_2)\,. \tag{7.318}$$

If $\phi_c = -\phi$, the separation is zero independently of z_1 and z_2 (perfect crabbing).
The crab crossing in the IPs of the HL-LHC for the clockwise and anticlockwise beams is illustrated with the relevant sign conventions in Figs. 7.2 - 7.5.

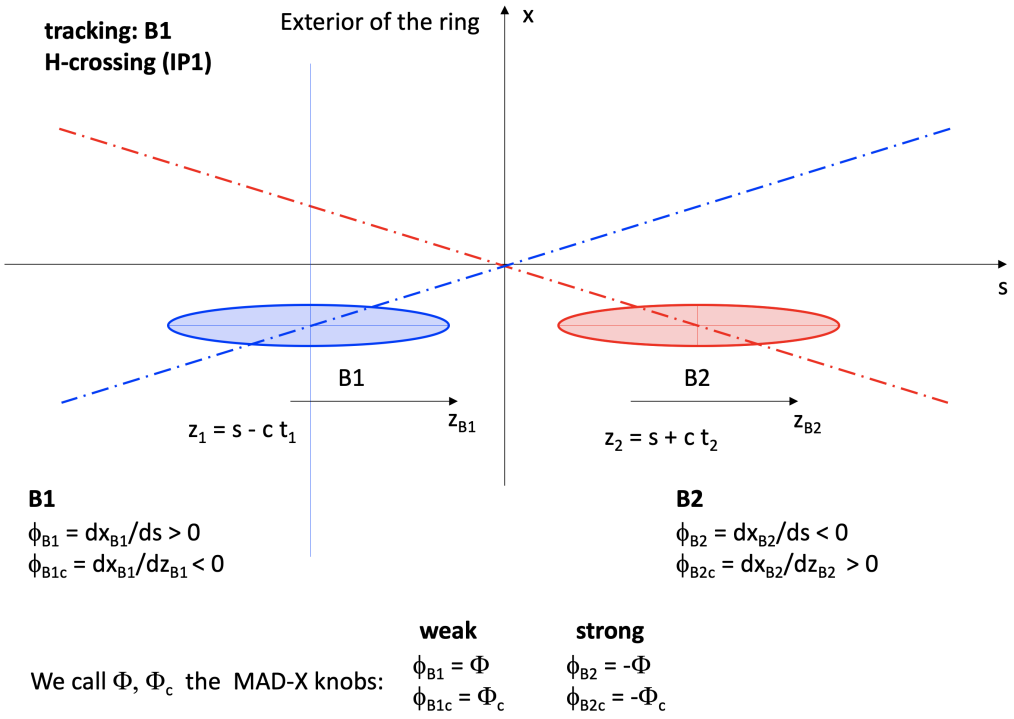

Figure 7.2: Crab crossing in the IP1 of the HL-LHC modeled for the tracking of the clockwise beam (beam 1).

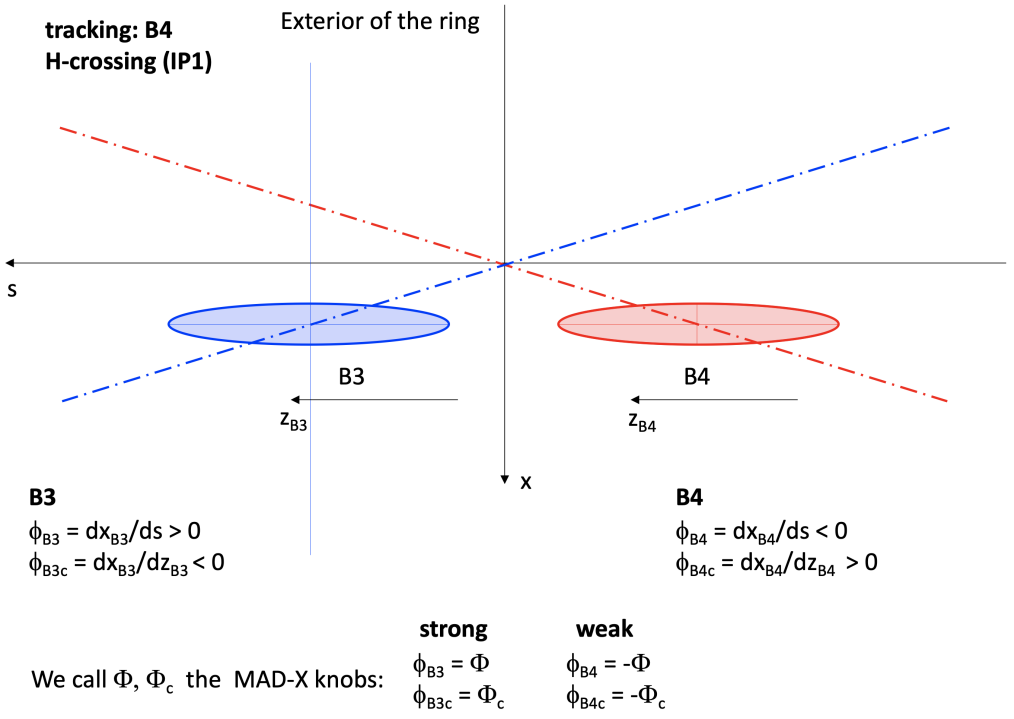

Figure 7.3: Crab crossing in the IP1 of the HL-LHC modeled for the tracking of the anticlockwise beam (beam 4).

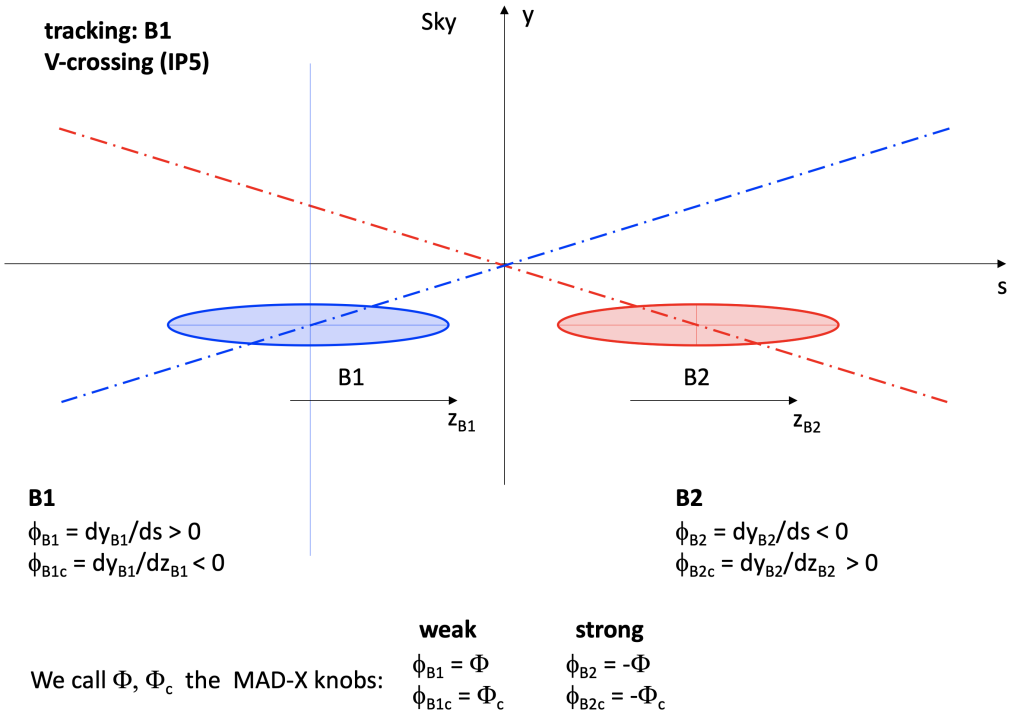

Figure 7.4: Crab crossing in the IP5 of the HL-LHC modeled for the tracking of the clockwise beam (beam 1).

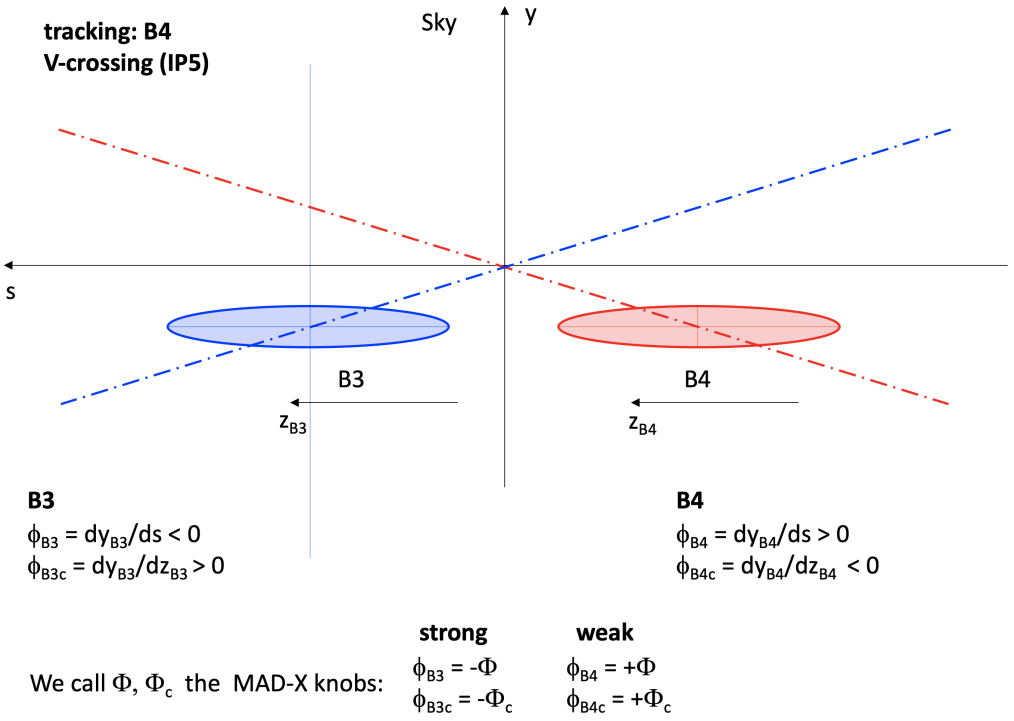

Figure 7.5: Crab crossing in the IP5 of the HL-LHC modeled for the tracking of the anticlockwise beam (beam 4).

7.8.7.1 Configuration of beam-beam lenses for beam 1

In order to model the HO interaction for a crab crossing, the "strong bunch" is sliced longitudinally using the constant charge method, and one beam-beam lens for each slice is installed in the sequence.
In particular, in the sequence of beam 1, the lens corresponding to a slice of the strong beam (beam 2) having longitudinal coordinate $z_2 = Z_2$ is installed at the location where the slice encounters the synchronous particle of the weak beam (see Eq. (7.313) with $z_1 = 0$):

$$s_{\text{lens}} = +\frac{Z_2}{2}\,. \tag{7.319}$$

The position of the strong beam at the lens can be found replacing Eq. (7.319) into Eq. (7.317):

$$X_2 = -s_{\text{lens}}(\phi + 2\phi_c)\,. \tag{7.320}$$

The effect of the crab bump alone is given by:

$$X_2^{\text{crab}} = -2\phi_c s_{\text{lens}} = -\phi_c Z_2\,. \tag{7.321}$$

Taking into account the RF curvature coming from the crab cavity frequency, the position of the slice at the beam-beam lens can be written as:

$$X_2^{\text{crab}} = -\phi_c \frac{L_{\text{ring}}}{2\pi h_{\text{CC}}} \sin\left(\frac{2\pi h_{\text{CC}}}{L_{\text{ring}}} Z_2\right) = -\phi_c \frac{L_{\text{ring}}}{2\pi h_{\text{CC}}} \sin\left(\frac{2\pi h_{\text{CC}}}{L_{\text{ring}}} 2s_{\text{lens}}\right)\,, \tag{7.322}$$

where h_{CC} is the harmonic number of the crab cavity and L_{ring} is the circumference of the ring.

7.8.8 Configuration of beam-beam lenses for beam 2

In the sequence of beam 2, we install the beam-beam lens for a slice of the strong beam (beam 1) having longitudinal coordinate $z_1 = Z_1$ at the location where the slice encounters the synchronous particle of the weak beam, (see Eq. (7.313) with $z_2 = 0$):

$$s_{\text{lens}} = \frac{Z_1}{2}\,. \tag{7.323}$$

The position of the strong beam at the lens can be found replacing Eq. (7.323) into Eq. (7.316):

$$X_1 = s_{\text{lens}}(\phi + 2\phi_c)\,. \tag{7.324}$$

The effect of the crab bump alone is given by:

$$X_1^{\text{crab}} = 2\phi_c s_{\text{lens}} = \phi_c Z_1\,. \tag{7.325}$$

Taking into account the RF curvature coming from the crab cavity frequency, the position of the slice at the beam-beam lens can be written as:

$$X_1^{\text{crab}} = \phi_c \frac{L_{\text{ring}}}{2\pi h_{\text{CC}}} \sin\left(\frac{2\pi h_{\text{CC}}}{L_{\text{ring}}} Z_1\right) = \phi_c \frac{L_{\text{ring}}}{2\pi h_{\text{CC}}} \sin\left(\frac{2\pi h_{\text{CC}}}{L_{\text{ring}}} 2s_{\text{lens}}\right)\,. \tag{7.326}$$

From Eqs. (7.322) and (7.326), we find that for lenses at the same longitudinal position s_{lens} the corresponding slices of the two beams $Z_1 = Z_2 = 2s_{\text{lens}}$ have opposite transverse coordinates:

$$X_1^{\text{crab}} = -X_2^{\text{crab}}\,. \tag{7.327}$$

7.8.8.1 Crab bump from twiss table

For a non-ideal crabbing, for example in the presence of a non-closure of the crab-bump, the realistic z-dependent orbit distortion introduced by the crab cavities can be characterized using the twiss, by installing orbit correctors at the position of the crab cavities that introduce the crab cavity deflection as seen at a certain reference position along the bunch z_{ref}. To obtain the effect on particles at different positions along bunch it is possible to apply the following scaling:

$$x\left(z\right) = x\left(z_{\text{ref}}\right) \frac{\sin\left(\frac{2\pi h_{\text{CC}}}{L_{\text{ring}}} z\right)}{\sin\left(\frac{2\pi h_{\text{CC}}}{L_{\text{ring}}} z_{\text{ref}}\right)}. \tag{7.328}$$

7.8.9 Step-by-step configuration procedure

Based on the method introduced in the previous sections, the following procedure has been implemented in pymask to configure the beam-beam lenses in the sixtrack and sixtracklib tracking model:

1. Inactive beam-beam lenses (not configured) are installed in both clockwise sequences (Beam 1 and Beam 2) at the locations of the HO and LR beam-beam encounters. As discussed in Sec. 7.8.7, at each IP a set of lenses is installed to model the HO, one corresponding to each bunch slice.

2. The MAD-X twiss and survey tables are computed for both clockwise sequences.

3. The transverse beam shapes (Σ-matrix) are extracted from the twiss table for all beam-beam lenses.

4. The positions of the beams at the beam-beam lenses in the lab frame are computed combining the information from the survey and twiss tables, as discussed in Sec. 7.8.1.

5. The beam-beam separations are computed, as discussed in Sec. 7.8.2.

6. For all HO interactions, the crossing plane and the crossing angle are identified, as discussed in Sec. 7.8.3.

7. The relevant quantities for the beam-beam lenses in the anticlockwise sequences (Beam 3 and Beam 4) are obtained from the data computed for the lenses in the clockwise sequences (Beam 1 and Beam 2), using the transformations described in Sec. 7.8.6.

8. The effect of the crab cavities is introduced by using the shape of the crab bumps obtained from twiss tables computed with orbit correctors at the locations of the cavities, as discussed in Sec. 7.8.7.

9. The information computed before is used to configure the beam-beam lenses in the MAD-X model of the sequence for which the tracking simulation will be performed, typically either Beam 1 or Beam 4.

10. The SixTrack input and the pysixtrack/sixtracklib input files are generated using the MAD-X model and the additional information computed as described above.

11. The closed orbit as computed from the MAD-X sequences is saved on file, for the generation of matched beam distributions and for the computation of the beam-beam dipolar kicks on the closed orbit, which are usually subtracted in weak-strong tracking simulations.

Chapter 8

Bhabha scattering and beamstrahlung

8.1 Bhabha scattering

In quantum electrodynamics (QED), the Coulomb attraction of two opposite charges (e.g. an electron and a positron) is called Bhabha scattering [35]. The mathematical treatment of Bhabha scattering can be done using the method of equivalent photons (Weizsäcker-Williams approach) [36, 37]. The essence of this method lies in the fact that the electromagnetic field of a relativistic charged particle, say the positron, is almost transversal and can therefore accurately be substituted by an appropriately chosen equivalent radiation field of photons. Thus, the cross section for the scattering of an electron with this positron (Bhabha scattering) can be approximated by that of the electron and an "equivalent" photon (Compton scattering). In this case, the equivalent photon corresponds to the exchanged virtual photon between the scattering primaries. The whole process, including the subsequent emission of bremsstrahlung photons can be treated in a numerical simulation as an inverse Compton scattering process [38]. In this, the virtual photons emitted by the positron will collide with the electron. Due to the relativistic dynamics of the participating leptons, the virtual photons have an energy which is often negligible compared to that of the leptons, thus we can treat them as real. The process is called inverse since here the electron will lose energy while the photons will gain energy, contrary to standard Compton scattering. The scattered photons are real and typically end up with an energy E'_γ comparable to the initial lepton energy E_e [39].

The generation of photons from radiative Bhabha scattering in Xsuite can be divided into 3 steps. First, the charge density of the opposite bunch slice at the location of the macroparticle in the soft-Gaussian approximation is computed [40]. From this one computes the integrated luminosity of the collision of the macroparticle with the virtual photons represented by the slice, integrated over the time of passing through the slice. Second, a set of virtual photons is generated corresponding to the total energy of the opposite slice. Third, the code iterates over these virtual photons and simulates the bremsstrahlung process as a series of inverse Compton scattering events between the macroparticle and each virtual photon.

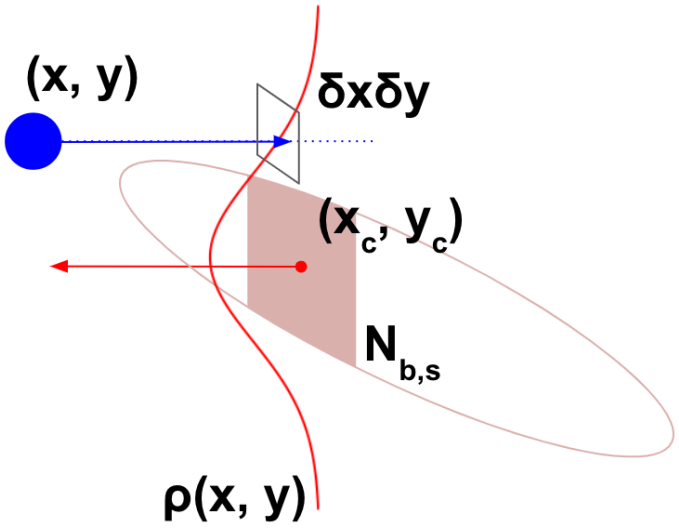

Figure 8.1: Schematic illustration of a single macroparticle from bunch 1 (blue) colliding with a single longitudinal slice of the opposing bunch 2 (red).

8.1.1 Luminosity Computation

Figure 8.1 illustratres how `Xfields` computes the integrated luminosity in a collision of a single macroparticle from one beam with a single slice of the opposing beam[1]. On the figure x, y denote the transverse coordinates of a macroparticle in the boosted and uncoupled frame, at the collision point with a slice of the opposing bunch, corresponding to the notation $\hat{\hat{x}}^*, \hat{\hat{y}}^*$ in the previous sections. The centroid (mean) coordinate of the opposing slice, with a bunch intensity of $N_{b,s}$, is denoted by x_c, y_c, in the boosted, uncoupled, transported reference frame of its own bunch. `Xfields` models the charge density of a longitudinal slice as a 2D Gaussian distribution $\rho(x, y)$. Considering an infinitesimal area $\delta x \delta y$ around the transverse position x, y of a given macroparticle at the collision point with the slice, one can write the number of charges with which this macroparticle will interact:

$$N_e(x, y) = N_{b,s} \rho(x, y) \delta x \delta y, \tag{8.1}$$

and the integrated luminosity of the macroparticle-slice collision:

$$L = \frac{N_{b,m} \cdot N_e(x, y)}{\delta x \delta y} = N_{b,m} N_{b,s} \rho(x, y), \tag{8.2}$$

where $N_{b,m}$ denotes the number of elementary charges per macroparticle.

[1]Note that this luminosity can be recorded in a table with the **flag_luminosity** flag of the `BeamBeamGaussian3D` element and **lumitable** keyword in the `Xline` internal log. The recorded entries must be summed up to get the total integrated luminosity of the collision. This method has an uncertainty of $\pm 10\%$ compared to the analytical formula.

8.1.2 Virtual Photon Generation

Equation (8.2) describes the integrated luminosity of primary-primary collisions. In order to simulate the collision of the primaries with virtual photons instead, `Xfields` uses the assumption that the virtual photon distribution $N_\gamma(x,y)$ is proportional to that of the primary charges:

$$N_\gamma(x,y) = nN_e(x,y), \tag{8.3}$$

where n is a proportionality factor denoting the number of virtual photons corresponding to one elementary charge. The number density spectrum of virtual photons is given by:

$$\frac{dn}{dxdQ^2} = \frac{\alpha}{2\pi}\frac{1+(1-x)^2}{x}\frac{1}{Q^2}, \tag{8.4}$$

where $x = \dfrac{\hbar\omega}{E_e} = \dfrac{E_\gamma}{E_e}$ is the total energy of the virtual photon normalized to the primary energy and Q^2 is the squared virtuality of the virtual photon [41].
The virtual photon energies and virtualities can be drawn using the method of inverse CDF (Cumulative Distribution Function) sampling. The sampling algorithm in `Xsuite` has been adapted from `GUINEA-PIG` [42], a Particle In Cell (PIC) based single beam-beam collision simulation software. For each macroparticle in the beam, we first compute the total amount of equivalent photons using the energy of the opposite bunch slice. Subsequently, the energy and virtuality of each photon will be sampled. In the current implementation all virtual photons inherit the dynamical variables of the strong bunch slice centroid. Note that the virtual photons sampled this way will also be "macroparticles" in the sense that they represent the dynamics of all virtual photons generated by all charges in a primary macroparticle.

8.1.3 Inverse Compton Scattering of Virtual Photons

We account for the proportionality of the primary charge and virtual photon distributions described by Eq. (8.3) by resampling the virtual photons for each macroparticle. With each photon, we simulate the bremsstrahlung process in the form of a set of inverse Compton scattering events. The number of Compton events can be described as:

$$R = \sigma_{C,tot}(s)L = \sigma_{C,tot}(s)N_{b,m}N_{b,s}\rho(x,y), \tag{8.5}$$

where $s \approx \dfrac{4E_\gamma E_e}{m_e^2c^4}$ is the center of mass energy squared of the photon-primary Compton interaction, normalized to the rest mass of the primary [43], and $\sigma_{C,tot}(s)$ denotes the total Compton scattering cross section, given by:

$$\sigma_{C,tot}(s) = \frac{2\pi r_e^2}{s}\left[\ln(s+1)\left(1-\frac{4}{s}-\frac{8}{s^2}\right).+\frac{1}{2}+\frac{8}{s}-\frac{1}{2(s+1)^2}\right], \tag{8.6}$$

with r_e being the classical electron radius. For each event, we sample the scattered photon energy from the differential cross section:

$$\frac{d\sigma_C}{dy} = \frac{2\pi r_e^2}{s}\left[\frac{1}{1-y} + 1 - y - \frac{4y}{s(1-y)} + \frac{4y^2}{s^2(1-y)^2}\right], \tag{8.7}$$

which describes the scattering of a beam of unpolarized photons on the primary charge [38]. Here $y = \frac{\hbar\omega'}{E_e} = \frac{E'_\gamma}{E_e}$ is the energy of the scattered photon in units of the total energy of the colliding primary. Given the energy E'_γ, we can compute the scattering angle of the primary and the photon as well as their momenta, using the constraints given by energy and momentum conservation. While the emitted photon spectrum corresponds to the sum of all charges represented by a macroparticle, a given macroparticle should represent the dynamics of a single primary charge. Thus, the dynamical variables of the macroparticles are updated according to energy and momentum conservation accounting for the emission of only a fraction of the photons. The latter are picked randomly based on a probability corresponding to the inverse of the number of charges per macroparticle.

8.2 Beamstrahlung

The implementation of beamstrahlung in `Xfields` is based on `GUINEA-PIG` [42]. In this section a high level summary of the modeling is presented. Further details can be found in [44].
`Xfields` samples the quantum theoretical synchrotron radiation spectrum $G(v, \xi)$:

$$G(v,\xi) = \frac{v^2}{(1-(1-\xi)v^3)^2}\left(G_1(y) + \frac{\xi^2 y^2}{1+\xi y}G_2(y)\right), \tag{8.8}$$

which is normalized such that $G(v=0,\xi) = 1$ and $G(v,\xi) \leq 1$ for all v and ξ. The variable ξ is defined as:

$$\xi = \frac{E_{crit}}{E} \tag{8.9}$$

and denotes the magnitude of the quantum correction, i.e. the critical energy normalized to the energy E of the primary particle in GeV undergoing the beamstrahlung process. The critical beamstrahlung energy is defined in the classical way as:

$$E_{crit} = \frac{3\hbar c\gamma^3}{2\rho} \tag{8.10}$$

The unitless variable y is related to the energy of the emitted beamstrahlung photon E_γ:

$$y = \frac{E_\gamma}{E_{crit}}\frac{1}{1-\frac{E_\gamma}{E}}. \tag{8.11}$$

Equation 8.11 can be expressed with the help of a uniform random variable v as follows:

$$y = \frac{v^3}{1 - v^3};\ v \in U[0,1]. \tag{8.12}$$

With these the number of beamstrahlung photons emitted in the interval $[v,\ v + \Delta v]$ during a time interval δ_t can be given as:

$$\Delta N_\gamma = p_0 G(v, \xi) \Delta v, \tag{8.13}$$

where

$$p_0 = \frac{2^{\frac{2}{3}}}{\Gamma(\frac{4}{3})} \frac{\alpha \gamma \delta_t}{\rho} \approx 25.4 \cdot \frac{E \delta_t}{\rho} \tag{8.14}$$

is a scaling factor dependent on the relativistic γ of the primary, the instantaneous bending radius ρ and the fine structure constant α. The bending radius of each macroparticle in the electromagnetic field of a given longitudinal slice of the opposite bunch is obtained from the radial kick:

$$F_r^* = r_{pp} \sqrt{F_x^{*2} + F_y^{*2}}, \tag{8.15}$$

$$\rho = \frac{1}{F_r^*}, \tag{8.16}$$

with $r_{pp} = \frac{1}{1+\delta} = \frac{p}{p_0}$. In the `Xfields` `BeamBeamGaussian3D` element the time interval δ_t is expressed as a longitudinal distance Δz, which is the distance the macroparticle travels between two consecutive longitudinal slices and it corresponds to the bin width of the longitudinal slicing.
Figure 8.2 shows the beamstrahlung photon number density $p_0 G(v, \xi)$ for a fixed value of p_0 and ξ. The area in the region C is the mean number of beamstrahlung photons emitted during an interval δ_t, i.e. a passage through one longitudinal slice of width Δz.
The functions $G_1(y)$ and $G_2(y)$ are defined as follows:

$$\begin{aligned} G_1(y) &= \frac{\sqrt{3}\Gamma(\frac{1}{3})}{2^{\frac{5}{3}}\pi} \int_y^\infty K_{\frac{5}{3}}(x) dx, \\ G_2(y) &= \frac{\sqrt{3}\Gamma(\frac{1}{3})}{2^{\frac{5}{3}}\pi} K_{\frac{2}{3}}(y). \end{aligned} \tag{8.17}$$

Equations 8.17 are evaluated numerically with the below approximate formulas:

$$\begin{aligned} &0 \le y \le 1.54 \\ &\quad G_1(y) = y^{-\frac{2}{3}}(1 - 0.8432885317 \cdot y^{\frac{2}{3}} + 0.1835132767 \cdot y^2 \\ &\qquad - 0.0527949659 \cdot y^{\frac{10}{3}} + 0.0156489316 \cdot y^4) \\ &\quad G_2(y) = y^{-\frac{2}{3}}(0.4999456517 - 0.5853467515 \cdot y^{\frac{4}{3}} \\ &\qquad + 0.3657833336 \cdot y^2 - 0.0695055284 \cdot y^{\frac{10}{3}} + 0.0191803860 \cdot y^4) \end{aligned} \tag{8.18}$$

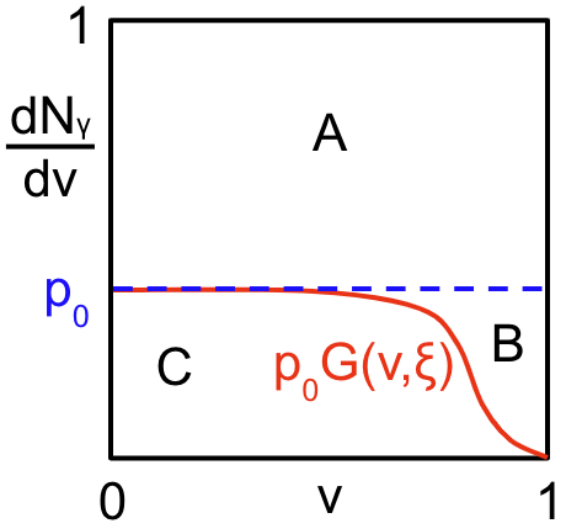

Figure 8.2: Schematic illustration of the number density function of beamstrahlung photons $p_0 G(v, \xi)$ (red curve) for a given p_0 (blue dashed line) and ξ, as a function of v.

$1.54 < y \leq 4.48$

$$G_1(y) = \frac{2.066603927 - 0.5718025331 \cdot y + 0.04243170587 \cdot y^2}{-0.9691386396 + 5.651947051 \cdot y - 0.6903991322 \cdot y^2 + y^3} \quad (8.19)$$
$$G_2(y) = \frac{1.8852203645 - 0.5176616313 \cdot y + 0.03812218492 \cdot y^2}{-0.4915880600 + 6.1800441958 \cdot y - 0.6524469236 \cdot y^2 + y^3}$$

$4.48 < y \leq 165.0$

$$G_1(y) = \frac{e^{-y}}{\sqrt{y}} \cdot \frac{1.0174394594 + 0.5831679349 \cdot y}{0.9949036186 + y} \quad (8.20)$$
$$G_2(y) = \frac{e^{-y}}{\sqrt{y}} \cdot \frac{0.2847316689 + 0.5830684600 \cdot y}{0.3915531539 + y}.$$

For $y > 165$ the model assumes no radiation. With these one can simulate beamstrahlung emission by first drawing a random uniform number p. The condition $p > p_0$ corresponds to region A on Fig. 8.2, therefore no photons are emitted. In the other case a second random uniform number v is drawn, and Eq. 8.8 is computed. If $p < p_0 G(v, \xi)$ is satisfied (region C) a photon is emitted with an energy

$$\frac{E_\gamma}{E} = \frac{\xi v^3}{1 - (1 - \xi) v^3}, \quad (8.21)$$

otherwise no photon is emitted (region B). The generated beamstrahlung photons are themselves macroparticles in the sense that they represent the dynamics of all photons generated by all charges in a primary macroparticle.

Chapter 9

Wakefields and impedances

9.1 Transverse wakefields

Transverse wakefields are defined such that the corresponding transverse kicks can be written as:

$$\Delta p_x = \frac{q^2 e^2}{m_0 \gamma \beta_0^2 c^2} \sum_{i,j,k,l \geq 0} x^k y^l \int_{-\infty}^{\infty} \bar{x}^i(z') \bar{y}^j(z') \lambda(z') W_x^{i,j,k,l}(z - z')\, dz' \tag{9.1}$$

$$\Delta p_y = \frac{q^2 e^2}{m_0 \gamma \beta_0^2 c^2} \sum_{i,j,k,l \geq 0} x^k y^l \int_{-\infty}^{\infty} \bar{x}^i(z') \bar{y}^j(z') \lambda(z') W_y^{i,j,k,l}(z - z')\, dz' \tag{9.2}$$

where $\bar{x}(z)$ and $\bar{y}(z)$ are the transverse centroid positions along the beam.
The convolution can be obtained numerically using the method of Section 11.2.
The lower order terms of the summation are often called as:

- $W_x^{0,0,0,0}$ constant x
- $W_y^{0,0,0,0}$ constant y
- $W_x^{1,0,0,0}$ dipolar x, or driving x
- $W_y^{0,1,0,0}$ dipolar y, or driving y
- $W_x^{0,1,0,0}$ dipolar xy, or driving xy
- $W_y^{1,0,0,0}$ dipolar yx, or driving yx
- $W_x^{0,0,1,0}$ quadrupolar x, or detuning x
- $W_y^{0,0,0,1}$ quadrupolar y, or detuning y
- $W_x^{0,0,0,1}$ quadrupolar xy, or detuning xy
- $W_y^{0,0,1,0}$ quadrupolar yx, or detuning yx

The z variable can be written as a function of time in the lab frame as:

$$z = -\beta_0 ct, \tag{9.3}$$

We call $\widehat{W}_{x,y}$ the wakefield defined as a function of time t:

$$\widehat{W}_{x,y}(t) = W_{x,y}\left(-\beta_0 ct\right) \tag{9.4}$$

$$W_{x,y}(z) = \widehat{W}_{x,y}\left(-\frac{z}{\beta_0 c}\right) \tag{9.5}$$

For ultrarelativistic beams we have:

$$\widehat{W}_{x,y}(t) = 0 \qquad \text{for } t < 0 \tag{9.6}$$

$$W_{x,y}(z) = 0 \qquad \text{for } z > 0 \tag{9.7}$$

The coefficient $1/\gamma\beta_0^2$ in Eqs. 9.1 and 9.2 comes from the fact that, if we have a force F_x acting on a length Δs, we can derive the corresponding kick as follows:

$$\Delta P_x = F_x \Delta t, \tag{9.8}$$

and substituting the P_x with the normalized one $p_x = \frac{P_x}{P_0}$ we find

$$\Delta p_x = \frac{F_x}{P_0}\Delta t = \frac{F_x}{P_0}\frac{\Delta s}{\beta_0 c}, \tag{9.9}$$

hence substituting $P_0 = m_0\gamma\beta_0 c$ we find

$$\Delta p_x = \frac{F_x}{m_0\gamma\beta_0^2 c^2}\Delta s. \tag{9.10}$$

9.2 Transverse impedances

The transverse beam coupling impedances $Z_{x,y}(\omega)$ are related to the wakefields through a Fourier transform (see [45, Eq. 1.216]):

$$\widehat{W}_{x,y}(t) = -\frac{j}{2\pi}\int_{-\infty}^{+\infty} d\omega\; e^{j\omega t} Z_{x,y}(\omega)\;, \tag{9.11}$$

$$Z_{x,y}(\omega) = j\int_{-\infty}^{+\infty} dt\; e^{-j\omega t}\widehat{W}_{x,y}(t)\;. \tag{9.12}$$

The equivalence between the two equations can be seen multiplying both sides of Eq. 9.11 by $e^{-j\omega' t}$ and integrating over t

$$\int_{-\infty}^{\infty} dt\; e^{-j\omega' t}\widehat{W}_{x,y}(t) = -\frac{j}{2\pi}\int_{-\infty}^{\infty} dt\;\int_{-\infty}^{+\infty} d\omega Z_{x,y}(\omega) e^{j(\omega-\omega')t} \tag{9.13}$$

$$= -\frac{j}{2\pi}\int_{-\infty}^{+\infty} d\omega\; Z_{x,y}(\omega)\int_{-\infty}^{\infty} dt\; e^{j(\omega-\omega')t}. \tag{9.14}$$

We now apply the following property of the Dirac δ function

$$\delta(\omega - \omega') = \frac{j}{2\pi} \int_{-\infty}^{\infty} dt\, e^{j(\omega-\omega')t}, \tag{9.15}$$

and we find

$$\int_{-\infty}^{\infty} dt\, e^{-j\omega' t} \widehat{W}_{x,y}(t) = -j \int_{-\infty}^{+\infty} d\omega\, Z_{x,y}(\omega)\delta(\omega - \omega') = -jZ_{x,y}(\omega'). \tag{9.16}$$

We can write the impedances also in terms of the wakefield expressed as a function of $z = -\beta_0 ct$ (using Eqs. 9.22 and 9.22):

$$W_{x,y}(z) = -\frac{j}{2\pi} \int_{-\infty}^{+\infty} d\omega\, e^{-j\omega \frac{z}{\beta_0 c}} Z_{x,y}(\omega)\,, \tag{9.17}$$

$$Z_{x,y}(\omega) = \frac{j}{\beta_0 c} \int_{-\infty}^{+\infty} dz e^{j\omega \frac{z}{\beta_0 c}} W_{x,y}(z)\,. \tag{9.18}$$

As the transverse wakes are real functions, the impedances satisfy the following symmetry properties:

$$\mathrm{Re}\left\{Z_{x,y}(-\omega)\right\} = -\,\mathrm{Re}\left\{Z_{x,y}(\omega)\right\} \tag{9.19}$$

$$\mathrm{Im}\left\{Z_{x,y}(-\omega)\right\} = \mathrm{Im}\left\{Z_{x,y}(\omega)\right\} \tag{9.20}$$

9.3 Longitudinal wakefield

Longitudinal wakefields are defined such that the corresponding kicks can be written as:

$$\Delta\delta = -\frac{q^2 e^2}{m_0 \gamma \beta_0^2 c^2} \int_{-\infty}^{+\infty} dz' \lambda(z') W_s(z - z')\,. \tag{9.21}$$

The minus sign is introduced such that a positive wake causes the particles to lose energy. The convolution can be obtained numerically using the method of Section 11.2.
Also in this case, we call $\widehat{W}_s$ the wakefield defined as a function of time t:

$$\widehat{W}_s(t) = W_s\left(\beta_0 ct\right) \tag{9.22}$$

$$W_s(z) = \widehat{W}_s\left(-\frac{z}{\beta_0 c}\right) \tag{9.23}$$

9.4 Longitudinal impedance

The longitudinal beam coupling impedances $Z_s(\omega)$ are related to the wakefields through a Fourier transform (see [45, Eq. 1.216]):

$$\widehat{W}_s(t) = \frac{1}{2\pi} \int_{-\infty}^{+\infty} d\omega\, e^{j\omega t} Z_s(\omega)\,, \tag{9.24}$$

$$Z_s(\omega) = \int_{-\infty}^{+\infty} dt\, e^{-j\omega t} \widehat{W}_s(t)\,. \tag{9.25}$$

We can write the impedances also in terms of the wakefield expressed as a function of $z = -\beta_0 ct$ (using Eqs. 9.22 and 9.22):

$$W_s(z) = \frac{1}{2\pi}\int_{-\infty}^{+\infty} d\omega\, e^{-j\omega\frac{z}{\beta_0 c}} Z_s(\omega)\,, \tag{9.26}$$

$$Z_s(\omega) = \frac{1}{\beta_0 c}\int_{-\infty}^{+\infty} dz e^{j\omega\frac{z}{\beta_0 c}} W_s(z)\,. \tag{9.27}$$

As the longitudinal wake is a real function, the conrresponding impedance satisfies the following symmetry properties:

$$\mathrm{Re}\left\{Z_s(-\omega)\right\} = \mathrm{Re}\left\{Z_s(\omega)\right\} \tag{9.28}$$

$$\mathrm{Im}\left\{Z_s(-\omega)\right\} = -\,\mathrm{Im}\left\{Z_s(\omega)\right\} \tag{9.29}$$

9.5 Analytical wakes

Resonator

Ultra-relativistic resonator with shunt impedance R, quality factor $Q > 1$ and resonant frequency f_r

- Longitudinal:

$$W_s(t) = \frac{\omega_r R}{Q} e^{-\alpha t}\left(\cos(\widehat{\omega}_r t) - \frac{\alpha}{\widehat{\omega}_r}\sin(\widehat{\omega}_r t)\right)\,, \tag{9.30}$$

$$Z_s(\omega) = \frac{R}{1 - jQ\left(\frac{\omega_r}{\omega} - \frac{\omega}{\omega_r}\right)}\,. \tag{9.31}$$

- Transverse:

$$W_{x,y}(t) = \frac{\omega_r^2 R}{Q\widehat{\omega}_r} e^{-\alpha t}\sin(\widehat{\omega}_r t)\,, \tag{9.32}$$

$$Z_{x,y}(\omega) = \frac{\omega_r}{\omega}\frac{R}{1 - jQ\left(\frac{\omega_r}{\omega} - \frac{\omega}{\omega_r}\right)}\,. \tag{9.33}$$

where $\omega_r = 2\pi f_r$, $\widehat{\omega}_r = \omega_r\sqrt{1 - \frac{1}{4Q^2}}$, $\alpha = \frac{\omega_r}{2Q}$. Ref: [45, Section 2.2]

Cylindrical thick wall

Cylindrical resistive wall wake, based on the "classic thick wall formula" (see e.g. [46, Chapter 2]) with resistivity ρ, permeability μ, radius r and length L:

- Longitudinal:

$$W_s(t) = -L\frac{1}{4\pi r}\sqrt{\frac{Z_0\rho}{\pi c}} t^{-\frac{3}{2}}\,, \tag{9.34}$$

$$Z_s(\omega) = L\left(1 + j\,\mathrm{sign}(\omega)\right)\frac{\rho}{2\pi r}\frac{1}{\delta_s(\omega)}\,, \tag{9.35}$$

where $\delta_s(\omega) = \sqrt{\frac{2\rho}{|\omega|}}$ is the frequency-dependent skin depth.
Note: the longitudinal resistive wall wake is negative for any value of t, while, with the adopted sign convention, longitudinal wakes should be positive for $t \to 0+$. This happens because the thick wall approximation is not valid for small t. Computing the wake numerically with IW2D shows that the resistive wall wake is actually positive close to zero and performs a few oscillations after which it agrees very well with the formula above. For applications where short range effects are relevant this model should not be used.

- Transverse:

$$W_{x,y}(t) = L\frac{1}{\pi r^3}\sqrt{\frac{cZ_0\rho}{\pi}}t^{-\frac{1}{2}}\,, \tag{9.36}$$

$$Z_{x,y}(\omega) = L(1 + j\,\mathrm{sign}(\omega))\frac{\rho}{\pi r^3}\frac{1}{\omega\sqrt{\varepsilon_0\mu_0}}\frac{1}{\delta_s(\omega)}\,. \tag{9.37}$$

Chapter 10

Intra-Beam Scattering

Intra-beam scattering (IBS) is the process of small angle, multiple Coulomb scattering of charged particles within the beam. It leads to a redistribution of the particle momenta in six-dimentional phase space.

10.1 Analytical Growth Rates

Theoretical models commonly characterize the effect of intra-beam scattering through growth rates, or growth times. The former is expressed in $\left[s^{-1}\right]$) and the latter in $[s]$. These govern the evolution of the rms beam sizes or rms emittances of the beam, depending on the convention used.

Growth rates (and growth times) can be expressed in either amplitude or emittance convention. The former governs the evolution of rms beam sizes while the latter governs that of rms emittances. The two conventions are equivalent by a factor 2 and conversion can be done as:

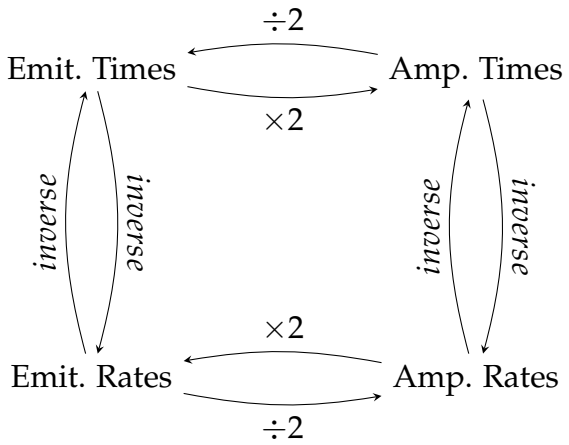

Figure 10.1: Illustration of the conversions between IBS growth rates and times, across emittance and amplitude conventions.

The growth rates themselves are expressed from the lattice optics as well as the beam properties.

In Xsuite, for consistency with synchrotron radiation damping times (see section 3.1), **the amplitude growth rates are computed**. The horizontal (K_x), vertical (K_y) and longitudinal (K_z) amplitude growth rates are defined as:

$$\begin{aligned} K_x &= \frac{1}{\tau_x} = \frac{1}{\varepsilon_x^{1/2}} \frac{d\varepsilon_x^{1/2}}{dt}, \\ K_y &= \frac{1}{\tau_y} = \frac{1}{\varepsilon_y^{1/2}} \frac{d\varepsilon_y^{1/2}}{dt}, \\ K_z &= \frac{1}{\tau_z} = \frac{1}{\varepsilon_z^{1/2}} \frac{d\varepsilon_z^{1/2}}{dt}, \end{aligned} \tag{10.1}$$

where (τ_x), (τ_y) and (τ_z) are the amplitude growth times.

Currently two different formalism are available to compute these growth rates. Both assume transverse and longitudinal Gaussian bunch profiles. Both rely on the computation of the Coulomb logarithm L_C, which in *xfields* is computed according to the expression in the Physics Vade Mecum [47]:

$$L_C = \ln\left(\frac{r_{max}}{r_{min}}\right) . \tag{10.2}$$

In Eq (10.2) r_{max} is taken as the smaller of σ_x and the Debye length, while r_{min} is taken as the larger of the classical distance of closest approach and the quantum diffraction limit from the nuclear radius.

10.1.1 Nagaitsev Formalism

One available formalism follows the approach introduced by S. Nagaitsev in [48]. It provides a fast computation method through symmetric elliptic integrals of the second kind, $R_D(x, y, z)$, defined as:

$$R_D(x, y, z) = \frac{3}{2} \int_0^\infty \frac{dt}{\sqrt{(t + x)(t + y)(t + z)^3}} . \tag{10.3}$$

Interestingly, this elliptic integral has the following special properties:

$$R_D(x, x, x) = x^{-3/2}, \tag{10.4}$$

$$R_D(x, y, z) + R_D(y, z, x) + R_D(z, x, y) = \frac{3}{\sqrt{xyz}} . \tag{10.5}$$

Thanks to Eq (10.5) only two evaluations of this integral are needed to obtain various simple terms from which one can compute the growth rates. Importantly, the computation time of this integral in Nagaitsev's approach does not scale with the size of the lattice.

First the a_x, a_y, a_s, a_1 and a_2 terms are computed:

$$\begin{aligned} a_x &= \frac{\beta_x}{\varepsilon_x}, a_y = \frac{\beta_y}{\varepsilon_y}, a_s = a_x \left(\frac{D_x^2}{\beta_x^2} + \Phi_x^2 \right) + \frac{1}{\sigma_p^2}, \\ a_1 &= \frac{1}{2}(a_x + \gamma^2 a_s), a_2 = \frac{1}{2}(a_x - \gamma^2 a_s) \, , \end{aligned} \tag{10.6}$$

where the $\Phi_{x,y}$ term is defined as:

$$\Phi_{x,y} = D'_{x,y} - \frac{\beta'_{x,y} D_{x,y}}{2\beta_{x,y}} \, . \tag{10.7}$$

Then the λ_1, λ_2 and λ_3 terms are computed:

$$\lambda_1 = a_y \, , \lambda_2 = a_1 + \sqrt{a_2^2 + \gamma^2 a_x^2 \Phi_x^2} \, , \lambda_3 = a_1 - \sqrt{a_2^2 + \gamma^2 a_x^2 \Phi_x^2} \, . \tag{10.8}$$

and used to compute three integrals R_1, R_2 and R_3 (though with Eq (10.5) only two need to be computed):

$$\begin{aligned} R1 &= \frac{1}{\lambda_1} R_D(\frac{1}{\lambda_2}, \frac{1}{\lambda_3}, \frac{1}{\lambda_1}) \, , \\ R2 &= \frac{1}{\lambda_2} R_D(\frac{1}{\lambda_3}, \frac{1}{\lambda_1}, \frac{1}{\lambda_2}) \, , \\ R3 &= \frac{1}{\lambda_3} R_D(\frac{1}{\lambda_1}, \frac{1}{\lambda_2}, \frac{1}{\lambda_3}) \, . \end{aligned} \tag{10.9}$$

Using all the above the S_p, S_x and S_{xp} terms are computed according to Eq (10.10):

$$\begin{aligned} S_p &= \frac{\gamma^2}{2} \left[2R_1 - R_2 \left(1 - \frac{3a_2}{\sqrt{a_2^2 + \gamma^2 a_x^2 \Phi_x^2}} \right) - R_3 \left(1 + \frac{3a_2}{\sqrt{a_2^2 + \gamma^2 a_x^2 \Phi_x^2}} \right) \right] \, , \\ S_x &= \frac{1}{2} \left[2R_1 - R_2 \left(1 + \frac{3a_2}{\sqrt{a_2^2 + \gamma^2 a_x^2 \Phi_x^2}} \right) - R_3 \left(1 - \frac{3a_2}{\sqrt{a_2^2 + \gamma^2 a_x^2 \Phi_x^2}} \right) \right] \, , \\ S_{xp} &= \frac{3\gamma^2 \Phi_x^2 a_x}{\sqrt{a_2^2 + \gamma^2 a_x^2 \Phi_x^2}} \left(R_3 - R_2 \right) \, . \end{aligned} \tag{10.10}$$

From these, one computes the integrals - called the *Nagaitsev integrals* in the *xfields* code base - I_x, I_y and I_z:

$$\begin{aligned} I_x &= \int_0^C \frac{\beta_x ds}{L\sigma_x\sigma_y} \left[S_x + \left(\frac{D_x^2}{\beta_x^2} + \Phi_x^2 \right) S_p + S_{xp} \right] \, , \\ I_y &= \int_0^C \frac{\beta_y ds}{L\sigma_x\sigma_y} \left(R_2 + R_3 - 2R_1 \right) \, , \\ I_z &= \int_0^C \frac{ds}{L\sigma_x\sigma_y} S_p \, . \end{aligned} \tag{10.11}$$

with C the circumference (or length) of the machine. Finally, the *emittance growth rates* in the horizontal, vertical and longitudinal planes are computed as:

$$\boxed{\frac{1}{\varepsilon_x}\frac{d\varepsilon_x}{dt} = \frac{1}{\varepsilon_x}\frac{Nr_0^2 cL_C}{12\pi\beta^3\gamma^5\sigma_z}I_x} \tag{10.12}$$

$$\boxed{\frac{1}{\varepsilon_y}\frac{d\varepsilon_y}{dt} = \frac{1}{\varepsilon_y}\frac{Nr_0^2 cL_C}{12\pi\beta^3\gamma^5\sigma_z}I_y} \tag{10.13}$$

$$\boxed{\frac{1}{\varepsilon_z}\frac{d\varepsilon_z}{dt} = \frac{1}{\sigma_p^2}\frac{Nr_0^2 cL_C}{12\pi\beta^3\gamma^5\sigma_z}I_z} \tag{10.14}$$

In the above N is the total beam intensity, r_0 the classical particle radius, c the speed of light in vacuum, L_C the Coulomb logarithm from Eq (10.2), β and γ the relativistic parameters of the beam and σ_z the bunch length.

Please note: Nagaitsev's computations yield emittance growth rates. In Xsuite these are computed as exposed above, and converted to amplitude growth rates before being returned to the user, as shown in Fig. 10.1.

Importantly, this formalism does not take into account vertical dispersion, and in the presence of D_y will yield an erroneous vertical growth rate. For machines with vertical dispersion, the Bjorken-Mtingwa formalism presented below is recommended.

10.1.2 Bjorken-Mtingwa Formalism

The IBS growth rates can also be computed according to the theory by Bjorken and Mtingwa [49]. The specific implementation follows that of the MAD-X code, for which modifications to the terms of B&M's theory have been made by Antoniou and Zimmermann to account for vertical dispersion non-ultrarelativistic beams [50].

In this formalism, growth rates are computed at every element in the lattice and averaged over the machine. For a given plane u (horizontal, vertical or longitudinal), the *emittance growth rate* is computed as:

$$T_u = \frac{Nr_0^2 cm^3 L_C \pi^2}{\gamma\Gamma}\left\langle \int_0^\infty \frac{d\lambda\lambda^{1/2}}{[\det(L+\lambda I)]^{1/2}}\left\{\operatorname{Tr} L^{(u)}\operatorname{Tr}\left(\frac{1}{L+\lambda I}\right) - 3\operatorname{Tr} L^{(u)}\left(\frac{1}{L+\lambda I}\right)\right\}\right\rangle \tag{10.15}$$

in which N is the total beam intensity, r_0 the classical particle radius, c the speed of light in vacuum, m the mass of the considered particle, L_C the Coulomb logarithm from Eq (10.2), γ the relativistic parameter of the beam, and Γ the six-dimensional phase space volume of the beam, defined as:

$$\Gamma = (2\pi)^3 (\beta\gamma)^3 m^3 \varepsilon_x\varepsilon_y\sigma_\delta\sigma_z \tag{10.16}$$

with σ_δ the relative momentum spread and σ_z the bunch length. One should note the expression for Γ is corrected by a factor $\sqrt{2}$ for coasting beams.
In Eq (10.15) λ is simply the integration variable, I is the 3x3 identity matrix, and L is the 3x3 matrix and the matrix L is defined as:

$$L = L^{(x)} + L^{(y)} + L^{(z)} \,, \tag{10.17}$$

where the plane-dependent matrices $L^{(x)}, L^{(y)}$ and $L^{(z)}$ are defined as:

$$L^{(x)} = \frac{\beta_x}{\epsilon_x} \begin{pmatrix} 1 & -\gamma\phi_x & 0 \\ -\gamma\phi_x & \gamma^2 H_x/\beta_x & 0 \\ 0 & 0 & 0 \end{pmatrix} \,, \tag{10.18}$$

$$L^{(y)} = \frac{\beta_y}{\epsilon_y} \begin{pmatrix} 0 & 0 & 0 \\ 0 & \gamma^2 H_y/\beta_y & -\gamma\phi_y \\ 0 & -\gamma\phi_y & 1 \end{pmatrix} \,, \tag{10.19}$$

$$L^{(z)} = \frac{\gamma^2}{\sigma_\delta^2} \begin{pmatrix} 0 & 0 & 0 \\ 0 & 1 & 0 \\ 0 & 0 & 0 \end{pmatrix} \,. \tag{10.20}$$

The $\Phi_{x,y}$ and $H_{x,y}$ terms are defined as:

$$\phi_{x,y} = D'_{x,y} - \frac{\beta'_{x,y} D_{x,y}}{2\beta_{x,y}} \,, \tag{10.21}$$

and

$$H_{x,y} = \frac{D_{x,y}^2 + \beta_{x,y}^2 \phi_{x,y}^2}{\beta_{x,y}} \,. \tag{10.22}$$

In [50] a new expression was derived for each growth rates, which is the implemented approach. In *xfields*, the computation of the growth rates takes the following steps. First the $a, b, c, a_x, b_x, a_y, b_y, a_z$ and b_z terms are computed as defined below:

$$a = \gamma^2 \left(\frac{H_x}{\varepsilon_x} + \frac{H_y}{\varepsilon_y} \right) + \frac{\gamma^2}{\sigma_\delta^2} + \left(\frac{\beta_x}{\varepsilon_x} + \frac{\beta_y}{\varepsilon_y} \right) \,, \tag{10.23}$$

$$b = \left(\frac{\beta_x}{\varepsilon_x} + \frac{\beta_y}{\varepsilon_y} \right) \left(\frac{\gamma^2 D_x^2}{\varepsilon_x \beta_x} + \frac{\gamma^2 D_y^2}{\varepsilon_y \beta_y} + \frac{\gamma^2}{\sigma_\delta^2} \right) + \frac{\beta_x \beta_y}{\varepsilon_x \varepsilon_y} \gamma^2 \left(\Phi_x^2 + \Phi_y^2 \right) + \frac{\beta_x \beta_y}{\varepsilon_x \varepsilon_y} \,, \tag{10.24}$$

$$c = \frac{\beta_x \beta_y}{\varepsilon_x \varepsilon_y} \left(\frac{\gamma^2 D_x^2}{\varepsilon_x \beta_x} + \frac{\gamma^2 D_y^2}{\varepsilon_y \beta_y} + \frac{\gamma^2}{\sigma_\delta^2} \right) \,, \tag{10.25}$$

$$\begin{aligned} a_x =& 2\gamma^2 \left(\frac{H_x}{\varepsilon_x} + \frac{H_y}{\varepsilon_y} + \frac{1}{\sigma_\delta^2} \right) - \frac{\beta_x H_y}{H_x \varepsilon_y} + \frac{\beta_x}{H_x \gamma^2} \left(\frac{2\beta_x}{\varepsilon_y} - \frac{\beta_y}{\varepsilon_y} - \frac{\gamma^2}{\sigma_\delta^2} \right) \\ & - 2\frac{\beta_x}{\varepsilon_x}\frac{\beta_y}{\varepsilon_y} + \frac{\beta_x}{\gamma^2 H_x} \left(\frac{6\beta_x}{\varepsilon_x} \gamma^2 \Phi_x^2 \right) , \end{aligned} \tag{10.26}$$

$$\begin{aligned} b_x =& \left(\frac{\beta_x}{\varepsilon_x} + \frac{\beta_y}{\varepsilon_y} \right) \left(\frac{\gamma^2 H_x}{\varepsilon_x} + \frac{\gamma^2 H_y}{\varepsilon_y} + \frac{\gamma^2}{\sigma_\delta^2} \right) - \gamma^2 \left(\frac{\beta_x^2}{\varepsilon_x^2} \Phi_x^2 + \frac{\beta_y^2}{\varepsilon_y^2} \Phi_y^2 \right) + \left(\frac{\beta_x}{\varepsilon_x} - \frac{4\beta_y}{\varepsilon_y} \right) \frac{\beta_x}{\varepsilon_x} \\ & + \frac{\beta_x}{\gamma^2 H_x} \left(\frac{\gamma^2}{\sigma_\delta^2} \left(\frac{\beta_x}{\varepsilon_x} - \frac{2\beta_y}{\varepsilon_y} \right) + \frac{\beta_x \beta_y}{\varepsilon_x \varepsilon_y} + \frac{6\beta_x \beta_y}{\varepsilon_x \varepsilon_y} \gamma^2 \Phi_x^2 + \gamma^2 \left(\frac{2\beta_y^2 \Phi_y^2}{\varepsilon_y^2} - \frac{\beta_x^2 \Phi_x^2}{\varepsilon_x^2} \right) \right) \\ & + \frac{\beta_x H_y}{\varepsilon_y H_x} \left(\frac{\beta_x}{\varepsilon_x} - \frac{2\beta_y}{\varepsilon_y} \right) \end{aligned} \tag{10.27}$$

$$\begin{aligned} a_y =& -\gamma^2 \left(\frac{H_x}{\varepsilon_x} + \frac{2H_y}{\varepsilon_y} + \frac{\beta_x}{\beta_y}\frac{H_y}{\varepsilon_x} + \frac{1}{\sigma_\delta^2} \right) + 2\gamma^4 \frac{H_y}{\beta_y} \left(\frac{H_y}{\varepsilon_y} + \frac{H_x}{\varepsilon_x} \right) \\ & + \frac{2\gamma^4 H_y}{\beta_y \sigma_\delta^2} - \left(\frac{\beta_x}{\varepsilon_x} - \frac{2\beta_y}{\varepsilon_y} \right) + \left(\frac{6\beta_y}{\varepsilon_y} \gamma^2 \Phi_y^2 \right) \end{aligned} \tag{10.28}$$

$$\begin{aligned} b_y =& \gamma^2 \left(\frac{\beta_y}{\varepsilon_y} - \frac{2\beta_x}{\varepsilon_x} \right) \left(\frac{H_x}{\varepsilon_x} + \frac{1}{\sigma_\delta^2} \right) + \left(\frac{\beta_y}{\varepsilon_y} - \frac{4\beta_x}{\varepsilon_x} \right) \frac{\gamma^2 H_y}{\varepsilon_y} + \frac{\beta_x \beta_y}{\varepsilon_x \varepsilon_y} \\ & + \gamma^2 \left(\frac{2\beta_x^2 \Phi_x^2}{\varepsilon_x^2} - \frac{\beta_y^2 \Phi_y^2}{\varepsilon_y^2} \right) + \frac{\gamma^4 H_y}{\beta_y} \left(\frac{\beta_x}{\varepsilon_x} + \frac{\beta_y}{\varepsilon_y} \right) \left(\frac{H_y}{\varepsilon_y} + \frac{1}{\sigma_\delta^2} \right) \\ & + \left(\frac{\beta_x}{\varepsilon_x} + \frac{\beta_y}{\varepsilon_y} \right) \gamma^4 \frac{H_x H_y}{\beta_y \varepsilon_x} - \gamma^4 \frac{H_y}{\beta_y} \left(\frac{\beta_x^2}{\varepsilon_x^2} \Phi_x^2 + \frac{\beta_y^2}{\varepsilon_y^2} \Phi_y^2 \right) + \frac{6\beta_x \beta_y}{\varepsilon_x \varepsilon_y} \gamma^2 \Phi_y^2 \end{aligned} \tag{10.29}$$

$$a_z = 2\gamma^2 \left(\frac{H_x}{\varepsilon_x} + \frac{H_y}{\varepsilon_y} + \frac{1}{\sigma_\delta^2} \right) - \frac{\beta_x}{\varepsilon_x} - \frac{\beta_y}{\varepsilon_y} \tag{10.30}$$

$$b_z = \left(\frac{\beta_x}{\varepsilon_x} + \frac{\beta_y}{\varepsilon_y} \right) \gamma^2 \left(\frac{H_x}{\varepsilon_x} + \frac{H_y}{\varepsilon_y} + \frac{1}{\sigma_\delta^2} \right) - 2\frac{\beta_x \beta_y}{\varepsilon_x \varepsilon_y} - \gamma^2 \left(\frac{\beta_x^2 \Phi_x^2}{\varepsilon_x^2} + \frac{\beta_y^2 \Phi_y^2}{\varepsilon_y^2} \right) \tag{10.31}$$

Finally, the *emittance growth rates* in the horizontal, vertical and longitudinal planes are computed as:

$$\boxed{\frac{1}{\varepsilon_x}\frac{d\varepsilon_x}{dt} = \frac{N r_0^2 c m^3 L_C \pi^2}{\gamma \Gamma} \left\langle \left[\frac{\gamma^2 H_x}{\varepsilon_x} \right] \int_0^\infty \frac{\lambda^{1/2} \left[a_x \lambda + b_x \right]}{(\lambda^3 + a\lambda^2 + b\lambda + c)} d\lambda \right\rangle} \tag{10.32}$$

$$\boxed{\frac{1}{\varepsilon_y}\frac{d\varepsilon_y}{dt} = \frac{N r_0^2 c m^3 L_C \pi^2}{\gamma \Gamma} \left\langle \left[\frac{\beta_y}{\varepsilon_y} \right] \int_0^\infty \frac{\lambda^{1/2} \left[a_y \lambda + b_y \right]}{(\lambda^3 + a\lambda^2 + b\lambda + c)} d\lambda \right\rangle} \tag{10.33}$$

$$\boxed{\frac{1}{\varepsilon_z}\frac{d\varepsilon_z}{dt} = \frac{Nr_0^2 cm^3 L_C \pi^2}{\gamma\Gamma}\left\langle\left[\frac{\gamma^2}{\sigma_\delta^2}\right]\int_0^\infty \frac{\lambda^{1/2}\left[a_z\lambda + b_z\right]}{\left(\lambda^3 + a\lambda^2 + b\lambda + c\right)}d\lambda\right\rangle} \tag{10.34}$$

where the constants in the common fraction term are the same as for Eq (10.15), λ is an integration variable and the angled bracket signify the averaging over the lattice, given the terms contained inside are arrays with one value per element.

Please note: Bjorken and Mtingwa's computations yield emittance growth rates. In Xsuite these are computed as exposed above, and converted to amplitude growth rates before being returned to the user, as shown in Fig. 10.1. where the constants in the common fraction term are the same as for Eq (10.15), λ is an integration variable and the angled bracket signifies the averaging over the lattice, given the terms contained inside are arrays with one value per element.

10.2 Steady-state emittances

The steady-state emittances in the presence of Synchrotron Radiation (SR), Quantum Excitation (QE), and Intra-Beam Scattering (IBS) emerge from a dynamic equilibrium, where the combined effect of these three phenomena balances each other out. More specifically, the QE and SR are accounted for through the natural emittances and SR damping constants, the IBS is described by its growth rates. Each of these effects depends on the optical functions along the storage ring. All the following equations remain valid independently of which formalism (Nagaitsev or Bjorken-Mtingwa) is used when computing the IBS growth rates. In addition, the SR damping constants and IBS growth rates follow the amplitude convention as defined in Eq. (3.15).

10.2.1 Steady-state emittances with QE, SR, and IBS

The steady-state emittances are solutions to a system of three ordinary differential equations describing the dynamic interplay of the QE, SR, and IBS. The system of differential equations can be solved numerically by computing the emittance evolution for a succession of infinitesimal time steps. The equations are as follows:

$$\frac{d\varepsilon_u}{dt} = -2\alpha_u^{SR}\left(\varepsilon_u - \varepsilon_{u,0}\right) + 2\alpha_u^{IBS}\varepsilon_u, \quad u = x, y, z \tag{10.35}$$

$\varepsilon_{u,0}$ is the natural emittance, ε_u the emittance, α_u^{SR} the SR damping constant and α_u^{IBS} the IBS growth rate. It can be noted that the IBS growth rates are a function of all three emittances ($\alpha_u^{IBS}(\varepsilon_x, \varepsilon_y, \varepsilon_z)$).
The steady-state emittance is reached when the emittance evolution reaches zero and leads to:

$$\varepsilon_u = \frac{\varepsilon_{u,0}}{1 - \alpha_u^{IBS}/\alpha_u^{SR}}, \quad u = x, y, z \tag{10.36}$$

Although mathematically correct, the equation assumes a finite vertical emittance. In the case of lepton storage rings, the vertical emittance is often negligible in the absence

of vertical dispersion or betatron coupling. As a result, the IBS growth rates would reach extremely large values when a near zero vertical emittance is considered. A finite vertical emittance is introduced through betatron coupling or an external excitation to overcome this limitation.

10.2.2 Steady-state emittances due to betatron coupling

In the presence of betatron coupling, emittance sharing occurs between the two transverse planes. The treatment of betatron coupling can be simplified by expressing it through the emittance coupling factor $\kappa = \tilde{\varepsilon}_y/\tilde{\varepsilon}_x$, the ratio of the perturbed vertical emittance to the horizontal one.
Based on the natural emittance, defined in Eq. (3.39) but written in a form [51] so that the horizontal damping partition number j_x appears:

$$\varepsilon_0 = C_q \frac{\gamma^2}{j_x} \frac{I_5}{I_2},$$

where $C_q = \frac{55}{32\sqrt{3}} \frac{\hbar}{m_e c} \approx 3.84 \times 10^{-13}$ m for electrons, γ the relativistic gamma and I_2, I_5 respectively the second and fifth radiation integrals.

$$\tilde{\varepsilon_0} = C_q \frac{\gamma^2}{\tilde{j_x}} \frac{\langle K^3 \mathcal{H} \rangle}{K^2}, \qquad \text{where} \quad \tilde{j_x} = \frac{j_x}{1+\kappa} + \frac{\kappa j_y}{1+\kappa} \tag{10.37}$$

Here, j_y represents the vertical damping partition number. After some simplifications and remembering $\tilde{\varepsilon}_0 = \tilde{\varepsilon}_x + \tilde{\varepsilon}_y$ we finally obtain:

$$\tilde{\varepsilon}_{x,0} = \frac{\tilde{\varepsilon}_0}{1+\kappa} = \frac{\tilde{\varepsilon}_0}{1+\kappa\frac{j_y}{j_x}}, \qquad \tilde{\varepsilon}_{y,0} = \frac{\kappa\tilde{\varepsilon}_0}{1+\kappa} = \frac{\kappa\tilde{\varepsilon}_0}{1+\kappa\frac{j_y}{j_x}} \tag{10.38}$$

Furthermore, the perturbed horizontal and vertical emittances can be expressed as a function of the ones without betatron coupling:

$$\tilde{\varepsilon}_x = \frac{\varepsilon}{1+\kappa\frac{j_y}{j_x}}, \quad \tilde{\varepsilon}_y = \frac{\kappa\varepsilon}{1+\kappa\frac{j_y}{j_x}}$$

It can be noted that total transverse emittance conservation occurs solely if $j_x = j_y$.
As a result, the transverse emittance evolution can be rewritten as:

$$\frac{d\tilde{\varepsilon}_u}{dt} = -2\alpha_u^{SR}\left(\tilde{\varepsilon}_u - \tilde{\varepsilon}_{u,0}\right) + 2\alpha_u^{IBS}\tilde{\varepsilon}_u, \quad u = x, y \tag{10.39}$$

And the steady-state transverse emittances become:

$$\tilde{\varepsilon}_u = \frac{\tilde{\varepsilon}_{u,0}}{1 - \frac{\alpha_u^{IBS}}{\alpha_u^{SR}\left(1+\kappa j_y/j_x\right)}}, \quad u = x, y \tag{10.40}$$

10.2.3 Steady-state emittances due to an external excitation

Alternatively, a finite vertical emittance can also be obtained by exciting the beam using the Pulse-Picking by Resonant Excitation (PPRE) method [52] in the vertical plane. In this situation, the horizontal and vertical planes are left uncoupled while the vertical emittance can be controlled. Nonetheless, the emittance coupling factor can still be employed. In this scenario, the emittance evolution follows Eq. (10.39) and the final emittance Eq. (10.36). Compared to the previous case, the total transverse emittance is not conserved even if $j_x = j_y$.

10.3 IBS Kicks

The approach of using analytical growth rates does not provide a way to study the interplay of IBS with arbitrary effects, such as space charge, electron clouds, beam-beam, etc. To do so, it is necessary to include IBS effects in tracking simulations together with other desired effects. In *xfields* two elements are available to model IBS effects in tracking simulations, both providing momenta kicks to tracked particles according to a specific formalism.

10.3.1 Analytical Kicks

A first element is available to provide momenta kicks based on analytical growth rates, according to the approach introduced by R. Bruce [53]. In *xfields* the computation of the kick is done as follows.

First, the beam intensity N, bunch length σ_z, momentum deviation σ_δ, and geometric emittances $\varepsilon_{x,y}$ are inferred from the tracked particles object. These are used to compute the analytical IBS growth rates. From these, each particle is given a momentum kick in each dimension according to:

$$\boxed{\Delta p_u = R\sigma_{p_u}\sqrt{2T_{IBS,u}T_{rev}\sigma_z\sqrt{\pi}\rho(z)}\ ;\ u = x, y, z} \tag{10.41}$$

Here R is a random number from the standard normal distribution; σ_{p_u} is the standard deviation of the momentum in plane u; $T_{IBS,u}$ is the *emittance growth rate* for plane u; T_{rev} is the revolution frequency and $\rho(z)$ is the longitudinal line density.

Note from the form of Eq (10.41) that only zero or strictly positive growth rates are valid, and as such this formalism is traditionally available above transition energy.

The longitudinal line density $\rho(z)$ is used as a weighting factor to provide a stronger kick to particles in the denser regions of the bunch. It is obtained by binning the longitudinal plane of the particle distribution and normalizing the values.

10.3.2 Kinetic Kicks

A second element is available to provide momenta kicks based on diffusion and friction terms from the kinetic theory of gases, as introduced by P. Zenkevich [54]. The momentum kick has a form similar to the Langevin equation:

$$\Delta p_u = -K_u p_u \sigma_z \sqrt{\pi}\rho(z)\Delta t + R\sigma_{p_u}\sqrt{2C_u\sigma_z\sqrt{\pi}\rho(z)\Delta t}\,; u = x, y, z \tag{10.42}$$

where K_u and C_u are functions of the friction and diffusion terms, respectively.

In *xfields* the exact implementation makes use of terms from the Nagaitsev formalism (see 10.1.1) as derived by M. Zampetakis [55]. First the a_x, a_y, a_s, a_1 and a_2 terms are computed according to Eq (10.6). Then the λ_1, λ_2 and λ_3 terms are computed according to Eq (10.8), to obtain the R_1, R_2 and R_3 elliptic integrals according to Eq (10.9).

New forms equivalent to the original diffusion and friction terms of the Approximate Model can be expressed from these. By first defining

$$q = \sqrt{a_2^2 + \gamma^2 a_x^2 \Phi_x^2}\,, \tag{10.43}$$

one can first compute:

$$\begin{aligned}
D_{x,x} &= \frac{1}{2}\left[2R_1 + R2\left(1 - \frac{a_2}{q}\right) + R_3\left(1 + \frac{a_2}{q}\right)\right], \\
D_{x,z} &= \frac{3\gamma^2\Phi_x^2 a_x}{q}\left(R_3 - R_2\right), \\
D_{y,y} &= R_2 + R_3, \\
D_{z,z} &= \frac{\gamma^2}{2}\left[2R_1 + R_2\left(1 + \frac{a_2}{q}\right) + R_3\left(1 - \frac{a_2}{q}\right)\right],
\end{aligned} \tag{10.44}$$

and then:

$$\begin{aligned}
K_x &= R_2\left(1 + \frac{a_2}{q}\right) + R_3\left(1 - \frac{a_2}{q}\right), \\
K_y &= 2R_1, \\
K_z &= \gamma^2\left[R_2\left(1 - \frac{a_2}{q}\right) + R_3\left(1 + \frac{a_2}{q}\right)\right].
\end{aligned} \tag{10.45}$$

The following integrals are computed from the above:

$$\begin{aligned}
D_{xi} &= \int_0^C \frac{\beta_x ds}{C\sigma_x\sigma_y}\left[D_{x,x} + \left(\frac{D_x^2}{\beta_x^2} + \Phi_x^2\right)D_{z,z} + D_{x,z}\right], \\
D_{yi} &= \int_0^C \frac{\beta_y ds}{C\sigma_x\sigma_y} D_{y,y}, \\
D_{zi} &= \int_0^C \frac{ds}{C\sigma_x\sigma_y} D_{z,z}\,.
\end{aligned} \tag{10.46}$$

$$
\begin{aligned}
F_{xi} &= \int_0^C \frac{\beta_x ds}{C\sigma_x\sigma_y}\left[K_x + \left(\frac{D_x^2}{\beta_x^2} + \Phi_x^2\right)K_z\right], \\
F_{yi} &= \int_0^C \frac{\beta_y ds}{C\sigma_x\sigma_y}K_x, \\
F_{zi} &= \int_0^C \frac{ds}{C\sigma_x\sigma_y}K_z\,.
\end{aligned} \tag{10.47}
$$

with C the circumference of the machine. Finally, the new diffusion coefficients are computed according to:

$$\boxed{G_x = \frac{1}{\varepsilon_x}\frac{Nr_0^2cL_C}{12\pi\beta^3\gamma^5\sigma_z}D_{xi}} \tag{10.48}$$

$$\boxed{G_y = \frac{1}{\varepsilon_y}\frac{Nr_0^2cL_C}{12\pi\beta^3\gamma^5\sigma_z}D_{yi}} \tag{10.49}$$

$$\boxed{G_z = \frac{1}{\sigma_\delta^2}\frac{Nr_0^2cL_C}{12\pi\beta^3\gamma^5\sigma_z}D_{zi}} \tag{10.50}$$

and the friction coefficients according to:

$$\boxed{F_x = \frac{1}{\varepsilon_x}\frac{Nr_0^2cL_C}{12\pi\beta^3\gamma^5\sigma_z}F_{xi}} \tag{10.51}$$

$$\boxed{F_y = \frac{1}{\varepsilon_y}\frac{Nr_0^2cL_C}{12\pi\beta^3\gamma^5\sigma_z}F_{yi}} \tag{10.52}$$

$$\boxed{F_z = \frac{1}{\sigma_\delta^2}\frac{Nr_0^2cL_C}{12\pi\beta^3\gamma^5\sigma_z}F_{zi}} \tag{10.53}$$

In the above N is the total beam intensity, r_0 the classical particle radius, c the speed of light in vacuum, L_C the Coulomb logarithm from Eq (10.2). β and γ are the relativistic parameters of the beam and σ_z the bunch length.

From these coefficients, each particle is given a momentum kick in each dimension according to:

$$\boxed{\Delta p_u = -F_u p_u T_{rev} 2\sqrt{\pi}\sigma_z\rho(z) + R\sigma_{p_u}\sqrt{T_{rev}G_u 2\sqrt{\pi}\sigma_z\rho(z)}\;;\, u = x, y, z} \tag{10.54}$$

Here R is a random number from the standard normal distribution; p_u and σ_{p_u} are the momentum and its standard deviation in plane u; T_{rev} is the revolution frequency and $\rho(z)$ is the longitudinal line density as defined previously (see 10.3.1).

Chapter 11

FFT solvers and convolutions

11.1 Notation for Discrete Fourier Transform

We will use the following notation for the Discrete Fourier Transform of a sequence of length M:

$$\hat{a}_k = \mathrm{DFT}_M(a_m) = \sum_{m=0}^{M-1} a_m \, e^{-j2\pi \frac{km}{M}} \quad \text{for } k \in 0, ..., M \tag{11.1}$$

The corresponding inverse transform is defined as:

$$a_n = \mathrm{DFT}_M^{-1}(\hat{a}_k) = \frac{1}{M} \sum_{k=0}^{M-1} \hat{a}_k \, e^{j2\pi \frac{km}{M}} \quad \text{for } m \in 0, ..., M \tag{11.2}$$

Multidimensional Discrete Fourier Transforms are obtained by applying sequentially 1D DFTs.. For example, in two dimensions:

$$\begin{aligned} \hat{a}_{k_x k_y} &= \mathrm{DFT}_{M_x M_y} \left\{ a_{m_x m_y} \right\} = \mathrm{DFT}_{M_y} \left\{ \mathrm{DFT}_{M_x} \left\{ a_{m_x m_y} \right\} \right\} \\ &= \sum_{m_x=0}^{M_x-1} e^{-j2\pi \frac{k_x m_x}{M_x}} \sum_{m_y=0}^{M_y-1} e^{-j2\pi \frac{k_y m_y}{M_y}} a_{m_x m_y} \end{aligned} \tag{11.3}$$

$$\begin{aligned} a_{n_x n_y} &= \mathrm{DFT}^{-1}_{M_x M_y} \left\{ a_{k_x k_y} \right\} = \mathrm{DFT}^{-1}_{M_y} \left\{ \mathrm{DFT}^{-1}_{M_x} \left\{ \hat{a}_{k_x k_y} \right\} \right\} \\ &= \frac{1}{M_x M_y} \sum_{k_x=0}^{M_x-1} e^{j2\pi \frac{k_x m_x}{M_x}} \sum_{k_y=0}^{M_y-1} e^{j2\pi \frac{k_y m_y}{M_y}} \hat{a}_{k_x k_y} \end{aligned} \tag{11.4}$$

11.2 FFT convolution - 1D case

The potential can be written as the convolution of a Green function with the charge distribution:

$$\phi(x) = \int_{-\infty}^{+\infty} \rho(x') \, G(x - x') dx' \tag{11.5}$$

We assume that the source is limited to the region $[0, L]$:

$$\rho(x) = \rho(x)\,\Pi_{[0,L]}\,(x) \tag{11.6}$$

where $\Pi_{[a,b]}(x)$ is a rectangular window function defined as:

$$\Pi_{[a,b]}(x) = \begin{cases} 1 & \text{for } x \in [a,b] \\ 0 & \text{elsewhere} \end{cases} \tag{11.7}$$

We are interested in the electric potential only the region occupied by the sources, so we can compute:

$$\phi_L(x) = \phi(x)\Pi_{[0,L]}\,(x) \tag{11.8}$$

We replace Eq. (11.6) and Eq. (11.8) into Eq.(11.5), obtaining:

$$\phi_L(x) = \Pi_{[0,L]}\,(x) \int_{-\infty}^{+\infty} \Pi_{[0,L]}\,(x')\,\rho(x')\,G(x-x')dx' \tag{11.9}$$

We apply the change of variable $x'' = x - x'$:

$$\phi_L(x) = \int_{-\infty}^{+\infty} \Pi_{[0,L]}\,(x)\,\Pi_{[0,L]}\,(x-x'')\,\rho(x-x'')\,G(x'')\,dx'' \tag{11.10}$$

The integrand vanishes outside the set of the (x, x'') defined by:

$$\begin{cases} 0 < x < L \\ 0 < (x - x'') < L \end{cases} \tag{11.11}$$

We flip the signs in the second equation, obtaining:

$$\begin{cases} 0 < x < L \\ -L < (x'' - x) < 0 \end{cases} \tag{11.12}$$

Combining the two equations we obtain:

$$-L < -L + x < x'' < x < L \tag{11.13}$$

i.e. the integrand is zero for $-L < x'' < L$. Therefore in Eq. (11.10) we can replace $G(x'')$ with its truncated version:

$$G_{2L}(x'') = G(x'')\,\Pi_{[-L,L]}\,(x'') \tag{11.14}$$

obtaining:

$$\phi_L(x) = \int_{-\infty}^{+\infty} \Pi_{[0,L]}\,(x)\,\Pi_{[0,L]}\,(x-x'')\,\rho(x-x'')\,G_{2L}(x'')dx'' \tag{11.15}$$

Since the two window functions force the integrand to zero outside the region $|x''| < L$ we can replace $G_{2L}(x'')$ with its replicated version:

$$G_{2LR}(x'') = \sum_{n=-\infty}^{+\infty} G_{2L}(x'' - 2nL) = \sum_{n=-\infty}^{+\infty} G(x'' - 2nL)\,\Pi_{[-L,L]}\,(x'' - 2nL) \tag{11.16}$$

obtaining:

$$\phi_L(x) = \int_{-\infty}^{+\infty} \Pi_{[0,L]}(x)\, \Pi_{[0,L]}\left(x - x''\right) \rho(x - x'')\, G_{2LR}(x'')dx'' \tag{11.17}$$

We can go back to the initial coordinate by substituting $x'' = x - x'$:

$$\phi_L(x) = \Pi_{[0,L]}(x) \int_{-\infty}^{+\infty} \rho(x')\, G_{2LR}(x - x')dx' \tag{11.18}$$

This is a cyclic convolution, so we can proceed as follows. We split the integral:

$$\phi_L(x) = \Pi_{[0,L]}(x) \sum_{n=-\infty}^{+\infty} \int_{2nL}^{2(n+1)L} \rho(x')\, G_{2LR}(x - x')\, dx' \tag{11.19}$$

In each term we replace $x''' = x' + 2nL$:

$$\phi_L(x) = \Pi_{[0,L]}(x) \sum_{n=-\infty}^{+\infty} \int_{0}^{2L} \rho(x''' - 2nL)\, G_{2LR}(x - x''' - 2nL)\, dx''' \tag{11.20}$$

We use the fact that $G_{2LR}(x)$ is periodic:

$$\begin{aligned} \phi_L(x) &= \Pi_{[0,L]}(x) \sum_{n=-\infty}^{+\infty} \int_{0}^{2L} \rho(x''' - 2nL)\, G_{2LR}(x - x''')dx''' \\ &= \Pi_{[0,L]}(x) \int_{0}^{2L} \sum_{n=-\infty}^{+\infty} \rho(x''' - 2nL)\, G_{2LR}(x - x''')dx''' \end{aligned} \tag{11.21}$$

We can define a replicated version of $\rho(x)$:

$$\rho_{2LR}(x) = \sum_{n=-\infty}^{+\infty} \rho(x - 2nL) \tag{11.22}$$

noting that this implies:

$$\rho_{2LR}(x) = 0 \quad \text{for } x \in [L, 2L] \tag{11.23}$$

We obtain:

$$\phi_L(x) = \Pi_{[0,L]}(x) \int_{0}^{2L} \rho_{2LR}(x')\, G_{2LR}(x - x')dx' \tag{11.24}$$

The function:

$$\phi_{2LR}(x) = \int_{0}^{2L} \rho_{2LR}(x')\, G_{2LR}(x - x')dx' \tag{11.25}$$

is periodic of period $2L$. From it the potential of interest can be simply calculated by selecting the first half period $[0, L]$:

$$\phi_L(x) = \Pi_{[0,L]}(x)\, \phi_{2LR}(x) \tag{11.26}$$

To compute the convolution in Eq. 11.25 we expand $\phi_{2LR}(x)$ in Fourier series:

$$\phi_{2LR}(x) = \sum_{k=-\infty}^{+\infty} \tilde{\phi}_k \, e^{j2\pi k \frac{x}{2L}} \tag{11.27}$$

where the Fourier coefficients are given by:

$$\tilde{\phi}_k = \frac{1}{2L} \int_0^{2L} \phi_{2LR}(x) \, e^{-j2\pi k \frac{x}{2L}} \, dx \tag{11.28}$$

We replace Eq. (11.25) into Eq. (11.28) obtaining:

$$\hat{\phi}_k = \frac{1}{2L} \int_0^{2L} \int_0^{2L} \rho_{2LR}(x') \, G_{2LR}(x - x') \, e^{-j2\pi k \frac{x}{2L}} \, dx' \, dx \tag{11.29}$$

With the change of variable $x'' = x - x'$ we obtain:

$$\tilde{\phi}_k = \frac{1}{2L} \int_0^{2L} \rho_{2LR}(x') e^{-j2\pi k \frac{x'}{2L}} dx' \int_0^{2L} G_{2LR}(x'') e^{-j2\pi k \frac{x''}{2L}} \, dx'' \tag{11.30}$$

where we recognize the Fourier coefficients of $\rho_{2LR}(x)$ and $G_{2LR}(x)$:

$$\tilde{\rho}_k = \frac{1}{2L} \int_0^{2L} \rho_{2LR}(x) \, e^{-j2\pi k \frac{x}{2L}} \, dx \tag{11.31}$$

$$\tilde{G}_k = \frac{1}{2L} \int_0^{2L} G_{2LR}(x) \, e^{-j2\pi k \frac{x}{2L}} \, dx \tag{11.32}$$

obtaining simply:

$$\hat{\phi}_k = 2L \, \hat{G}_k \, \hat{\rho}_k \tag{11.33}$$

I assume to have the functions $\rho_{2LR}(x)$ and $G_{2LR}(x)$ sampled (or averaged) with step:

$$h_x = \frac{2L}{M} = \frac{L}{N} \tag{11.34}$$

I can approximate the integrals in Eqs. (11.31) and (11.32) as:

$$\tilde{\rho}_k = \frac{1}{M} \sum_{n=0}^{M-1} \rho_{2LR}(x_n) \, e^{-j2\pi \frac{kn}{M}} = \frac{1}{M} \hat{\rho}_k \tag{11.35}$$

$$\tilde{G}_k = \frac{1}{M} \sum_{n=0}^{M-1} G_{2LR}(x_n) \, e^{-j2\pi \frac{kn}{M}} = \frac{1}{M} \hat{G}_k \tag{11.36}$$

where we recognize the Discrete Fourier Transforms:

$$\hat{\rho}_k = \mathrm{DFT}_M \left\{ \rho_{2LR}(x_n) \right\} \tag{11.37}$$

$$\hat{G}_k = \mathrm{DFT}_M \left\{ G_{2LR}(x_n) \right\} \tag{11.38}$$

Using Eq. (11.27) we can obtain a sampled version of $\phi(x)$:

$$\phi_{2LR}(x_n) = \sum_{n=0}^{M-1} \tilde{\phi}_k \, e^{j2\pi \frac{kn}{M}} \tag{11.39}$$

where we have assumed that $\phi(x)$ is sufficiently smooth to allow truncating the sum. Using Eqs. (11.33), (11.35) and (11.36) we obtain:

$$\phi_{2LR}(x_n) = 2L \sum_{n=0}^{M-1} \tilde{G}_k \, \tilde{\rho}_k \, e^{j2\pi \frac{kn}{M}} = \frac{2L}{M^2} \sum_{n=0}^{M-1} \hat{G}_k \, \hat{\rho}_k \, e^{j2\pi \frac{kn}{M}} \tag{11.40}$$

This can be rewritten as:

$$\phi_{2LR}(x_n) = \frac{1}{M} \sum_{n=0}^{M-1} (h_x \hat{G}_k) \, \hat{\rho}_k \, e^{j2\pi \frac{kn}{M}} = \mathrm{DFT}_M^{-1} \left\{ \phi_k \right\} \tag{11.41}$$

where

$$\hat{\phi}_k = h_x \hat{G}_k \, \hat{\rho}_k \tag{11.42}$$

We call "Integrated Green Function" the quantity:

$$G_{2LR}(x_n) = h_x G_{2LR}(x_n) \tag{11.43}$$

we introduce the corresponding Fourier transform:

$$\hat{G}_k^{\mathrm{int}} = \mathrm{DFT}_M \left\{ G_{2LR}^{\mathrm{int}}(x_n) \right\} \tag{11.44}$$

Eq. (11.42) can be rewritten as:

$$\boxed{\hat{\phi}_k = \hat{G}_k^{\mathrm{int}} \, \hat{\rho}_k} \tag{11.45}$$

In summary the potential at the grid nodes can be computed as follows:

1. We compute the Integrated Green function at the grid points in the range $[0, L]$:

$$G_{2LR}^{\mathrm{int}}(x_n) = \int_{x_n - \frac{h_x}{2}}^{x_n + \frac{h_x}{2}} G(x) dx \tag{11.46}$$

2. We extend to the interval $[L, 2L]$ using the fact that in this interval:

$$G_{2LR}^{\mathrm{int}}(x_n) = G_{2LR}^{\mathrm{int}}(x_n - 2L) = G_{2LR}^{\mathrm{int}}(2L - x_n) \tag{11.47}$$

   where the first equality comes from the periodicity of $G_{2LR}^{\mathrm{int}}(x)$ and the second from the fact that $G(x)$ is an even function (i.e. $G(x) = G(-x)$). Note that for $x_n \in [L, 2L]$ we have that $2L - x_n \in [0, L]$ so we can reuse the values computed at the previous step.

3. We transform it:

$$\hat{G}_k^{\mathrm{int}} = \mathrm{DFT}_{2N} \left\{ G_{2LR}(x_n) \right\} \tag{11.48}$$

4. We assume that we are given $\rho(x_n)$ in the interval $[0, L]$. From this we can obtain $\rho_{2LR}(x_n)$ over the interval $[0, 2L]$ simply extending the sequence with zeros (see Eq. (11.23)).

5. We transform it:

$$\hat{\rho}_k = \mathrm{DFT}_{2N} \left\{ \rho_{2LR}(x_n) \right\} \tag{11.49}$$

6. We compute the potential in the transformed domain:

$$\hat{\phi}_k = \hat{G}_k^{\text{int}} \hat{\rho}_k \quad \text{for } k \in [0, 2N] \tag{11.50}$$

7. We inverse-transform:

$$\phi_{2LR}(x_n) = \text{DFT}_{2N}^{-1} \left\{ \hat{\phi}_k \right\} \tag{11.51}$$

which provides the physical potential in the range $[0, L]$:

$$\phi(x_n) = \phi_{2LR}(x_n) \quad \text{for } x_n \in [0, L] \tag{11.52}$$

11.3 Extension to multiple dimensions

The procedure described above can be extended to multiple dimensions by applying the same reasoning for all coordinates. This gives the following procedure:

1. We compute the Integrated Green function at the grid points in the volume $[0, L_x] \times [0, L_y] \times [0, L_z]$:

$$G_{2LR}^{\text{int}}(x_{n_x}, y_{n_y}, z_{n_z}) = \int_{x_{n_x} - \frac{h_x}{2}}^{x_{n_x} + \frac{h_x}{2}} dx \int_{y_{n_y} - \frac{h_y}{2}}^{y_{n_y} + \frac{h_y}{2}} dy \int_{z_{n_z} - \frac{h_z}{2}}^{z_{n_z} + \frac{h_z}{2}} dz \, G(x, y, z) \tag{11.53}$$

2. We extend to the region $[0, 2L_x] \times [0, 2L_y] \times [0, 2L_z]$ using the fact that:

$$G_{2LR}^{\text{int}}(x_n, y_n, z_n) = G_{2LR}^{\text{int}}(x_n - 2L_x, y_n, z_n) = G_{2LR}^{\text{int}}(2L_x - x_n, y_n, z_n) \\ \text{for } x_n \in [L_x, 2L_x], y_n \in [0, 2L_y], z_n \in [0, 2L_z] \tag{11.54}$$

$$G_{2LR}^{\text{int}}(x_n, y_n, z_n) = G_{2LR}^{\text{int}}(x_n, y_n - 2L_y, z_n) = G_{2LR}^{\text{int}}(x_n, 2L_y - y_n, z_n) \\ \text{for } y_n \in [L_y, 2L_y], x_n \in [0, 2L_x], z_n \in [0, 2L_z] \tag{11.55}$$

$$G_{2LR}^{\text{int}}(x_n, y_n, z_n) = G_{2LR}^{\text{int}}(x_n, y_n, z_n - 2L_z) = G_{2LR}^{\text{int}}(x_n, y_n, 2L_z - z_n) \\ \text{for } z_n \in [L_z, 2L_z], x_n \in [0, 2L_x], y_n \in [0, 2L_y] \tag{11.56}$$

This allows reusing the values computed at the previous step.

3. We transform it:

$$\hat{G}_{k_x k_y k_z}^{\text{int}} = \text{DFT}_{2N_x 2N_y 2N_z} \left\{ G_{2LR}(x_n, y_n, z_n) \right\} \tag{11.57}$$

4. We assume that we are given $\rho(x_n, y_n, z_n)$ in the region $[0, L_x] \times [0, L_y] \times [0, L_z]$. From this we can obtain $\rho_{2LR}(x_n)$ over the region $[0, 2L_x] \times [0, 2L_y] \times [0, 2L_z]$ simply extending the matrix with zeros (see Eq. (11.23)).

5. We transform it:

$$\hat{\rho}_{k_x k_y k_z}^{\text{int}} = \text{DFT}_{2N_x 2N_y 2N_z} \left\{ \rho_{2LR}(x_n, y_n, z_n) \right\} \tag{11.58}$$

6. We compute the potential in the transformed domain:

$$\hat{\phi}_{k_x k_y k_z} = \hat{G}^{\text{int}}_{k_x k_y k_z} \hat{\rho}_{k_x k_y k_z} \quad \text{for } k_{x/y/z} \in [0, 2N_{x/y/z}] \tag{11.59}$$

7. We inverse-transform:

$$\phi_{2LR}(x_n, y_n, z_n) = \text{DFT}^{-1}_{2N_x 2N_y 2N_z} \left\{ \hat{\phi}_{k_x k_y k_z} \right\} \tag{11.60}$$

which provides the physical potential in the region $[0, L_x] \times [0, L_y] \times [0, L_z]$:

$$\phi(x_n, y_n, z_n) = \phi_{2LR}(x_n, y_n, z_n) \text{ for } (x_n, y_n, z_n) \in [0, L_x] \times [0, L_y] \times [0, L_z] \tag{11.61}$$

11.4 Green functions for 2D and 3D Poisson problems

3D Poisson problem, free space boundary conditions

For the equation:

$$\nabla^2 \phi(x, y, z) = -\frac{1}{\varepsilon_0} \rho(x, y, z) \tag{11.62}$$

where:

$$\nabla = \left(\frac{\partial}{\partial x}, \frac{\partial}{\partial y}, \frac{\partial}{\partial z} \right) \tag{11.63}$$

the solution can be written as

$$\phi(x, y, z) = \iiint_{-\infty}^{+\infty} \rho(x', y', z')\, G(x - x', y - y', z - z')\, dx'\, dy'\, dz' \tag{11.64}$$

where:

$$G(x, y, z) = \frac{1}{4\pi\varepsilon_0} \frac{1}{\sqrt{x^2 + y^2 + z^2}} \tag{11.65}$$

The corresponding integrated Green function [56]. can be written as:

$$G^{\text{int}}_{2LR}(x_{n_x}, y_{n_y}, z_{n_z}) = \int_{x_{n_x}-\frac{h_x}{2}}^{x_{n_x}+\frac{h_x}{2}} dx \int_{y_{n_y}-\frac{h_y}{2}}^{y_{n_y}+\frac{h_y}{2}} dy \int_{z_{n_z}-\frac{h_z}{2}}^{x_{n_z}+\frac{h_z}{2}} dz\, G(x,y,z) \tag{11.66}$$

$$\begin{aligned}
&= + F\left(x_{n_x}+\frac{h_x}{2}, y_{n_x}+\frac{h_y}{2}, z_{n_x}+\frac{h_z}{2}\right) && (11.67)\\
&\quad - F\left(x_{n_x}+\frac{h_x}{2}, y_{n_x}+\frac{h_y}{2}, z_{n_x}-\frac{h_z}{2}\right) && (11.68)\\
&\quad - F\left(x_{n_x}+\frac{h_x}{2}, y_{n_x}-\frac{h_y}{2}, z_{n_x}+\frac{h_z}{2}\right) && (11.69)\\
&\quad + F\left(x_{n_x}+\frac{h_x}{2}, y_{n_x}-\frac{h_y}{2}, z_{n_x}-\frac{h_z}{2}\right) && (11.70)\\
&\quad - F\left(x_{n_x}-\frac{h_x}{2}, y_{n_x}+\frac{h_y}{2}, z_{n_x}+\frac{h_z}{2}\right) && (11.71)\\
&\quad + F\left(x_{n_x}-\frac{h_x}{2}, y_{n_x}+\frac{h_y}{2}, z_{n_x}-\frac{h_z}{2}\right) && (11.72)\\
&\quad + F\left(x_{n_x}-\frac{h_x}{2}, y_{n_x}-\frac{h_y}{2}, z_{n_x}+\frac{h_z}{2}\right) && (11.73)\\
&\quad - F\left(x_{n_x}-\frac{h_x}{2}, y_{n_x}-\frac{h_y}{2}, z_{n_x}-\frac{h_z}{2}\right) && (11.74)
\end{aligned}$$

where $F(x,y,z)$ is a primitive of $G(x,y,z)$, which can be obtained as:

$$F(x,y,z) = \int_{x_0}^{x} dx \int_{y_0}^{y} dy \int_{z_0}^{x} dz\, G(x,y,z) \tag{11.75}$$

with (x_0, y_0, z_0) being an arbitrary starting point.
An expression for $F(x,y,z)$ is the following

$$F(x,y,z) = \frac{1}{4\pi\varepsilon_0} \iiint \frac{1}{\sqrt{x^2+y^2+z^2}} dxdydz \tag{11.76}$$

$$\begin{aligned}
&= \frac{1}{4\pi\varepsilon_0}\left[-\frac{z^2}{2}\arctan\left(\frac{xy}{z\sqrt{x^2+y^2+z^2}}\right) - \frac{y^2}{2}\arctan\left(\frac{xz}{y\sqrt{x^2+y^2+z^2}}\right)\right. && (11.77)\\
&\quad - \frac{x^2}{2}\arctan\left(\frac{yz}{x\sqrt{x^2+y^2+z^2}}\right) + yz\ln\left(x+\sqrt{x^2+y^2+z^2}\right) && (11.78)\\
&\quad \left. + xz\ln\left(y+\sqrt{x^2+y^2+z^2}\right) + xy\ln\left(z+\sqrt{x^2+y^2+z^2}\right)\right] && (11.79)
\end{aligned}$$

Note that we need to choose the first cell center to be in (0,0,0) for evaluation of the integrated Green function. Therefore the cell edges have non zero coordinates and the denominators in the formula will always be non-vanishing.

2D Poisson problem, free space boundary conditions

For the equation:

$$\nabla_{\perp}^2 \phi(x,y) = -\frac{1}{\varepsilon_0}\rho(x,y) \tag{11.80}$$

where:

$$\nabla = \left(\frac{\partial}{\partial x}, \frac{\partial}{\partial y}\right) \tag{11.81}$$

the solution can be written as

$$\phi(x,y) = \iint_{-\infty}^{+\infty} \rho(x',y')\, G(x-x', y-y')\, dx'\, dy' \tag{11.82}$$

where:

$$G(x,y) = -\frac{1}{4\pi\varepsilon_0} \log\left(\frac{x^2+y^2}{r_0^2}\right) \tag{11.83}$$

where r_0 is arbitrary constant which has no effect on the evaluated fields (changes the potential by an additive constant).
The corresponding integrated Green function can be written as:

$$G_{2LR}^{\text{int}}(x_{n_x}, y_{n_y}) = \int_{x_{n_x}-\frac{h_x}{2}}^{x_{n_x}+\frac{h_x}{2}} dx \int_{y_{n_y}-\frac{h_y}{2}}^{y_{n_y}+\frac{h_y}{2}} dy\, G(x,y,z) \tag{11.84}$$

$$= + F\left(x_{n_x} + \frac{h_x}{2}, y_{n_x} + \frac{h_y}{2}\right) \tag{11.85}$$

$$- F\left(x_{n_x} + \frac{h_x}{2}, y_{n_x} - \frac{h_y}{2}\right) \tag{11.86}$$

$$- F\left(x_{n_x} - \frac{h_x}{2}, y_{n_x} + \frac{h_y}{2}\right) \tag{11.87}$$

$$+ F\left(x_{n_x} - \frac{h_x}{2}, y_{n_x} - \frac{h_y}{2}\right) \tag{11.88}$$

where $F(x,y)$ is a primitive of $G(x,y)$, which can be obtained as:

$$F(x,y) = \int_{x_0}^{x} dx \int_{y_0}^{y} dy\, G(x,y) \tag{11.89}$$

where (x_0, y_0) is an arbitrary starting point.
An expression for $F(x,y)$ is the following (where we have chosen $r_0 = 1$):

$$F(x,y) = -\frac{1}{4\pi\varepsilon_0} \iint \ln\left(x^2+y^2\right) dx/, dy \tag{11.90}$$

$$= \frac{1}{4\pi\varepsilon_0}\left[3xy - x^2 \arctan(y/x) - y^2 \arctan(x/y) - xy \ln\left(x^2+y^2\right)\right] \tag{11.91}$$

Note that we need to choose the first cell center to be in (0,0) for evaluation of the integrated Green function. Therefore the cell edges have non zero coordinates and the denominators in the formula will always be non-vanishing.

11.5 Generalization to observation interval different from source interval

The potential generated by a source $\rho(x)$ can be written as the convolution of a Green function with the charge distribution:

$$\phi(x) = \int_{-\infty}^{+\infty} \rho(x')\, G(x - x') dx' \tag{11.92}$$

We assume that the source is limited to the region $[a, b]$:

$$\rho(x) = \rho(x)\, \Pi_{[a,b]}(x) \tag{11.93}$$

where $\Pi_{[a,b]}(x)$ is a rectangular window function defined as:

$$\Pi_{[a,b]}(x) = \begin{cases} 1 & \text{for } x \in [a, b] \\ 0 & \text{elsewhere} \end{cases} \tag{11.94}$$

We are interested in the electric potential in a given region $[c, d]$, so we can compute:

$$\phi_{cd}(x) = \phi(x) \Pi_{[c,d]}(x) \tag{11.95}$$

We combine Eqs. (11.93), (11.95) and (11.92), obtaining:

$$\phi_{cd}(x) = \Pi_{[c,d]}(x) \int_{-\infty}^{+\infty} \Pi_{[a,b]}(x')\, \rho(x')\, G(x - x') dx' \tag{11.96}$$

We apply the change of variable $x'' = x - x'$:

$$\phi_{cd}(x) = \int_{-\infty}^{+\infty} \Pi_{[c,d]}(x)\, \Pi_{[a,b]}(x - x'')\, \rho(x - x'')\, G(x'')\, dx'' \tag{11.97}$$

The integrand vanishes outside the set of the (x, x'') defined by the two window functions:

$$\begin{cases} c < x < d \\ a < (x - x'') < b \end{cases} \tag{11.98}$$

We flip the signs in the second equation, obtaining:

$$\begin{cases} c < x < d \\ -b < (x'' - x) < -a \end{cases} \tag{11.99}$$

Combining the two equations we obtain:

$$c - b < -b + x < x'' < -a + x < d - a \tag{11.100}$$

i.e. the integrand is not zero for $c - b < x'' < d - a$. Therefore in Eq. (11.97) we can replace $G(x'')$ with its truncated version:

$$G_{\text{tr}}(x'') = G(x'')\, \Pi_{[c-b,\, d-a]}(x'') \tag{11.101}$$

obtaining:

$$\phi_{cd}(x) = \int_{-\infty}^{+\infty} \Pi_{[c,d]}(x)\, \Pi_{[a,b]}\left(x - x''\right) \rho(x - x'')\, G_{\text{tr}}(x'')dx'' \tag{11.102}$$

We can go back to the initial coordinate by substituting $x'' = x - x'$:

$$\phi_{cd}(x) = \Pi_{[c,d]}(x) \int_{-\infty}^{+\infty} \rho(x')\, G_{\text{tr}}(x - x')dx' \tag{11.103}$$

We call:

$$L_1 = b - a \tag{11.104}$$
$$L_2 = d - c \tag{11.105}$$

The measure of the set on which $G_{\text{tr}}(x'')$ is non zero is

$$(d - a) - (c - b) = L_1 + L_2 \tag{11.106}$$

We define L such that:

$$L_1 + L_2 = 2L \tag{11.107}$$

Since the two window functions in Eq. 11.102 force the integrand to zero outside the region $c - b < x'' < d - a$ of measure $2L$, we can replace $G_{\text{tr}}(x'')$ with its replicated version:

$$G_R(x'') = \sum_{n=-\infty}^{+\infty} G_{\text{tr}}(x'' - 2nL) = \sum_{n=-\infty}^{+\infty} G(x'' - 2nL)\, \Pi_{[c-b,\, d-a]}\left(x'' - 2nL\right) \tag{11.108}$$

obtaining:

$$\phi_{cd}(x) = \int_{-\infty}^{+\infty} \Pi_{[c,d]}(x)\, \Pi_{[a,b]}\left(x - x''\right) \rho(x - x'')\, G_R(x'')dx'' \tag{11.109}$$

We can go back to the initial coordinate by substituting $x'' = x - x'$:

$$\phi_{cd}(x) = \Pi_{[c,d]}(x) \int_{-\infty}^{+\infty} \rho(x')\, G_R(x - x')dx' \tag{11.110}$$

This is a cyclic convolution, so we can proceed as follows. We split the integral:

$$\phi_{cd}(x) = \Pi_{[c,d]}(x) \sum_{n=-\infty}^{+\infty} \int_{2nL}^{2(n+1)L} \rho(x')\, G_R(x - x')\, dx' \tag{11.111}$$

In each term we replace $x''' = x' + 2nL$:

$$\phi_{cd}(x) = \Pi_{[c,d]}(x) \sum_{n=-\infty}^{+\infty} \int_{0}^{2L} \rho(x''' - 2nL)\, G_R(x - x''' - 2nL)\, dx''' \tag{11.112}$$

We use the fact that $G_R(x)$ is periodic:

$$\begin{aligned}\phi_{cd}(x) &= \Pi_{[c,d]}(x) \sum_{n=-\infty}^{+\infty} \int_0^{2L} \rho(x''' - 2nL)\, G_R(x - x''') dx''' \\ &= \Pi_{[c,d]}(x) \int_0^{2L} G_R(x - x''') \sum_{n=-\infty}^{+\infty} \rho(x''' - 2nL)\, dx'''\end{aligned} \tag{11.113}$$

We can define a replicated version of $\rho(x)$:

$$\rho_R(x) = \sum_{n=-\infty}^{+\infty} \rho(x - 2nL) \tag{11.114}$$

We obtain:

$$\phi_{cd}(x) = \Pi_{[c,d]}(x) \int_0^{2L} \rho_R(x')\, G_R(x - x') dx' \tag{11.115}$$

The function:

$$\phi_R(x) = \int_0^{2L} \rho_R(x')\, G_R(x - x') dx' \tag{11.116}$$

is periodic of period $2L$. Replacing in Eq. 11.115 we see that the potential of interest can be simply calculated by selecting the right interval $[c, d]$:

$$\phi_{cd}(x) = \Pi_{[c,d]}(x)\, \phi_R(x) \tag{11.117}$$

To compute the convolution in Eq. 11.116 we expand $\phi_R(x)$ in a Fourier series starting from $x = c$:

$$\phi_R(x) = \sum_{k=-\infty}^{+\infty} \tilde{\phi}_k\, e^{j2\pi k \frac{x}{2L}} \tag{11.118}$$

where the Fourier coefficients are given by:

$$\tilde{\phi}_k = \frac{1}{2L} \int_0^{2L} \phi_R(x)\, e^{-j2\pi k \frac{x}{2L}}\, dx \tag{11.119}$$

We replace Eq. (11.116) into Eq. (11.119) obtaining:

$$\tilde{\phi}_k = \frac{1}{2L} \int_0^{2L} \int_0^{2L} \rho_R(x')\, G_R(x - x')\, e^{-j2\pi k \frac{x}{2L}}\, dx'\, dx \tag{11.120}$$

With the change of variable $x'' = x - x'$ we obtain:

$$\tilde{\phi}_k = \frac{1}{2L} \int_0^{2L} \rho_R(x') e^{-j2\pi k \frac{x'}{2L}} dx' \int_0^{2L} G_R(x'') e^{-j2\pi k \frac{x''}{2L}}\, dx'' \tag{11.121}$$

where we recognize the Fourier coefficients of $\rho_R(x)$ and $G_R(x)$:

$$\tilde{\rho}_k = \frac{1}{2L} \int_0^{2L} \rho_R(x)\, e^{-j2\pi k \frac{x}{2L}}\, dx \tag{11.122}$$

$$\tilde{G}_k = \frac{1}{2L} \int_0^{2L} G_R(x)\, e^{-j2\pi k \frac{x}{2L}}\, dx \tag{11.123}$$

obtaining simply:

$$\tilde{\phi}_k = 2L\,\tilde{G}_k\,\tilde{\rho}_k \tag{11.124}$$

We assume to have the functions $\rho_R(x)$ and $G_R(x)$ sampled (or averaged) with step:

$$h_x = \frac{2L}{M} \tag{11.125}$$

We assume that all intervals have size multiple of h_x. So we can define:

$$N_1 = L_1/h_x \tag{11.126}$$
$$N_2 = L_2/h_x \tag{11.127}$$

We call:

$$\rho_{Rn} = \rho_R\left(a + nh_x\right) \tag{11.128}$$
$$\phi_{Rn} = \phi_R\left(c + nh_x\right) \tag{11.129}$$
$$G_{Rn} = G_R\left(c - b + nh_x\right) \tag{11.130}$$

By construction in the range $0 \leq n < M$:

$$\rho_{Rn} \equiv \rho_n = \begin{cases} \rho\left(a + nh_x\right) & \text{for } 0 \leq n < N_1 \\ 0 & \text{for } N_1 \leq n < M \end{cases} \tag{11.131}$$

$$G_{Rn} \equiv G_n = G\left(c - b + nh_x\right) \text{ for } 0 \leq n < M \tag{11.132}$$

We can approximate the integral as follows:

$$\tilde{\rho}_k = \frac{1}{2L}\int_0^{2L} \rho_R(x)\, e^{-j2\pi k\frac{x}{2L}}\, dx = \frac{1}{2L}\int_a^{a+2L} \rho_R(x)\, e^{-j2\pi k\frac{x}{2L}}\, dx \tag{11.133}$$
$$\simeq \frac{h_x}{2L}\sum_{n=0}^{M-1} \rho_R(a + nh_x)\, e^{-j2\pi k\frac{a+nh_x}{2L}} = e^{-j2\pi k\frac{a}{2L}}\frac{1}{M}\sum_{n=0}^{M-1} \rho_{Rn} e^{-j2\pi\frac{kn}{M}} \tag{11.134}$$

We recognize the Discrete Fourier Transform:

$$\tilde{\rho}_k = e^{-j2\pi k\frac{a}{2L}}\frac{1}{M}\mathrm{DFT}_M\left\{\rho_{Rn}\right\} = e^{-j2\pi k\frac{a}{2L}}\frac{1}{M}\hat{\rho}_k \tag{11.135}$$

and similarly we can obtain

$$\tilde{\phi}_k = e^{-j2\pi k\frac{c}{2L}}\frac{1}{M}\mathrm{DFT}_M\left\{\phi_{Rn}\right\} = e^{-j2\pi k\frac{c}{2L}}\frac{1}{M}\hat{\phi}_k \tag{11.136}$$

$$\tilde{G}_k = e^{-j2\pi k\frac{c-b}{2L}}\frac{1}{M}\mathrm{DFT}_M\left\{G_{Rn}\right\} = e^{-j2\pi k\frac{c-b}{2L}}\frac{1}{M}\hat{G}_k \tag{11.137}$$

Replacing in Eq. 11.124 we obtain

$$\hat{\phi}_k = h_x e^{j2\pi k\frac{b-a}{2L}}\hat{\rho}_k\hat{G}_k = h_x e^{j2\pi k\frac{N_1}{M}}\hat{\rho}_k\hat{G}_k \tag{11.138}$$

11.6 Compressed FFT convolution

We assume that the source has the form

$$\rho(x) = \sum_{j=A}^{B-1} \rho_j^{\text{loc}}(x - jP) \tag{11.139}$$

where $\rho_j^{\text{loc}}(x)$ is limited to the interval $[a, b]$.
We are interested in the potential in a set of intervals given by:

$$[c + iP,\ d + iP] \quad \text{for } i = C, ..., D - 1 \tag{11.140}$$

The contribution of the j-th term of ρ to ϕ int the i-th interval:

$$\phi_{ij}(x) = \int_{-\infty}^{+\infty} \rho_j^{\text{loc}}(x' - jP)\, G_{i-j}^{\text{tr}}(x - x')dx' \tag{11.141}$$

where:

$$G_l^{\text{tr}}(x'') = G(x'')\, \Pi_{[c-b+lP,\ d-a+lP]}\left(x''\right) \tag{11.142}$$

We define a local version of G^{tr} as

$$G_l^{\text{tr, loc}}(x) = G_l^{\text{tr}}(x + lP) = G(x + lP)\, \Pi_{[c-b,\ d-a]}\left(x\right) \tag{11.143}$$

obtaining:

$$\phi_{ij}(x) = \int_{-\infty}^{+\infty} \rho_j^{\text{loc}}(x' - jP)\, G_{i-j}^{\text{tr, loc}}(x - x' - (i-j)P)dx' \tag{11.144}$$

We replace $x' = x' - jP$:

$$\phi_{ij}(x) = \int_{-\infty}^{+\infty} \rho_j^{\text{loc}}(x')\, G_{i-j}^{\text{tr, loc}}(x - x' - iP)dx' \tag{11.145}$$

We define a local version of ϕ:

$$\phi_{ij}^{\text{loc}}(x) = \phi_{ij}(x + iP) \tag{11.146}$$

obtaining:

$$\phi_{ij}^{\text{loc}}(x) = \int_{-\infty}^{+\infty} \rho_j^{\text{loc}}(x')\, G_{i-j}^{\text{tr, loc}}(x - x')dx' \tag{11.147}$$

I explicit all the pies:

$$\phi_{ij}^{\text{loc}}(x) = \int_{-\infty}^{+\infty} \Pi_{[a,b]}(x')\Pi_{[c-b,\ d-a]}(x - x')\rho_j^{\text{loc}}(x')\, G_{i-j}^{\text{tr, loc}}(x - x')dx' \tag{11.148}$$

Again, we want to find the region in x where this is non-zero:

$$a < x' < b \tag{11.149}$$
$$c - b < x - x' < d - a \tag{11.150}$$

from which:

$$c - b + x' < x < d - a + x' \tag{11.151}$$
$$c - b + a < x < d - a + b \tag{11.152}$$

So we find that $\phi_{ij}^{\text{loc}}(x)$ is non-zero in the region:

$$c - L_1 < x < d + L_1 \tag{11.153}$$

The total potential in the i-th interval of interest:

$$\phi_i^{\text{loc}}(x) = \sum_{j=A}^{B-1} \phi_{ij}^{\text{loc}}(x) = \sum_{j=A}^{B-1} \int_{-\infty}^{+\infty} \rho_j^{\text{loc}}(x')\, G_{i-j}^{\text{tr, loc}}(x - x')dx' \tag{11.154}$$

Since all terms in the sum are zero outside the region defined by Eq. 11.153 also $\phi_i^{\text{loc}}(x)$ is zero outside the same interval, which is larger by $2L_1$ compared to the set of interest $[c, d]$.
We build:

$$G^{\text{aux}}(x) = \sum_{l=C-B+1}^{D-A-1} G_l^{\text{tr, loc}}(x - lL_{\text{aux}}) \tag{11.155}$$

where:

$$L_{\text{aux}} = L_1 + L_2 \tag{11.156}$$

and

$$\rho^{\text{aux}}(x) = \sum_{j=A}^{B-1} \rho_j^{\text{loc}}(x - jL_{\text{aux}}) \tag{11.157}$$

and we define

$$\phi^{\text{aux}}(x) = \int_{-\infty}^{+\infty} \rho^{\text{aux}}(x')\, G^{\text{aux}}(x - x')dx' \tag{11.158}$$

We extract a segment of it:

$$\phi_i^{\text{aux, loc}}(x) = \phi^{\text{aux}}(x + iL_{\text{aux}})\Pi_{[c,d]}(x) \tag{11.159}$$

We replace Eq. 11.155:

$$\phi_i^{\text{aux, loc}}(x) = \Pi_{[c,d]}(x) \int_{-\infty}^{+\infty} \rho^{\text{aux}}(x')\, G^{\text{aux}}(x - x' + iL_{\text{aux}})dx' \tag{11.160}$$

We replace Eq. 11.157 and Eq. 11.155:

$$\phi_i^{\text{aux, loc}}(x) = \Pi_{[c,d]}(x) \int_{-\infty}^{+\infty} \sum_{j=A}^{B-1} \rho_j^{\text{loc}}(x' - jL_{\text{aux}}) \sum_{l=C-B+1}^{D-A-1} G_l^{\text{tr, loc}}(x - x' + (i-l)L_{\text{aux}})dx' \tag{11.161}$$

$$= \Pi_{[c,d]}(x) \sum_{l=C-B+1}^{D-A-1} \sum_{j=A}^{B-1} \int_{-\infty}^{+\infty} \rho_j^{\text{loc}}(x' - jL_{\text{aux}})\, G_l^{\text{tr, loc}}(x - x' + (i-l)L_{\text{aux}})dx' \tag{11.162}$$

We change variable $x'' = x' - (i-l)L_{\text{aux}}$

$$\phi_i^{\text{aux, loc}}(x) = \sum_{l=C-B+1}^{D-A-1} \sum_{j=A}^{B-1} \int_{-\infty}^{+\infty} \Pi_{[c,d]}(x) \rho_j^{\text{loc}}(x'' + (i-l-j)L_{\text{aux}})\, G_l^{\text{tr, loc}}(x - x'') dx'' \tag{11.163}$$

The integrand is nonzero for:

$$c < x < d \tag{11.164}$$
$$a < x'' + (i-l-j)L_{\text{aux}}) < b \tag{11.165}$$
$$c - b < x - x'' < d - a \tag{11.166}$$

I subtract the first and the last:

$$a < x'' + (i-l-j)L_{\text{aux}}) < b \tag{11.167}$$
$$-b < -x'' < -a \tag{11.168}$$

I flip the last

$$a < x'' + (i-l-j)L_{\text{aux}}) < b \tag{11.169}$$
$$a < x'' < b \tag{11.170}$$

The two are compatible only if

$$l = i - j \tag{11.171}$$

This means that in the double sum only the terms satisfying Eq. 11.171 are nonzero, hence:

$$\phi_i^{\text{aux, loc}}(x) = \Pi_{[c,d]}(x) \sum_{j=A}^{B-1} \int_{-\infty}^{+\infty} \rho_j^{\text{loc}}(x''+)\, G_{i-j}^{\text{tr, loc}}(x - x'') dx'' \tag{11.172}$$

Comparing against Eq. 11.154 we find:

$$\Pi_{[c,d]}(x) \phi_i^{\text{aux, loc}}(x) = \Pi_{[c,d]}(x) \phi_i^{\text{loc}}(x) \tag{11.173}$$

Using Eq. 11.159 we obtain:

$$\Pi_{[c,d]}(x) \phi_i^{\text{loc}}(x) = \Pi_{[c,d]}(x) \phi^{\text{aux}}(x + iL_{\text{aux}}) \tag{11.174}$$

To compute the convolution in Eq. 11.158 we can use the results from the previous section.
We call:

$$N_S = B - A \tag{11.175}$$
$$N_T = D - C \tag{11.176}$$
$$\tag{11.177}$$

The support of $\rho^{\text{aux}}(x)$ is:

$$[a + AL_{\text{aux}}, a + BL_{\text{aux}}] \text{ having size } N_S L_{\text{aux}} \tag{11.178}$$

The support of $G^{\text{aux}}(x)$ is:

$$[c - b + (C - B + 1)L_{\text{aux}}, c - b + (D - A)L_{\text{aux}}] \text{ having size } (N_S + N_T - 1)\, L_{\text{aux}} \tag{11.179}$$

Using a sampling step h_x, we can define:

$$N_1 = L_1/h_x \tag{11.180}$$
$$N_2 = L_2/h_x \tag{11.181}$$
$$N_{\text{aux}} = L_{\text{aux}}/h_x = N_1 + N_2 \tag{11.182}$$

The number of samples in the support of $G^{\text{aux}}(x)$ is

$$M_{\text{aux}} = (N_S + N_T - 1)N_{\text{aux}} \tag{11.183}$$

We define

$$G^{\text{aux}}_m = G^{\text{aux}}\left(c - b + (C - B + 1)L_{\text{aux}} + mh_x\right) \text{ for } 0 \leq m < M_{\text{aux}} \tag{11.184}$$

Replacing Eq. 11.155:

$$G^{\text{aux}}_m = \sum_{l=C-B+1}^{D-A-1} G^{\text{tr, loc}}_l(c - b + (C - B + 1)L_{\text{aux}} + mh_x - lL_{\text{aux}}) \tag{11.185}$$
$$= \sum_{l=C-B+1}^{D-A-1} G(c - b + (C - B + 1)L_{\text{aux}} + lP + h_x(m - lN_{\text{aux}})) \times \tag{11.186}$$
$$\Pi_{[c-b,\, d-a]}(c - b + (C - B + 1)L_{\text{aux}} + h_x(m - lN_{\text{aux}})) \tag{11.187}$$

We define:

$$G^{\text{segm}}_{l,n} = G(c - b + (C - B + 1)L_{\text{aux}} + lP + nh_x)\Pi_{[c-b,\, d-a]}(c - b + (C - B + 1)L_{\text{aux}} + nh_x)$$
$$\text{for } 0 \leq n < N_{\text{aux}} \text{ and } (C - B + 1) \leq l < (D - A) \tag{11.188}$$

So we can write:

$$G^{\text{aux}}_m = \sum_{l=C-B+1}^{D-A-1} G^{\text{segm}}_{l,m-lN_{\text{aux}}} \tag{11.189}$$

We define:

$$\rho^{\text{aux}}_m = \begin{cases} \rho^{\text{aux}}\left(a + AL_{\text{aux}} + mh_x\right) & \text{for } 0 \leq m < N_S N_{\text{aux}} \\ 0 & \text{for } N_S N_{\text{aux}} \leq m < M_{\text{aux}} \end{cases} \tag{11.190}$$

We can use the result from before linking the DFTs of these sequences:

$$\hat{\phi}^{\text{aux}}_k = h_x e^{j2\pi k \frac{(B-A-1)L_{\text{aux}} + (b-a)}{(N_S+N_T-1)L_{\text{aux}}}} = h_x e^{j2\pi k \frac{(N_S-1)N_{\text{aux}} + N_1}{(N_S+N_T-1)N_{\text{aux}}}} \hat{\rho}^{\text{aux}}_k \hat{G}^{\text{aux}}_k \tag{11.191}$$

The inverse DFT of $\hat{\phi}^{\text{aux}}_k$ provides:

$$\phi^{\text{aux}}_m = \phi^{\text{aux}}\left(c + CL_{\text{aux}} + mh_x\right) \quad \text{for } 0 \leq m < N_T N_{\text{aux}} \tag{11.192}$$

Bibliography

[1] G. Ripken. Non-linear canonical equations of coupled synchro-betatron motion and their solutions within the framework of a non-linear six-dimensional (symplectic) tracking program for ultrarelativistic protons. Technical Report 85-084, DESY, 1985.

[2] D.P. Barber, G. Ripken, and F. Schmidt. A non-linear canonical formalism for the coupled synchro-betatron motion of protons with arbitrary energy. Technical Report 87-36, DESY, 1987.

[3] G. Ripken and F. Schmidt. A symplectic six-dimensional thin-lens formalism for tracking. Technical Report DESY 95-63 and CERN/SL/95-12(AP), DESY, CERN, 1995.

[4] K. Heinemann, G. Ripken, and F. Schmidt. Construction of nonlinear symplectic six-dimensional thin-lens maps by exponentiation. Technical Report 95-189, DESY, 1995.

[5] D.P. Barber, K. Heinemann, G. Ripken, and F. Schmidt. Symplectic thin-lens transfer maps for SIXTRACK: Treatment of bending magnets in terms of the exact hamiltonian. Technical Report 96-156, DESY, 1996.

[6] L.H.A. Leunissen, F. Schmidt, and G. Ripken. 6D beam-beam kick including coupled motion. Technical report, 2001.

[7] A. Latina and R. De Maria. RF multipole implementation. Technical report, CERN-ATS. 2012-088.

[8] E. Forest. *Beam Dynamics: A New Attitude and Framework*. Harcourt Academic Publisher, 1999.

[9] Andrzej Wolski. *Beam dynamics in high energy particle accelerators*. World Scientific, 2014.

[10] F. Willeke and G. Ripken. Methods of beam optics. Technical Report 88-114, DESY, 1988.

[11] F. C. Iselin. The mad program (methodical accelerator design) - physics methods manual. Technical Report CERN/SL/92-?? (AP), CERN, 1992.

[12] Y. Luo, P. Cameron, S. Peggs, and D. Trbojevic. Possible phase loop for the global betatron decoupling. Technical Report CAD/AP/174, Brookhaven National Laboratory, Upton, NY 11973, USA, October 4 2004.

[13] Rhodri Jones. Measuring Tune, Chromaticity and Coupling. 5 2020.

[14] Eirik Jaccheri Hoydalsvik, Tobias Hakan Bjorn Persson, and Rogelio Tomas Garcia. Evaluation of the closest tune approach and its MAD-X implementation. 2021.

[15] Albert Hofmann. *The Physics of Synchrotron Radiation*. Cambridge Monographs on Particle Physics, Nuclear Physics and Cosmology. Cambridge University Press, 2004.

[16] H Burkhardt. Monte Carlo generator for synchrotron radiation. Technical report, CERN, Geneva, 1990.

[17] Alexander W. Chao. Evaluation of beam distribution parameters in an electron storage ring. *Journal of Applied Physics*, 50(2):595–598, 07 2008.

[18] Georg H. Hoffstaetter. *High-Energy Polarized Proton Beams: A Modern View*, volume 218 of *Springer Tracts in Modern Physics*. Springer, Berlin, Heidelberg, 2006.

[19] David C. Sagan. *Bmad Reference Manual*. Cornell Laboratory for Accelerator-Based Sciences and Education, 2025. Available at `https://www.classe.cornell.edu/bmad/`.

[20] A. W. Chao. Evaluation of Radiative Spin Polarization in an Electron Storage Ring. *Nucl. Instrum. Meth.*, 180:29, 1981.

[21] Ya. S. Derbenev and A. M. Kondratenko. Polarization kinematics of particles in storage rings. *Sov. Phys. JETP*, 37:968–973, 1973.

[22] Michael Boge. Analysis of spin depolarizing effects in electron storage rings. Other thesis, 5 1994.

[23] S. R. Mane. Electron Spin Polarization in High-Energy Storage Rings. 1. Derivation of the Equilibrium Polarization. *Phys. Rev. A*, 36:105–119, 1987.

[24] D. P. Barber and G. Ripken. Radiative polarization, computer algorithms and spin matching in electron storage rings. 7 1999.

[25] Zhe Duan, Mei Bai, Desmond P. Barber, and Qing Qin. A monte-carlo simulation of the equilibrium beam polarization in ultra-high energy electron (positron) storage rings. *Nuclear Instruments and Methods in Physics Research Section A: Accelerators, Spectrometers, Detectors and Associated Equipment*, 793:81–91, 2015.

[26] K Hirata, H Moshammer, and F Ruggiero. A Symplectic Beam-Beam Interaction with Energy Change. *SLAC-PUB-10055*, Dec 2017.

[27] Kohji Hirata. Don't be afraid of beam-beam interactions with a large crossing angle. Technical Report SLAC-PUB-6375, 1994.

[28] G Iadarola, R De Maria, and Y Papaphilippou. Modelling and implementation of the "6D" beam-beam interaction. *CERN-ACC- SLIDES-2018-001*, Dec 2017.

[29] SixTrack Project website. `http://cern.ch/sixtrack`.

[30] SixTrackLib source code repository. `http://github.com/SixTrack/SixTrackLib`.

[31] G Iadarola, R De Maria, and Y Papaphilippou. 6D beam-beam interaction step-by-step. *CERN-ACC-NOTE-2018-0023*, Dec 2017.

[32] W Herr and T Pieloni. Beam-Beam Effects. *in Proceedings of CAS - CERN Accelerator School: Advanced Accelerator Physics Course, 18 - 29 Aug 2013, Trondheim, Norway, CERN-2014-009*, 2014.

[33] Mad-X beam-beam macros, source code repository. `https://github.com/lhcopt/beambeam_macros`.

[34] MAD-X Project website. `http://cern.ch/madx`.

[35] D. Griffiths. *Introduction to elementary particles*. 2nd rev. version, Wiley, 2008.

[36] C. Weizsäcker. Ausstrahlung bei Stössen sehr schneller Elektronen. *in Zeitschrift Für Physik, vol. 88, Sep. 1934, pp. 612-625.* `https://doi.org/10.1007/BF01333110`.

[37] E. Williams. Correlation of certain collision problems with radiation theory. *in Kong. Dan. Vid. Sel. Mat. Fys. Med., vol. 13N4, 1935, pp. 1-50.* `https://inspirehep.net/literature/1377275`.

[38] D. Schulte. Study of electromagnetic and hadronic background in the interaction region of the TESLA collider. Apr. 1997. `https://cds.cern.ch/record/331845`.

[39] F. Arutyunian and V. Tumanian. The Compton effect on relativistic electrons and the possibility of obtaining high energy beams. *in Physics Letters, vol. 4, 1963, pp. 176-178.* `https://doi.org/10.1016/0031-9163(63)90351-2`.

[40] M. Bassetti and G. Erskine. Closed expression for the electrical field of a two-dimensional Gaussian charge. 1980. `https://cds.cern.ch/record/122227`.

[41] F. Halzen and A. Martin. *Quarks and Leptons: An Introductory Course in Modern Particle Physics*. 1984. `http://www.gammaexplorer.com/wp-content/uploads/2014/03/Quarks-and-Leptons-An-Introductory-Course-in-Modern-Particle-Physics.pdf`.

[42] `GUINEA-PIG` repository. `https://gitlab.cern.ch/clic-software/guinea-pig-legacy`.

[43] I. Ginzburg, G. Kotkin, V. Serbo, and V. Telnov. Colliding ge and gg beams based on the single-pass e±e- colliders (VLEPP type). *in Nuclear Instruments And Methods In Physics Research, vol. 205, pp. 47-68.*, 1983. https://www.sciencedirect.com/science/article/pii/0167508783901734.

[44] Kaoru Yokoya. A Computer Simulation Code for the Beam-beam Interaction in Linear Colliders. 10 1985. https://inspirehep.net/literature/218375.

[45] Nicolas Mounet. The LHC Transverse Coupled-Bunch Instability, 2012. Presented 2012.

[46] A. W. Chao. *Physics of collective beam instabilities in high-energy accelerators*. 1993.

[47] H. L, Anderson. *AIP 50th Anniversary: Physics Vade Mecum*. American Institute of Physics, 1981.

[48] Sergei Nagaitsev. Intrabeam Scattering Formulas for Fast Numerical Evaluation. *Phys. Rev. ST Accel. Beams*, 8:064403, 5 2005.

[49] James Bjorken and Sekazi Mtingwa. Intrabeam scattering. In *Particle Accelerators*, pages 115–143. Gordon and Breach Science Publishers, 1983.

[50] F. Antoniou and F. Zimmermann. Revision of Intrabeam Scattering with Non-Ultrarelativistic Corrections and Vertical Dispersion for MAD-X. Technical report, Cern, Geneva, 2012.

[51] Shyh-yuan Lee. *Accelerator Physics (Fourth Edition)*. World Scientific Publishing Company, 2018.

[52] Ji-Gwang Hwang, Marten Koopmans, Markus Ries, Andreas Schälicke, and Roman Muller. Analytical and numerical analysis of longitudinally coupled transverse dynamics of pulse picking by resonant excitation in storage rings serving timing and high-flux users simultaneously. *Nuclear Instruments and Methods in Physics Research Section A: Accelerators, Spectrometers, Detectors and Associated Equipment*, 2019.

[53] Bruce R, Jowett J. M, Blaskiewicz M, and Fischer W. Time Evolution of the Luminosity of Colliding Heavy-Ion Beams in BNL Relativistic Heavy Ion Collider and CERN Large Hadron Collider. *Physical Review Special Topics - Accelerators and Beams*, 13(9), 2010.

[54] Zenkevich P, Boine-Frankenheim O, and Bolshakov A. A new Algorithm for the Kinetic Analysis of Intra-Beam Scattering in Storage Rings. *Nuclear Instruments and Methods in Physics Research Section A: Accelerators, Spectrometers, Detectors and Associated Equipment*, 561(2):284–288, 2006.

[55] M. Zampetakis, F. Antoniou, F. Asvesta, H. Bartosik, Y. Papaphilippou, and A.S. Hernández. Interplay of Space Charge and Intra-Beam Scattering in the LHC Ion Injector Chain. 2023.

[56] Ji Qiang, Miguel A. Furman, and Robert D. Ryne. A parallel particle-in-cell model for beam–beam interaction in high energy ring colliders. *Journal of Computational Physics*, 198(1):278–294, 2004.